ISSN 2587-1366

TUJE

TURKISH JOURNAL OF ENGINEERING

VOLUME 4 ISSUE 1 JANUARY 2020

Dr. Ghazi DROUBI
Robert Gordon University Engineering Faculty
Scotland, UK

JOURNAL SECRETARY

Nida DEMİRTAŞ
nidademirtas@mersin.edu.tr

TURKISH JOURNAL OF ENGINEERING (TUJE)

Turkish Journal of Engineering (TUJE) is a multi-disciplinary journal. The Turkish Journal of Engineering (TUJE) publishes the articles in English and is being published 4 times (January, April, July and October) a year. The Journal is a multidisciplinary journal and covers all fields of basic science and engineering. It is the main purpose of the Journal that to convey the latest development on the science and technology towards the related scientists and to the readers. The Journal is also involved in both experimental and theoretical studies on the subject area of basic science and engineering. Submission of an article implies that the work described has not been published previously and it is not under consideration for publication elsewhere. The copyright release form must be signed by the corresponding author on behalf of all authors. All the responsibilities for the article belongs to the authors. The publications of papers are selected through double peer reviewed to ensure originality, relevance and readability.

AIM AND SCOPE

The Journal publishes both experimental and theoretical studies which are reviewed by at least two scientists and researchers for the subject area of basic science and engineering in the fields listed below:

Aerospace Engineering
Environmental Engineering
Civil Engineering
Geomatic Engineering
Mechanical Engineering
Geology Science and Engineering
Mining Engineering
Chemical Engineering
Metallurgical and Materials Engineering
Electrical and Electronics Engineering
Mathematical Applications in Engineering
Computer Engineering
Food Engineering

PEER REVIEW PROCESS

All submissions will be scanned by iThenticate® to prevent plagiarism. Author(s) of the present study and the article about the ethical responsibilities that fit PUBLICATION ETHICS agree. Each author is responsible for the content of the article. Articles submitted for publication are priorly controlled via iThenticate ® (Professional Plagiarism Prevention) program. If articles that are controlled by iThenticate® program identified as plagiarism or self-plagiarism with more than 25% manuscript will return to the author for appropriate citation and correction. All submitted manuscripts are read by the editorial staff. To save time for authors and peer-reviewers, only those papers that seem most likely to meet our editorial criteria are sent for formal review. Reviewer selection is critical to the publication process, and we base our choice on many factors, including expertise, reputation, specific recommendations and our own previous experience of a reviewer's characteristics. For instance, we avoid using people who are slow, careless or do not provide reasoning for their views, whether harsh or lenient. All submissions will be double blind peer reviewed. All papers are expected to have original content. They should not have been previously published and it should not be under review. Prior to the sending out to referees, editors check that the paper aim and scope of the journal. The journal seeks minimum three independent referees. All submissions are subject to a double blind peer review; if two of referees gives a negative feedback on a paper, the paper is being rejected. If two of referees gives a positive feedback on a paper and one referee negative, the editor can decide whether accept or reject. All submitted papers and referee reports are archived by journal Submissions whether they are published or not are not returned. Authors who want to give up publishing their paper in TUJE after the submission have to apply to the editorial board in written. Authors are responsible from the writing quality of their papers. TUJE journal will not pay any copyright fee to authors. A signed Copyright Assignment Form has to be submitted together with the paper.

PUBLICATION ETHICS

Our publication ethics and publication malpractice statement is mainly based on the Code of Conduct and Best-Practice Guidelines for Journal Editors. Committee on Publication Ethics (COPE). (2011, March 7). Code of Conduct and Best-Practice Guidelines for Journal Editors. Retrieved from http://publicationethics.org/files/Code%20of%20Conduct_2.pdf

PUBLICATION FREQUENCY

The TUJE accepts the articles in English and is being published 4 times (January, April, July and October) a year.

CORRESPONDENCE ADDRESS

Journal Contact: tuje@mersin.edu.tr

CONTENTS

Volume 4 – Issue 1

ARTICLES

Turkish Journal of Engineering

Turkish Journal of Engineering (TUJE)
Vol. 4, Issue 1, pp. 1-8, January 2020
ISSN 2587-1366, Turkey
DOI: 10.31127/tuje.571020
Research Article

NEW REGULATION TO REGISTER THE ANOMALOUS CONSTRUCTIONS AND FINANCE URBAN REGENERATION PROJECTS IN TURKEY: DEVELOPMENT PEACE

Yüksel Boz *[1] and Tayfun Çay [2]

[1] Hacettepe University, Faculty of Engineering, Geomatics Engineering, Ankara, Turkey
ORCID ID 0000 – 0002 – 8135 – 8308
yboz@hacettepe.edu.tr

[2] Konya Technical University, Faculty of Engineering and Natural Sciences, Geomatics Engineering, Konya, Turkey
ORCID ID 0000 – 0002 – 4661 – 5583
tcay@selcuk.edu.tr

* Corresponding Author
Received: 28/05/2019 Accepted: 30/07/2019

ABSTRACT
In the past year a brand new term, Development Peace, has been introduced by the Ministry of Environment and Urbanization of Turkey (MEUT) to register the constructions contrary to development and finance urban regeneration activities. Development Peace has been announced as a regulation in order to establish agreement between the owners of the irregular constructions and the government by providing Construction Registration Deed (CRD) on condition that a certain payment must be made based on the property value. The irregular properties except those constructed on private land and on public land reserved for social facilities will benefit from the regulation. Development Peace covers all kinds of constructions that are not in accordance with the Development Law. In May 18th, 2018 a temporary article explaining this new regulation has been added to the Development Law No. 3194 in Turkey. The anomalous constructions are not a newly discovered problem in Turkey and come from the past. The MEUT has taken the initiative and offered a solution for the majority of the buildings in Turkey. The Development Peace, in addition to its many benefits for the people owning irregular properties, will support urban regeneration projects with the income collected through its implementation. While the government forgives the citizens involved in illegitimacy, the law abiding citizens might be demoralized as the formers are getting rewarded. Development Peace-like regulations might have a pitfall such as encouraging the people that have tendency to violate laws. Therefore, the government should take precautions instead of authorizing irregular constructions. On the other hand, this new regulation covers all kinds of constructions no matter how resilient they are against natural hazards (esp. earthquakes), which is the other flawed side of the regulation.

Keywords: *Development Peace, Urban Regeneration, Construction Registration Deed, Irregular Construction, Turkey*

1. INTRODUCTION

Development Peace is a new term introduced by the MEUT to find solutions to the constructions contrary to the development plans, unauthorized, or contradictory to the appendices of the permits given (Ministry of Environment and Urbanization, 2018a). In Official Gazette (No. 30425 and Date: May 18th, 2018) Law on Restructuring of Tax and Some Other Debts and Making Changes on Some Laws (original title: Vergi ve Diğer Bazı Alacakların Yeniden Yapılandırılması ile Bazı Kanunlarda Değişiklik Yapılmasına İlişkin Kanun) has been published and a temporary article (No. 16) has been added to the Development Law No. 3194 by that Law (Official Gazette, 2018a). The purpose of the temporary article is to explain the content of the Development Peace regulation. The information covered in this study are mostly based on this explanatory temporary article of Development Law.

In the booklet prepared by the MEUT to introduce the Development Peace, the former Minister (Mehmet Ozhaseki) stated their happiness for having the citizens and the Government forgive eachother by means of the Development Peace (Ministry of Environment and Urbanization 2018a). In the booklet, the mutual forgiveness are described by the term "helalleşmek". "Helalleşmek" is a term that does not have a direct corresponding in English vocabulary and is used between two or more parties in case they have rights on each other and they forgive each other by paying some compensation or without any compensation, disclaiming any right.

The objective of the Development Peace is to register the constructions that are contradictory to the development plans, unauthorized, or contradictory to the appendices of the permits given. In this way, it is aimed to provide legality for the irregular constructions. These constructions will be registered by providing Construction Registration Deed (CRD).

2. STATEMENT OF THE PROBLEM

The irregular constructions covered by the new regulation include housings, commercial properties, agricultural constructions, solar power plants etc. The majority of these anomalous constructions consist of housings. In Turkey, the housings contrary to the development plans comprise over 50% of the housings constructed, which corresponds 13 million individual housing units. The residents in these buildings are mostly low-income citizens. The housings incompatible with the development plans were mainly constructed between 1950 and 2000. The development-based issues between the citizens and the municipalities resulted in piling up the files in the courts and the municipalities, for some reasons, are not able to manage to demolish the buildings contradictory to the development plans. On the other hand, the residents of the buildings in dispute are not able to get water, electricity, and natural gas services connected to their houses and are making use of these services unlawfully. As the irregular residential and commercial units are not registered, they cannot be pledged as collateral and not be used as an economic asset (Ministry of Environment and Urbanization, 2018a).

3. THE SCOPE OF THE DEVELOPMENT PEACE

The constructions, which are unauthorized or contradictory to the appendices of the permits given, in urban and rural areas will be in the scope of the Development Peace provided that they had been constructed before December 31th, 2017. Bosphorous coastal band, Sultanahmet and Suleymaniye Regions of the Historical Peninsula, and Gelibolu Historical Area will be out of the scope. Figure 1 shows a view from the Historical Peninsula, İstanbul (Emlaknews, 2018). The area where the Development Peace will not be applied has been surrounded and highlighted in Figure 2 (Ministry of Environment and Urbanization, 2018b). The constructions built on another's property and on public land reserved for social service areas are also out of the scope. If the CRD-given constructions are on the land owned by municipalities, the owners of these constructions can pay the market value of the property of the municipality and gain the ownership (Ministry of Environment and Urbanization, 2018a).

Fig. 1. A view of the Historical Peninsula, Istanbul (Source: Emlaknews, 2018)

The condominiums that had been built in defiance of development plans have property ownership problems due to lack of occupancy permits. After getting the CRDs, if all the owners in a condominium give consent and cede the areas coinciding with public spaces (roads, green fields, parks etc.), type conversion and apartment ownership will be recorded without seeking for occupancy permit at the directorates of land registry. In that case, a payment must be made as much as the amount paid while getting CRD.

Fig. 2. The area (surrounded and highlighted) excluded from Development Peace in Historical Peninsula, Istanbul (Source: Ministry of Environment and Urbanization, 2018b)

After these procedures, exchange operations of the constructions will be legitimized, the property tax will

be collected on the basis of property type 'building', which was being collected based on the property type 'plot' before, and tax loss will be avoided by this way. Since the construction servitude and property ownership will be provided, it will be feasible to perform banking operations such as pledging the buildings as collateral and getting mortgage loan (Ministry of Environment and Urbanization, 2018a).

The constructions built on public land will be provided with CRD under the condition that the owners must apply to the Ministry of Environment and Urbanization and pay the market value of the plot, on which the construction built (Ministry of Environment and Urbanization, 2018a).

4. FORMER PRACTICES BEFORE DEVELOPMENT PEACE IN TURKEY

The activities against development and construction laws are called as development crime. The laws about shanty/squatter's houses (in Turkish: gecekondu) can also be related to development crime (Keleş, 2015). The term "gecekondu" is used for the illegitimate houses and literally means "built overnight" (Türker-Devecigil, 2005). The constructions that were built without the required permissions and those that were not built in accordance with the previously obtained construction permission deeds are subject to punishment of fine or partly/full demolishment. In Turkey, the situation in which the owners of the anomalous constructions are forced to pay certain amount of money or forgiven without any payment is called as development (or zoning) amnesty (Keleş, 2015).

Indeed, the anomalous constructions must be demolished in case of implementing the laws. However, the demolishment attempts encounter resistance of pressure groups in terms of subjectivity. On the other hand, in terms of objectivity, it has been almost a permanent rule that the anomalous constructions are forgiven from time to time as the demolishment of those constructions means loss of national wealth (Keleş, 2015). Akalın (2018) states that development amnesty-like regulations punish the cities instead of the people committing crime towards cities.

The legal regulations before development peace were mainly based on legalizing the gecekondu houses. Whilst the recent regulation, Development Peace, is a government declaration, the former regulations were all enacted as laws. Since the gecekondu phenomenon gained importance in 1940s, many laws had been enacted whose numbers are 5218, 5288, 6188, 7367, 775, 1990, 2805, 2981, 3290, 3366 (Keleş, 2015; Official Gazette, 1948a, 1948b, 1953, 1959, 1966, 1976, 1983, 1984, 1986, 1987).

When the former regulations are compared to the recent one, Development Peace, it will be noticed that the most of the old practices targeted only gecekondu houses whereas Development Peace comprises all types of constructions (not only houses). Gecekondu houses sooner or later gain legitimacy by government actions (Buğra, 1998). The earliest regulations (e.g. Law No. 5218, 5228) were mainly about allocating land, based on some conditions, to the citizens living in the municipality. Some of the requirements to benefit from the past regulations were as follows (Official Gazette, 1948a, 1948b, 1953, 1966, 1983, 1984, 1986, 1987):

- To have been stayed within the boundaries of the municipality at least one year (Law No. 5218),
- Not having any dwelling or any plot of land to build a house (Law No. 5218),
- The worth of the plot to be assigned will be paid by installments without any interest in ten years (Law No. 5218),
- In the case of having more than one unauthorized dwellings within the municipality boundary, the provisions of the law are utilized for only one of them (Law No. 5218),
- In order to get a plot that belongs to the municipality, the person or his/her spouse must not own any dwelling or plot (Law No. 5228),
- The people obtained plots from the municipality must start constructing their houses in one year after receiving the plots and after expiration of that one year-period they must complete the construction within two years (Law No. 5228),
- The people that are the owners of the dwellings, which were built without any permit in areas not suitable for housing or that were built in areas suitable for housing, but not having required permits are provided with housing units by the municipality on condition that the owner of the illegitimate house must demolish the anomalous structure and remove the salvage before the allocation of the house by the municipality (Law No. 6188).
- The plots in the gecekondu prevention zone are primarily given to the citizens that became houseless due to the rehabilitation and clearance of the gecekondu houses and the citizens that do not have any dwelling unit (Law No. 775),
- According to the provisions of this law, the citizens which will be allocated with plots must be poor or low-income, they and their spouses or their minor children are required to not having any plot suitable for building a house inside the boundaries of any municipality (Law No. 775, Law No. 2805),
- The right holder, whose gecekondu is not preserved, will be provided with plot in the same area or in another gecekondu prevention zone (Law No. 2805),
- The dwellings contrary to the development law, whether those that will be preserved or the ones that will be preserved after rehabilitation, are subject to payments such as permit fee, fine payment and worth of the plot in order to be issued permanent or temporary permit and residential usage license (Law No. 2805),
- Bosphorus and Dardanelles, the places defined or will be defined according to Law No. 2863, military forbidden zones and security zones are out of scope (Law No. 2981),
- In case of having a gecekondu on a private land, consent of the owner of that private land must be obtained in order to benefit from this law (Law No. 2981),
- The land owner can demand to sell the land to the person who has gecekondu on that land according to the market value determined by the court. The gecekondu owner can make cash payment or (if the land and gecekondu owners agree on it) payments by installments (Law No. 3290),

- In the areas determined by rehabilitation development plan or cadastral plan, the right holders can be directly provided with title deed instead of title assignment deed (Law No. 3366).

More detailed information about development amnesty regulations in Turkey can be found in Akalın (2018). As some of them listed above, the former legislations, which were considered as development amnesty, had regulations such as allocating plots to the people letting them built houses or providing people with firm houses on condition that clearing out the gecekondu houses. On the other hand, the new regulation, Development Peace, has a broader spectrum since it comprises all types of constructions including houses. Development Peace also differs from the past practices with regard to its scope as given in Section 3 entitled "The Scope of the Development Peace".

5. DEVELOPMENT AMNESTY IN OTHER COUNTRIES

As irregular settlements like gecekondu is not a phenomenon peculiar only to Turkey (Keleş, 1978), development amnesty is not as well. In other countries it is not unusual to observe development amnesty regulations. In South Cyprus, an amnesty regulation had been announced as a one-off opportunity covering the anomalous buildings built before April 8th, 2011. The construction date must be validated by an oath of architect/civil engineer. In addition to the property owners, developers could apply to benefit from the amnesty and in case they miss to apply, they would be required to pay fine. The issued document within the scope of the amnesty was Certificate of Completion and all available problems of the buildings with irregularities could be solved with this certificate (Koutsolambros, 2011).

Another amnesty regulation was prepared for the buildings that had unregistered construction work in City of Alameda, California, United States. The construction works of the buildings without any permit such as adding another room, remodeling kitchen, plumbing work for another sink were considered within the scope of the regulation. The unregistered dwelling units were also covered by that program. The subject properties would be inspected by a City Inspector in order to make sure there is not any safety issues related to the construction (City of Alameda, 2017).

In Township of Marlboro, New Jersey, United States, a building/zoning amnesty program has been announced that covers the buildings with irregularities based on defined codes. The construction works performed without required permits will not be subject to any fine. The buildings that have unpermitted construction works such as finished basements, fences, outdoor kitchens, driveway stanchions etc. will be covered by the amnesty program (Township of Marlboro, 2019).

In Italy, the people done building violations can benefit from two types of amnesty: formal building amnesty (Sanatoria) and substantial building amnesty (Condono). If anybody starts construction work without a building permit, they need to file a Sanatoria to regularize the ongoing work. In case of a construction work against building rules, this issue needs to be solved by a government action, Condono law. The Condono laws establish the types of building irregularities and certain dates before which people should apply. In case of buying or selling a property, it is must be made sure that the permit or amnesty issues had been solved for that property (Studio Legale Metta, 2019).

The most noticeable difference between Turkey and other countries based on the established development (building/zoning) amnesties is that in Turkey development amnesty actions are taken by the central government as laws or declarations, while in the other countries, especially in North America, the development amnesties are regulated as local government (municipalities) programs and these programs mainly cover the extra work done as additions to the existing buildings.

Compared to the other countries, Turkey`s amnesty regulations for the irregular constructions are quite comprehensive leading to expectations for similar actions in the future and irresponsible behaviors. Sustainable amnesty anticipation is a troublesome situation threatening the sustainable planned development.

6. THE APPLICATION PROCEDURE FOR THE CONSTRUCTION REGISTRATION DEED

Applications will be made over e-government gateway (www.turkiye.gov.tr) or by applying to the institutions authorized by the MEUT. The applications could also be followed on e-government gateway (Ministry of Environment and Urbanization, 2018a). The e-government gateway is an internet site that provides access to all public services from a single source. This internet site has been in use since 2006. The citizens can perform queries on such as tax debt, traffic tickets based on the license plate, criminal record, case file and many others. On e-government gateway, under the menu 'Newly Added Services', there is a section titled 'Development Peace Registration Operations' (e-government gateway, 2018). The citizens can make registration application or verify construction registration deed under this section (Fig. 3). In Fig. 3, the page content has been given in English as well. In case the citizens need help, the Environment and Urbanization Provincial Directorates will be available for any information and support needed.

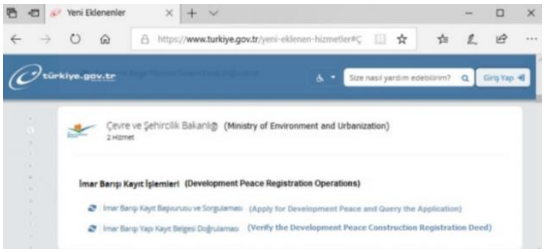

Fig. 3. 'Newly Added Services' page of e-government gateway (Source: e-government gateway, 2018)

The information needed to be entered over e-government gateway are as follows (Ministry of Environment and Urbanization, 2018c):

- e-government gateway password
- A valid phone number
- A valid e-mail address
- Address of the construction to be declared
- If title deed is present for the construction, the block and plot number for that construction
- Total construction area; areas of the residential and commercial properties separately (m^2)
- Number of residential and commercial units in the construction
- Unit tax value of the land or plot (TRY/m^2) (can be obtained from the relevant municipality)
- The area of the plot of the construction; if available the area in the land register, if not the declared area (m^2)
- Construction class (will be selected from the options offered by the system)
- Specifying the contradiction to the development legislation
- Pictures of the construction and the part having the contradiction, one for each (in jpg, jpeg, or png formats)

Applications has begun in June 2018 and will continue until June 15th, 2019 (Posta Gazette, 2019). In order to calculate the amount that the owners need to pay to get CRD is calculated by summing up the value of the plot and the cost of the building on that plot and taking %3 of that sum for the residential units and %5 of the sum for the commercial units. Value of the plots is the market value calculated from Sales Comparison approach. Cost of the constructions is calculated based on the declaration entitled "Rules and Procedures to Provide Construction Registration Deed" that is published by MEUT. In this declaration, the fifth article covers the unit cost price to calculate the approximate costs of the constructions.

The unit cost prices are: 200 TRY/m^2 for the ordinary agricultural constructions, 600 TRY/m^2 for one to two-storey buildings and simple industrial constructions, 1,000 TRY/m^2 for three to seven-storey buildings and integrated industrial constructions, 1,600 TRY/m^2 for eight-storey or higher buildings, 2,000 TRY/m^2 for the luxury buildings, villas, shopping malls, hospitals, hotels (Ministry of Environment and Urbanization 2018d). The unit cost prices for the other construction types, which have been added to the declaration in 20 September 2018, are as follows: 2,000,000 TRY/MW for power plants, 1,500 TRY/m^2 for ports, harbors, and shipyards, 150 TRY/m^2 for retaining walls, fill areas, pools, sports areas, and other constructions not having building characteristics (Official Gazette, 2018b).

The deadline of the payments for CRD was first announced as December 31th, 2018. The MEUT has stated that in case of need, the period of application and payment can be extended by the Cabinet of Ministers (Ministry of Environment and Urbanization 2018a). As indicated by the MEUT, the payment deadline had been extended until June 30th, 2019, whereas the application deadline is June 15th, 2019 (Posta Gazette, 2019). Another update has been put into action with respect to the payment deadline just before it expired. In accordance with the presidential decree dated 1 July 2019 and numbered 30818, the applicants of CRD applied before 15 July 2019 will be able to make their payments by 31 December 2019 (Ministry of Environment and Urbanization, 2019).

7. THE RELATION OF DEVELOPMENT PEACE AND URBAN REGENERATION

The collected fund from the regulation 'Development Peace' will be recorded as income in State budget and will be used to be prepared for the risks of earthquakes and other natural hazards, and finance the urban regeneration projects. The municipalities implementing urban regeneration projects will be provided loan with zero interest provided that they prefer 100% native construction materials (Ministry of Environment and Urbanization, 2018a).

As of July 20th, 2018, the number of applications to get CRD was 2,614,570. Among these applications, the housings have the highest number (2,340,450). The number of applications for the commercial properties, agricultural constructions, and solar power plants were 223,428, 50,611, and 81, respectively. The number of the irregular constructions that have been issued with CRD is 133,064 and an income of 659,506,741 TRY has been collected by providing CRDs. This income will be used in favor of urban regeneration projects. The cities having the highest number of applications have been given in Table 1 (Ministry of Environment and Urbanization, 2018e).

Table 1. The cities having the highest number of applications as of July 20th, 2018

City	Number of Applications
Istanbul	484,875
Izmir	242,604
Konya	156,613
Kocaeli	124,639
Bursa	123,039
Ankara	93,344
Gaziantep	76,605
Hatay	71,738
Antalya	70,739

Since the application deadline has been extended until June15th, 2019, as of May 7th, 2019, the number of applications to get CRD has reached 9,698,238 and 16.5 billion TRY has been collected corresponding the applications (Posta Gazette, 2019).

The issued CRD will be valid until the reconstruction of the construction or the urban regeneration project. In case of the reconstruction the constructions, the development legislation in effect will be enforced and the CRD will not provide any acquired right (Ministry of Environment and Urbanization, 2018a).

8. DISCUSSION AND CONCLUSIONS

In the booklet prepared by the MEUT to introduce the Development Peace, the outcomes of the Development Peace are given as below:

- The owners applied to take advantage of Development Peace and obtained CRD will get water, electricity, and natural gas services connected to their constructions.
- There will be no need to worry for the owners obtained CRD, relating to having their constructions demolished by the municipalities.
- The decisions taken for the demolishment according to the Development Law will be revoked and uncollectible fines will be omitted.
- The owners obtained CRD will be able to use their properties as an asset having economical value. This is highly important benefit of the regulation, since the irregular properties will gain formal representation and their confined potential value will be revealed as signified by De Soto (2000).
- In condominiums, apartment ownership for each residential unit will be established at the directorates of land registry by making the designated payments.

As pointing out the fact that the buildings incompatible with the development plans comprise over 50% of the buildings in Turkey, Development Peace has been announced by the MEUT as a solution to the constructions that are contradictory to the development plans, unauthorized, or contradictory to the appendices of the permits given. The Development Peace might seem as a problem solver as the irregular settlements and constructions will gain legality and the urban regeneration projects will be financed by this way. The government explains this regulation as mutual forgiveness and making peace with the citizens that have irregular constructions. However, the land where irregular constructions exist is not merely under the ownership of the government and the government should not decide on these properties on its own. The other citizens respectful to the laws also have rights on these properties. While the government forgives the citizens involved in infraction, the law abiding citizens might be demoralized as the formers are getting rewarded. Development Peace-like regulations might encourage the people that have tendency to violate laws. The government should take precautions instead of authorizing irregular constructions. The municipalities could benefit from the technologic advancements to monitor anomalous constructions, record the changes in the field, and create databases. Today there is a wide range of opportunities for the municipalities to utilize in their areas of responsibility such as satellite images, aerial photographs, Airborne-LiDAR (Light Detection And Ranging), Geographic Information Systems (GIS), Unmanned Aerial Vehicles (UAVs, drones).

In a constantly developing world, instead of temporary solutions, permanent approaches must be developed. Development Peace and similar regulations should not become a government policy. At first glance, the Development Peace seems to give a chance to low-income citizens to gain legitimacy for their irregular settlements. As stated above, however, these group of people are not the only beneficiaries of the regulation. The constructions built contradictory to the development plans or to the appendices of the permits given are within the scope of the regulation. That means the multi-storey buildings, commercial properties, industrial buildings will benefit from the regulation as well. The profits of the owners of these properties are incomparable with the payments that needed to be paid by the owners to obtain CRD. In other words, the high-income citizens most likely will make enormous gains. Considering that the irregular constructions comprise the majority of the constructions in Turkey, the income expected from Development Peace regulation for the purpose of financing regeneration projects could be substantial. The question is that who will take the advantage of the regulation? Is it the government and the municipalities or the high-income owners that own high value properties?

From valuation point of view, the commercial properties cannot be valued as residential properties. In the Development Peace regulation, as stated before, both types of properties will be valued in the same way. The only difference is the percentage to be paid by the owners to get CRD. In valuation profession, the commercial properties are appraised by income approach instead of sales comparison approach as they yield income. In case of valuing income generating properties inappropriately, the gain from issuing CRD for this kind of properties will be less than normal.

Earliest form (July 2018) of the declaration of the MEUT entitled "Rules and Procedures to Provide Construction Registration Deed" has been changed in September 2018 and seems to be changed by the time of progress. The Development Peace regulation has newly put into action and it is likely to have further changes as the deficiencies discovered.

The Development Peace might seem in favor of the people occupying irregular constructions. While this kind of regulations make certain parts of community delighted, the law-abiding side of the society will be demoralized. Although the Development Peace is the most comprehensive action of the government with respect to irregular constructions as yet, it may cause expectations in the citizens such as the government might put into action similar regulations in the future as well. The government should develop policies to avoid irregularity and not to encourage the people having tendency to break the rules.

On the other hand, the rationale behind the urban regeneration projects in Turkey is mainly declared as constructing earthquake resistant buildings. However, this new regulation covers all kinds of constructions no matter how resilient they are against natural hazards (esp. earthquakes). While promoting durable constructions, legitimizing vulnerable buildings at the same time is another flawed side of the regulation and needs further consideration.

REFERENCES

Akalın, M., (2018). *Kente Karşı İşlenen Suçların Faili: İmar Afları* [The Perpetrator of the Crimes Committed Towards the City: Development Peace], IKSAD Publications.

Buğra, A., (1998). The Immoral Economy of Housing in Turkey, *International Journal of Urban and Regional Research*, Vol. 22, Issue 2, 303-317.

City of Alameda (2017). Amnesty Program for Undocumented Construction. Available at: https://www.alamedaca.gov/files/sharedassets/public/ala

meda/comm-services/formsandhandouts/building/amnesty_program_for_undocumented_construction.pdf (Accessed 20 July 2019).

De Soto H., (2000). The Mystery of Capital, Why Capitalism Triumphs in the West and Fails Everywhere Else, Bantam Press.

Emlaknews, (2018). Tarihi Yarımada'ya Elektrikli Araç Düzenlemesi Yolda [The Regulation for Use of Electric Vehicles on Its Way for the Historical Peninsula]. Available at: https://www.emlaknews.com.tr/haberler/tarihi-yarimadaya-elektrikli-arac-duzenlemesi-yolda-285382/ (Accessed 06 July 2018).

e-government gateway, (2018). Yeni Eklenen Hizmetler [Newly Added Services]. Available at: https://www.turkiye.gov.tr/yeni-eklenen-hizmetler (Accessed 06 July 2018).

Keleş, R., (1978). *100 Soruda Türkiye'de Şehirleşme, Konut ve Gecekondu* [Urbanization, Housing, and Gecekondu in Turkey by 100 Questions], Genişletilmiş 2. Baskı [Comprehensive 2nd Edition], Gerçek Yayınevi.

Keleş, R., (2015). *Kentleşme Politikası* [Urbanization Policy], 14. Baskı [14th Edition], İmge Kitabevi.

Koutsolambros, Y., (2011). Planning Amnesty Explained. Available at: https://news.cyprus-property-buyers.com/wp-content/uploads/2011/09/Amnesty.pdf (Accessed 21 July 2019).

Ministry of Environment and Urbanization, (2018a). İmar Barışı [Development Peace], Booklet. Available at: http://webdosya.csb.gov.tr/db/imarbarisi/icerikler/brosur-20180603111057.pdf (Accessed 05 July 2018).

Ministry of Environment and Urbanization, (2018b). Available at: http://webdosya.csb.gov.tr/db/imarbarisi/icerikler/tar-h-yarimada-20180601150242.pdf (Accessed 05 July 2018).

Ministry of Environment and Urbanization, (2018c). E-Devlet Kapısı Üzerinden Yapılacak Müracaatta Gereken Bilgiler [The Information Needed for the Application Over E-Government Gateway]. Available at: http://imarbarisi.csb.gov.tr/e-devlet-kapisi-uzerinden-yapilacak-muracaatta-gereken-bilgiler-i-86161 (Accessed 03 July 2018).

Ministry of Environment and Urbanization, (2018d). Yapı Kayıt Belgesi Verilmesine İlişkin Usul ve Esaslar [Rules and Procedures to Provide Construction Registration Deed]. Available at: https://imarbarisi.csb.gov.tr/yapi-kayit-belgesi-verilmesine-iliskin-usul-ve-esaslar-i-86171 (Accessed 06 July 2018).

Ministry of Environment and Urbanization, (2018e). Bakan Kurum "İmar Barışı" Son Verileri Açıkladı [Minister Kurum Declared Last Data About "Development Peace"]. Available at: https://İmarbarisi.Csb.Gov.Tr/Bakan-Kurum-İmar-Barisi-Son-Verileri-Acikladi-Haber-229095 (Accessed 24 September 2018).

Ministry of Environment and Urbanization, (2019). İmar Barışı Ödeme Süresinin Uzatılmasına İlişkin Duyuru [Announcement About Extending the Payment Period of Development Peace]. Available at: https://imarbarisi.csb.gov.tr/imar-barisi-odeme-suresinin-uzatilmasina-iliskin-duyuru-haber-240279 (Accessed 27 July 2019).

Official Gazette (1948a). Ankara Belediyesine, Arsa ve Arazisinden Belli Bir Kısmını Mesken Yapacaklara 2490 Sayılı Kanun Hükümlerine Bağlı Olmaksızın ve Muayyen Şartlarla Tahsis ve Temlik Yetkisi Verilmesi Hakkında Kanun [Law on Authorization of Municipality of Ankara for Allocating and Assigning Some Part of Its Land to the People Willing to Build Houses]. Available at: http://www.resmigazete.gov.tr/arsiv/6938.pdf (Accessed 15 July 2019).

Official Gazette (1948b). Bina Yapımını Teşvik Kanunu [Law on Encouragement of Building Construction]. Available at: http://www.resmigazete.gov.tr/arsiv/6950.pdf (Accessed 15 July 2019).

Official Gazette (1953). Bina Yapımını Teşvik ve İzinsiz Yapılan Binalar Hakkında Kanun [Law on Encouragement of Building Construction and the Buildings Constructed without Permission]. Available at: http://www.resmigazete.gov.tr/arsiv/8470.pdf (Accessed 15 July 2019).

Official Gazette (1959). Hazineden Belediyelere Devredilecek Arazi ve Arsalar Hakkında Kanun [Law on Land and Plots to be Transferred from Treasury to the Municipalities]. Available at: http://www.resmigazete.gov.tr/arsiv/10265.pdf (Accessed 15 July 2019).

Official Gazette (1966). Gecekondu Kanunu [Gecekondu Law]. Available at: http://www.resmigazete.gov.tr/arsiv/12362.pdf (Accessed 16 July 2019).

Official Gazette (1976). Gecekondu Kanununda Bazı Değişiklikler Yapılması Hakkında Kanun [Law on Making Some Amendments to the Gecekondu Law]. Available at: http://www.resmigazete.gov.tr/arsiv/15588.pdf (Accessed 16 July 2019).

Official Gazette (1983). İmar ve Gecekondu Mevzuatına Aykırı Olarak Yapılan Yapılara Uygulanacak İşlemler ve 6785 Sayılı İmar Kanununun Bir Maddesinin Değiştirilmesi Hakkında Kanun [Law on Procedures to be Applied for the Constructions Build Contrary to Development and Gecekondu Legislation and Amending One Article of the Development Law Numbered 6785]. Available at: http://www.resmigazete.gov.tr/arsiv/17994.pdf (Accessed 16 July 2019).

Official Gazette (1984). İmar ve Gecekondu Mevzuatına Aykırı Yapılara Uygulanacak Bazı İşlemler ve 6785 Sayılı İmar Kanununun Bir Maddesinin Değiştirilmesi Hakkında Kanun [Law on Procedures to be Applied for the Constructions Contrary to Development and Gecekondu Legislation and Amending One Article of the Development Law Numbered 6785]. Available at: http://www.resmigazete.gov.tr/arsiv/18335.pdf (Accessed 17 July 2019).

Official Gazette (1986). 24.2.1984 Tarih ve 2981 Sayılı Kanunun Bazı Maddelerinin Değiştirilmesi ve Bu Kanuna Bazı Maddeler Eklenmesi Hakkında Kanun [Law on Amending Some Articles of the Law Dated 24 February 1984 and Numbered 2981 and Adding Some Articles to That Law]. Available at: http://www.resmigazete.gov.tr/arsiv/19130.pdf (Accessed 17 July 2019).

Official Gazette (1987). 3290 Sayılı Kanun ile Değişik 2981 Sayılı Kanunun Bazı Maddelerinin Değiştirilmesine İlişkin Kanun [Law on Amending Some Articles of the Law Numbered 2981 that has been Amended by the Law Numbered 3290]. Available at: http://www.resmigazete.gov.tr/arsiv/19471.pdf (Accessed 17 July 2019).

Official Gazette, (2018a). Vergi ve Diğer Bazı Alacakların Yeniden Yapılandırılması ile Bazı Kanunlarda Değişiklik Yapılmasına İlişkin Kanun [Law on Restructuring of Tax and Some Other Debts and Making Changes on Some Laws]. Available at: http://www.mevzuat.gov.tr/MevzuatMetin/1.5.7143.pdf (Accessed 05 July 2018).

Official Gazette, (2018b). Yapı Kayıt Belgesi Verilmesine İlişkin Usul ve Esaslarda Değişiklik Yapılmasına Dair Usul ve Esaslar [Rules and Procedures in Respect of Making Changes in Rules and Procedures to Provide Construction Registration Deed]. Available at: http://www.resmigazete.gov.tr/main.aspx?home=http://www.resmigazete.gov.tr/eskiler/2018/09/20180926.htm&main=http://www.resmigazete.gov.tr/eskiler/2018/09/20180926.htm (Accessed 22 September 2018).

Posta Gazette (2019). İmar Barışı'nda Son Fırsat [Last Chance for Development Peace]. Available at: https://www.posta.com.tr/imar-barisinda-son-firsat-2151184 (Accessed 08 May 2019).

Studio Legale Metta, (2019). Italian Building Permit and Violations. Available at: https://www.studiolegalemetta.com/en/italian-building-permit-violations/ (Accessed 25 July 2019).

Township of Marlboro, (2019). Building/Zoning Permit Amnesty Program. Available at: https://www.marlboro-nj.gov/notices/2019/Building-zoningDept-Amnesty-LetterLF.pdf (Accessed 20 July 2019).

Türker-Devecigil, P., (2005). Urban Transformation Projects as a Model to Transform Gecekondu Areas in Turkey: The Example of Dikmen Valley-Ankara, *European Journal of Housing Policy*, Vol. 5, No. 2, 211-219.

Turkish Journal of Engineering

Turkish Journal of Engineering (TUJE)
Vol. 4, Issue 1, pp. 9-16, January 2020
ISSN 2587-1366, Turkey
DOI: 10.31127/tuje.579869
Research Article

UTILIZING A GEOMECHANICAL CLASSIFICATION TO PRELIMINARY ANALYSIS OF ROCK SLOPE STABILITY ALONG ROADWAY D340- 41.42, SOUTHWEST OF TURKEY: A CASE STUDY

Ahmed Ibraheem Mohamed *[1] and Ali Ferat Bayram [2]

[1] Konya Teknik University, Natural Science And Engineering Faculty, Department of Geological Engineering, Konya, Turkey
ORCID ID 0000 – 0001 – 9226 – 0982
Ahmed.mohamed@selcuk.edu.tr

[2] Konya Teknik University, Natural Science And Engineering Faculty, Department of Geological Engineering, Konya, Turkey
ORCID ID 0000 – 0001 – 5210 – 7836
fbayram@selcuk.edu.tr

* Corresponding Author
Received: 19/06/2019 Accepted: 28/08/2019

ABSTRACT
Road construction is mostly passed through mountainous regions or hilly terrains in Turkey like in all world. In hence, roadway construction and widening are being constructed through blasting and excavation, leading to rock slope instabilities and failures then poses threats to life and property. The reasons for failure sometime after construction are likely due to the deterioration of rock masses in cut slopes. However, slope instability and failures mainly occur due to adverse slope geomorphological complexities, joint discontinuities, weathering, man-made activities, unloading; and several induced factors such as seasonal heavy rainfall events, snow coverage, etc. The objectives of this paper are therefore to identify the most significant parameters influencing the behavior of cut slope rock masses with employing SMR ,and to perform a preliminary slope instability assessment along roadway D340- 41.42, southwest of Turkey, where slopes located in a region of Taurus's rugged terrains with known complex geometry, then propose a suitable control measures to mitigate potential failures of rock slope stability. In this study, 19 rock cuts are selected based on the observed failure mechanisms, slope geometry and materials. A systematic site investigation incorporating relevant engineering geological and geotechnical parameters were carried out in detail. Based on slope instability observations and SMR results rating, concluded that these slopes were widely controlled by discontinuities (structurally controlled failures). As well, SMR classification scheme was successfully used for failure classification in Taurus's terrains. Finally, slope flattening with various angles method, wire mesh, toe support by detached rock blocks and drainage ditches re-design are proposed as a remedial measurement to protect road slope stability from failure.

Keywords: *Slope Stability Failures, Rock Mass Classification, SMR Classification System, Roadway D340- 41.42, Turkey*

1. INTRODUCTION

Stability assessment is of essential importance for planning and construction of infrastructure, including roads in hilly terrain (Basahel and Mitri, 2017; Lenka, *et al.*, 2018). Slope stability in hilly regions is easily affected and frequent failures are present all over the world. In Turkey, most road networks and some railway tracks are passed through hilly terrains, such as Taurus's rugged terrains in the present study. So, these roadways construction and widening are being constructed through blasting and excavation, this blasting creates new fractures in the rock slopes poses threats to life and property.

In Taurus precarious, slopes are well known for their instability due to the dynamic nature of slopes, geomorphological complexities, joint discontinuities, weathering, long period snowfall which sometimes cause the roads to be completely closed, in addition to heavy and sustained rainfall, and ongoing activity. This constraint sometimes causing disruption of traffic along this important hill route and creating recurrent economic loss to the state exchequer.

To avoid these troubles, it is then very important to assess engineering geological properties of the lithological units with elaborated investigations for stability of slopes, in hence, this paper highlights utilizing SMR classification after (Romana, 1985) developed for rock slope stability assessment, then classify the rock mass of the investigated slopes into different slope classes of Turkey, according their vulnerability to failure along roadway D340- 41.42, southwest of Turkey, where slopes located in a region of Taurus's rugged terrains known with complex geometry.

In order to examine cut slope and assess their stabilities, a systematic site investigations incorporating relevant engineering geological and geotechnical parameters have been carried out in detail, this work was accomplished with scan-line technique suggested by (ISRM, 2007), during investigation all field observations / measurements, characterization of rock mass for all slope instability analysis were recorded, Also, slope instability modes were identified too. Finally, and to mitigate the endangered cut slopes from failure, the strengthening measurements and many remedial solutions were proposed.

2. GEOLOGICAL DESCRIPTION

The studied roadway cut is located within the Central Taurus Belt, it is a part of D-340 along a major highway connecting between Konya and Alanya cities, lying southwest of Turkey with coordinates (36°58'52" N;32°27'32"E) and (36°44'54" N;32°27'55"E) (Fig. 1).

Geologically, roadway D340-42.41 region was covered by shallow marine sedimentary rocks that resulted from deposition of limestone, clayey limestone and recrystallized limestones during the Early-Middle Cambrian. Exposed lithological units along studied roadway were belong to "Gevne group "varied from Kusakdagi formation (Pk) to Dedebeleni formation (Jd) with some Quaternary deposits and recent slope debris (Q) (Fig. 2), ranged in age from Jurassic - Upper Jurassic (Dedebeleni formation) to Upper Permian (Kusakdagi formation) (Turan, 1990).

The studied roadway was a problematic due to the existence of lithological units with variable characters which mainly comprised of micritic limestone, reefal limestone, clayey limestone, mudstone, sandstone, conglomerate; and Quaternary clastic deposits comprised of gravel-sand-silt and clay (Fig. 1)

However, during field studies the observed cut slopes are located within four formations are: 1) Kusakdagi formation (Pk) (Upper Permian) comprised of bituminous - fossiliferous and reefal limestone beds described in field with grey-black color, moderate - thickly bedded, moderately to highly weathered, hard, and moderately jointed, and thin abundant algal limestone with interbedded of shale and quartzite. 2) Beyreli formation (Tb) (Middle -Upper Triassic) was a sequence layers varied from light gray, hard, slightly-moderately weathered, well bedded sandy recrystallized limestone, sandstoe, shale to light brownish colors of mudstones and micro-conglomerates beds characterized with moderately-highly weathered, highly jointed 3) Camici formation (Jc) (Jurassic?) recognized by colored with red clayey, thick and conglomerate - dominated sandstones, mudstones. This conglomerate was reddish, coarse grained with poor rounded shape, slightly-moderately weathered and medium strong; and Dedebeleni formation (Jd) (Upper Jurassic) dominantly comprised of limestone and micritic limestone with soft morphological clay and silt, claystone- clayey limestone alternated with re-crystalized and little dolomitic limestone, these units characterized with light gray to white colored, limestone hard to extremely hard, highly jointed.

Structurally, the study area is repeatedly affected by folded, uplifted - thrusting and erosion activities through Early Cimmerian Orogeny (Turan, 1990), thus, this led to a rugged terrain like Taurus ranged in elevation between (1052-1403 m) above sea level and form a dendritic drainage pattern which was observed during field studies too.

The researched roadway stretch was an extensively deformed, this observed obviously by making up major thrust fault namely "Gevne thrust fault" accompanied by transional faults, then led to form deeply valley namely "Gevne stream" as a weakness planes induced most of slope instabilities exposed along this road.

Therefore, most of the observed failure modes (planer, wedge, toppling) in the field were controlled by discontinuities. In addition to several climatic factors directly and indirectly widely induce road slope instability such as seasonal heavy included rainfall events and snow coverage on open spaces and site-specific roadway traffic (Trenouth and Gharabaghi, 2016).

These factors combined with the erosion and man-made activity, water run-off and groundwater mainly cause to slope instabilities. Briefly, the factors impact on roadway lifetime are consecutive and myriad, could be argued.

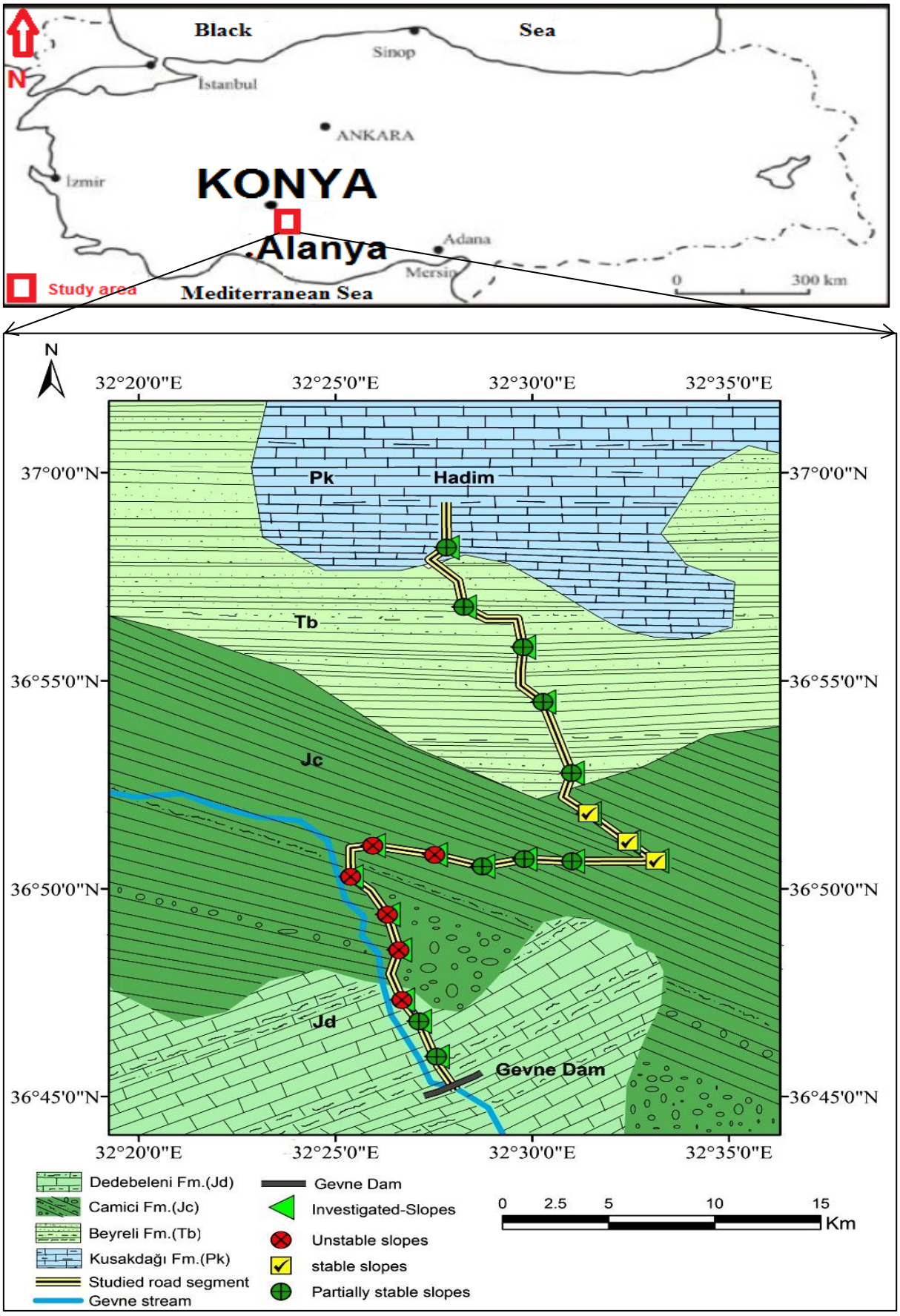

Fig. 1. Location and Geological map of study area, *modified from* Directorate of Mineral and Explorations (MTA, 1985).

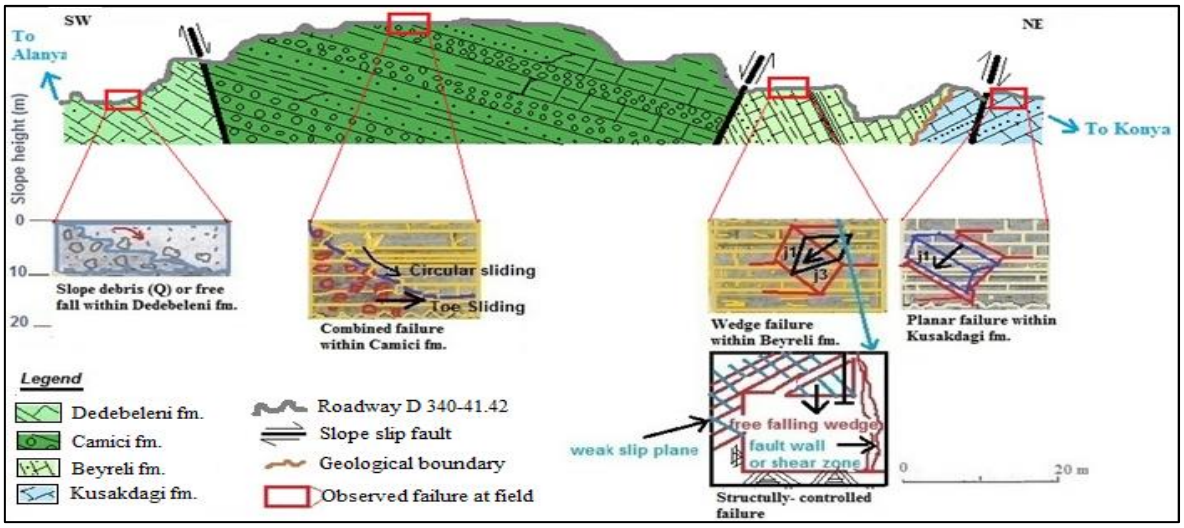

Fig. 2. Geological sketch showing discontinuity impact on failures modes observed along roadway D340-41.42.

3. APPLICABILITY OF ROCK MASS CLASSIFICATION TO SLOPE STABILITY

In rock mass classification system, most of the methodology is proposed to identify the quantitative condition of road slopes (Saranaathan, 2015). In general, the slope stability determination methods depending on the material involved (Sonmez *et al.*, 1998) . However, many authors have applied geostatistics to investigate slope stability assessment in a rock mass (Aksoy, 2008; Harrison and Hudson, 2000; Liu and Chen, 2007; Morales *et al.*, 2019; Pastor *et al.*, 2019; Tomas *et al.*, 2012) qualitative and quantitative methods have been used to detect and predict rock slope stabilities, As is well known, Rock Mass Classification calculated based of RMR, is probably one of the most widely used classifications (Pantelidis, 2009; Romana, 1997) is mainly used and developed to perform slope stability and examine failure of rock cut slopes, but largely accepted, endorsed and used in current paper classification system is slope mass rating (SMR) (Romana, 1985; Romana *et al.*, 2003) specifically designed for calibration of slopes, which basically modified from basic Rock Mass Rating (RMR_{basic}).

3.1. APPLICATION OF SLOPE MASS RATING (SMR)

For evaluating the stability of rock slopes, (Romana,1985) proposed a classification system called the "slope mass rating" (SMR) system (Table 1). SMR is basically obtained from Bieniawski's rock mass rating (RMR) by subtracting adjustment factors of the joint–slope relationship and adding a factor depending on method of excavation.

Romana (1985) established a relationship to find 'Slope Mass Rating 'depending on the RMR_{basic} index (Bieniawski, 1989) and a factorial adjustment factors that depict the geometrical relationship between discontinuities affecting the rock mass and the slope (F1, F2, F3) (Table 2), slope excavation method (F4) (Table 3). It is completely depend on the geometrical relationship slope and discontinuities orientation with observed failure modes in field (Table 4). The final calculation is of the form:

$$SMR = RMR_{basic} + (F1.F2.F3) + F4 \quad \ldots\ldots\ldots\ldots\ldots \quad (1)$$

Where: (RMR_{basic}) is evaluated according to (Bieniawski, 1979) by adding the ratings of five parameters (see Table 5). F1, F2, and F3 are adjustment factors related to joint orientation with respect to slope orientation, and F4 is the correction factor for method of excavation:

i) F1 – depends on parallelism between joints and slope face strikes. It is in range from 1.00 (when both are near parallel) to 0.15 (when the angle between them is more than 30°).

ii) F2 refers to joint dip angle in the planar mode of failure, in a sense, is a measure of the probability of joint shear strength. This value varies from 1.00 (for joint dipping more than 45°) to 0.15 (for joints dipping less than 20°).

iii) F3 reflects the relationship between slope face and joint dip. Conditions are fair when slope face and joint are parallel. When the slope dips 10° more than joints, very unfavorable condition occur. The adjustment factor for the method of excavation F4 depends on whether one deals with a natural slope or one excavated by pre-splitting, smooth blasting, mechanical excavation, or poor blasting. Based on the SMR results, the studied slopes are classified into different instability classes with risks descriptions according to the following Table:

Table 1. Description of SMR classes (Romana, 1985).

Class	SMR	Descript-ion	Stability	Failure probability
V	0- 20	Very bad	*C. unstable	0
IV	21-40	Bad	unstable	0.2
III	41-60	Fair	*P.stable	0.4
II	61-80	Good	stable	0.6
I	81-100	*V.good	*C.stable	0.9

*V: very; *C: completely; *P: Partially.

Table 2. Adjustment ratings for F1, F2, and F3 (Romana, 1985, modified by (Anbalagan,*et al.*, 1992))

Case of slope failure	Very favourable	Favourable	Fair	Unfavourable	Very unfavourable
P | αj-αs|	> 30º				
T | αj-αs-180|		30-20º	20-10º	10-5º	< 5º
W | αj-αs|					
P/T/W F1	0.15	0.40	0.70	0.85	1.00
P | βj |	< 20º	20-30º	30-35º	35- 45º	> 45º
W | βj |					
P/W F2	0.15	0.40	0.70	0.85	1.00
T F2	1.00	1.00	1.00	1.00	1.00
P βj- βs	> 10º	10- 0º	0º	0- (-10º)	< (-10º)
W βj- βs					
T βj+βs	<110º	110-120º	>120º	-	-
P/T/W F3	0	- 6	-25	-50	-60

FAILURE: P planar; W wedge; T toppling. DIP DIRECTION: α j discontinuity; α s slope. DIP: βj discontinuity; βs: slope .

Table 3. Adjustment factor F4 for the method of excavation (Romana, 1985).

Excavation method	F4 value		
Presplitting	+10	Normal blasting or mechanical excavation	0
Smooth blasting	+8	Deficient blasting	- 8
Natural slope	+15		

4. CASE STUDY

In this study, Slope Mass Rating (SMR) after (Romana, 1985) was used to determine the slope stability and examine their stability conditions, in order to do this,19 road cuts have been chosen in the study area along roadway D340- 41.42. A detailed field investigation with seven scanlines, 10 m each has been carried out in the different selected localities of the study area.

This investigation involved record of both quantitative and qualitative recording of various rock masses parameters with an emphasis on collect the required geological and geotechnical data/measurements for finding both RMR and SMR. The methodology of current study can be summarized by the following main steps:

1- Determination of the six parameters related to RMR_{basic} for each investigated slope, to find SMR values.

2- Collection of field data related to discontinuities in term of spacing, orientation (dip/strike) with respect to slope, conditions of joints, ground water, Rock Quality Designation (RQD %); and Rock strength of rock material. Here, it is worth to mention that RQD % rating was calculated by field survey using mean discontinuities spacing (Palmstrom, 2005; Singh and Goel, 1999) from this relationship; RQD % = (115 -3.3 jv), where jv is the volumetric joint count.

3- Based on the field investigations, investigate and record, then finding Romana's rating adjustments (F1, F2, F3) and assess excavation method (F4) parameters, to determine the respective Slope Mass Rating (SMR values).

4- According to SMR values classify of the rock slope stability into different instability classes with risks consequently.

5. RESULTS AND DISCUSSION

As well as, this study was meant to assess then classify the rock mass of the investigated slopes along roadway D340- 41.42 into different slope classes according their vulnerability to landslide employing SMR classification. The carried - out investigation involved 19 rock slopes (S1-S19) along this roadway (Fig. 1).

Most of the investigated slopes comprise three sets of discontinuities (J1, J2, J3) along dip with some randomly oriented sets forming blocks of different sizes, these joints, slope conditions; and related adjustment factors (F1, F2, F3) were studied in detail, then evaluated according to Tables 2,3. Joints - slope measurements parameters at different locations were given in Table 4 too. Most of the encountered failure modes regarding to the geometrical relationship between joints and slope were controlled by fracturing.

In this study, RMR_{basic} rating values and SMR rating values were calculated too. RMR_{basic} rating values ranges from 61 to 72 (Table 5), SMR rating values ranges from 30.30 to 68.10 (Table 6). These ratings were assigned to each parameter. From these results it was found that, some slopes despite have a moderate to high RMR_{basic} values with good quality of rock mass, but it was remained unstable and prone to failure.

For example, in the Table 5, S3-S6, S7- S8 rock slopes although, have medium to high values of RMR_{basic} (both are 66), but have the lower SMR values in Table 6. (30.30, 36.25 respectively).

Obviously, this may be due to effect of joints orientation and excavation method (blasting) on the slope instability which denoted in the previous equation with (F4).

Accordingly, slope stability condition for all nineteen (19) rock slopes were assessed and classified in (Table 7) into five potential failure classes based on their

Table 4. Slope – discontinuities orientation relationship with observed failure modes in field. (DD = Dip direction, DA = Dip amount)

Rock slope No.	Slope orientation DD / DA	Bedding plane	Joints orientation			Observed failure in field
		DD / DA	J1 (DD / DA)	J2 (DD / DA)	J3 (DD / DA)	
S1 - S2	089/41-68	210/34-35	222/70	355/80	098/90	Wedge J1&J3
S3 - S6	087/30-37	180/30-35	280/82	030/83	140/87	Planar J1,Toppling J1,2,3
S7 - S8	105/34	255/37	225/80	349/72	115/ 70	Planar j2
S9 - S11	115/44	270/40	235/87	045/56	135/85	Planar J1; Wedge J1&J3
S12 - S14	112/40	220/31-40	225/82	025/85	100/64	block failure, Rockfall
S15 - S17	095/55	310/20-40	188/83	030/90	125/75	Toppling J1,J2,J3
S18 - S19	110/87	230/40	230/65	045/65	-	wedge J1&J2

Table 5. RMR classification based on estimated (RMR_{basic}) values parameters for the studied rock slopes

Rock slope No. →		S1-S2	S3-S6	S7-S8	S9-S11	S12-S14	S15-S17	S18-S19
USC rating (R1)		12	8	11	13	12	10	12
RQD rating % (R2)		13	12	13	17	12	14	13
Discontinuities spacing Rating (R3)		8	10	9	8	10	8	10
Discontinuities condition rating (R4)	Persistence	6	6	5	4	5	4	4
	Aperture	1	1	2	4	1	3	1
	Roughness	6	5	5	6	5	5	4
	Infilling	6	4	5	4	3	6	5
	Weathering	3	3	2	3	4	4	4
	Total	**22**	**21**	**19**	**21**	**18**	**22**	**18**
Ground water rating (R5)		14	15	14	13	14	13	15
Discontinuities orientation (R6)		0	0	0	0	- 5	0	0
RMRbasic		69	66	66	72	66	67	68
RMR*		69	66	66	72	61	67	68
Rock mass class		Good	Good	Good	Good	Good	Good	Good
RMR description		II	II	II	II	II	II	II

RMR* = ∑classification parameters (R1+R..+R5) + Discontinuity orientation adjustment (R6)

Table 6. Results of SMR Rating values for studied rock cut slopes.

Rock slope No.	RMR basic	Observed failure	The factorial adjustment factors				SMR** rating
			F1	F2	F3	F4	
S1 - S2	69	Wedge J1&J3	0.85	0.85	-25	+8	58.93
S3 - S6	66	Planar J1, Toppling J1,2,3	0.85	0.70*	-60	0	30.30
S7 - S8	66	Planar j2	0.70	0.85	-50	0	36.25
S9 - S11	72	Planar J1; Wedge J1&J3	0.85	0.85	-25	0	53.93
S12 -S14	61	Free rock falling	0.15	1.00	-6	+8	68.10
S15 - S17	67	Toppling J1,J2,J3	0.85	0.70	-25	0	52.12
S18 - S19	68	Wedge J1&J2	0.70	0.70	-50	0	43.50

0.70* is an average value for planar and Toppling, SMR** = RMR_{basic}+ (F1.F2.F3) + F4

Table 7. Slope stability assessment of roadway D340 - 41.42 slopes according to classes and SMR values in Table 6.

Rock slope No.	SMR** value	Class No.	Slope description	Stability	Inferred failure from SMR	Failure Probability %
S1 - S2	58.93	III	Fair	Partially stable	Planar along some joints or many wedge failure	40
S3 - S6	30.30	IV	Bad	unstable	Planar or Big Wedge	60
S7 - S8	36.25	IV	Bad	unstable	Planar or Big Wedge	60
S9 - S11	53.93	III	Fair	Partially stable	Planar along some joints or many wedge failure	40
S12 -S14	68.10	II	Good	stable	Some block failure	20
S15 - S17	52.12	III	Fair	Partially stable	Planar along some joints or many wedge failure	40
S18 - S19	43.50	III	Fair	Partially stable	Planar along some joints or many wedge failure	40

SMR values in Table 6, and according to all obtained results, the probability of failure for all studied slopes have been computed as inserted in Table 7. and compared to the observed values, then represented in Fig. 3 too.

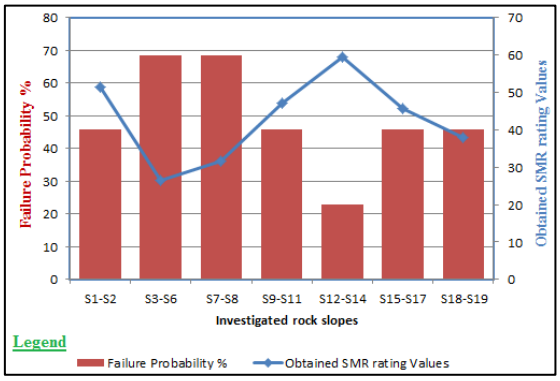

Fig. 3 Failure Probability according to their SRM rating values for the investigated slopes in the current study.

From this figure it was found there is a reverse relationship between SMR rating values and probability of failure (failure probability increases with decreasing of SMR values). Furthermore, slope stability analysis for nineteen investigated rock slopes have been explained in Table 7 and Fig. 4, then categorized into partially stable, unstable, and completely stable. slope stability analysis was classified with taking into account multiple considerations of anticipated conditions during field study.

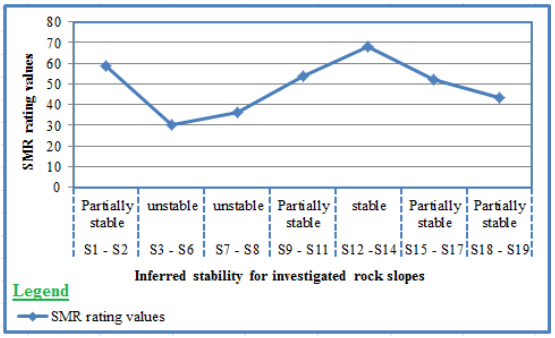

Fig. 4 Slope stability analysis for the investigated slopes in the current study.

Consequently, we can classify these failures modes as a "structurally - controlled failures". This can reasonably be expected because the study area was repeatedly affected by folded, uplifted – thrusting through Early Cimmerian Orogeny. In addition to impact of severe weather conditions such as climates heavy rains, snow, etc..; and man-made activities, therefore, field studies and obtained results have shown that there is a positive correlation between joints - slope parameters and failure modes (planer, wedge, toppling).

Also, in this study, we propose that slope flattening with various angles method, wire mesh; and toe support by detached rock blocks are suitable remedial solutions to ensure slope stability of the studied roadway from failure. On the other hand, it is inferred that rock bolting is not suitable for the cut slope of this study due to the highly fractured nature of the rock mass. If any, as shown in Fig. 5, re-design of roadside drainage ditch to protect sensitive rock slopes from failure can be optimized, where drainage is generally used to mitigate larger rockslides and failures.

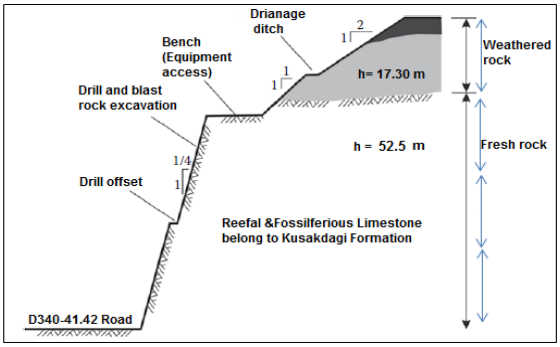

Fig. 5 suitable proposed solution by Slope flattening with various angles for investigated rock slope No.17

6. CONCLUSION

Utilizing SMR classification (Romana, 1985) which we sought to test in this paper, an adjustment factors (F1, F2, F3) and excavation method (F4) were considered in this study. From this study, it was found that SMR can be applicable to thickly-massive and extremely rocks like massive limestone of this study, because this rock will need to a heavy blasting, this blasting creates new fractures in the rock slopes, So, the effects of the new fractures on rock slopes with SMR classification as (F4) factor can be estimated. Probably some correction should be added for the block size (relative to slope height).

Also, in this study, SMR was successfully used for failure modes classification assessment in rocky and hilly areas (like Taurus in present study). In hence, from the current study we inferred that a detailed study should be carried out where SMR is less than 40 (S3-S8 in Table 5), and further studies need to be done to determine the cause of the differences that occur.

Moreover, it was found that the preliminary analysis with limited data RMR and SMR is more suitable. The detailed analysis requires more data and a comprehensive study of each layer.

Consequently, the geologist and geotechnical engineers works at General Directorate of Highways in Turkey are encouraged to use this classification in the initial evaluation of rocky slopes instabilities conditions, it is a practical, easy tool and it does not require much time.

ACKNOWLEDGEMENT

The authors thank **S**cientific Research Projects Support Fund (BAP) in Konya Technical University, Turkey; for their financial support and providing the necessary laboratory facilities to complete this research. As well, we express their sincere gratitude to Prof. Dr. Ihsan Özkan for his frequent discussions and suggestions during the study.

REFERENCES

Aksoy, C. (2008). Review of rock mass rating classification: historical developments, applications, and restrictions. *Journal of mining science, 44*(1), 51-63.

Anbalagan, R., Sharma, S.and Raghuvanshi, T. (1992). Rock mass stability evaluation using modified SMR approach. *In the Proceedings 6th Natural Symposium on Rock Mechanics,p258-268.*

Basahel, H.and Mitri, H. (2017). Application of rock mass classification systems to rock slope stability assessment: A case study. *Journal of rock mechanics and geotechnical engineering, 9*(6), 993-1009.

Bieniawski, Z. (1979). The geomechanics classification in rock engineering applications. *In the 4th ISRM Congress.*

Bieniawski, Z. (1989). Engineering rock mass classifications: a complete manual for engineers and geologists in mining, civil, and petroleum engineering: *Wiley- interscience Publication,,NEW YORK,240 p.*

Harrison, J. P.and Hudson, J. A. (2000). Engineering rock mechanics: *part 2: illustrative worked examples (Vol. 2): Elsevier.*

I.S.R.M. (2007). The complete ISRM suggested methods for rock characterization, testing and monitoring: 1974-2006: *International Soc. for Rock Mechanics, Commission on Testing Methods.*

Lenka, S. K., Panda, S. D., Kanungo, D. P.,. (2018). Slope Mass Assessment of Road Cut Rock Slopes Along Karnprayag to Narainbagarh Highway in Garhwal Himalayas, India. *In the Workshop on World Landslide Forum.*

Liu, Y.-C.and Chen, C.-S. (2007). A new approach for application of rock mass classification on rock slope stability assessment. *Engineering Geology, 89*(1-2), 129-143.

Morales, M., Panthi, K.and Botsialas, K. (2019). Slope stability assessment of an open pit mine using three-dimensional rock mass modeling. *Bulletin of Engineering Geology and the Environment*, 1-16.

M.T.A. (1985). General Directorate of Mineral and Research Explorations,Turkey, *Geological maps of Turkey,scale 1:100,000.*

Palmstrom, A. (2005). Measurements of and correlations between block size and rock quality designation (RQD). *Tunnelling and Underground Space Technology, 20*(4), 362-377.

Pantelidis, L. (2009). Rock slope stability assessment through rock mass classification systems. *International Journal of Rock Mechanics and Mining Sciences, 46*(2), 315-325.

Pastor, J. L., Riquelme, A. J., Tomás, R.,. (2019). Clarification of the slope mass rating parameters assisted by SMRTool, an open-source software. *Bulletin of Engineering Geology and the Environment*, 1-12.

Romana, M. (1985). New adjustment ratings for application of Bieniawski classification to slopes. *In the Proceedings of the international symposium on role of rock mechanics, Zacatecas, Mexico.*

Romana, M. (1997). El papel de las clasificaciones geomecánicas en el estudio de la estabilidad de taludes. *In the IV Simposio Nacional sobre taludes y laderas inestables. Comunicaciones* (In spanish).

Romana, M., Serón, J. B.and Montalar, E. (2003). SMR geomechanics classification: application, experience and validation. *In the 10th ISRM Congress.*

Saranaathan, S. (2015). Different research techniques and models in rock mass rating and slope stability analysis. *Journal of Chemical and Pharmaceutical Research, 7*(7), 160-168.

Singh, B.and Goel, R. K. (1999). Rock mass classification: a practical approach in civil engineering, *(Vol. 46): Elsevier Science; 1 edition (May 19, 1999).*

Sonmez, H., Ulusay, R.and Gokceoglu, C. (1998). A practical procedure for the back analysis of slope failures in closely jointed rock masses. *International Journal of Rock Mechanics and Mining Sciences, 35*(2), 219-233.

Tomas, R., Cuenca, A., Cano, M.,. (2012). A graphical approach for slope mass rating (SMR). *Engineering Geology journal, 124*, 67-76.

Trenouth, W. R.and Gharabaghi, B. (2016). Highway runoff quality models for the protection of environmentally sensitive areas. *Journal of Hydrology, 542*, 143-155.

Turan.A. (1990). Geology, stratigraphy and tectonic development of Hadim (Konya) and southwest of Taurus. *PhD. thesis published, Selcuk University, higher education board, documentation center. YÖK database,240 p.*

Turkish Journal of Engineering

Turkish Journal of Engineering (TUJE)
Vol. 4, Issue 1, pp. 17-22, January 2020
ISSN 2587-1366, Turkey
DOI: 10.31127/tuje.583975
Research Article

OPTIMAL DESIGN OF POWER TRANSFORMER TANK USING ANT/FIREFLY HYBRID HEURISTIC ALGORITHM

Mehmet Zile *[1]

[1] Mersin University, Erdemli Applied Technology and Business School, Department of Information Systems and Information Technology, Mersin, Turkey
ORCID ID 0000 – 0002 – 0457 – 2124
mehmetzile@yahoo.com

* Corresponding Author
Received: 28/06/2019 Accepted: 02/09/2019

ABSTRACT
Power transformers are one of the most important and expensive components of power transmission lines. Reducing costs in the manufacture of power transformers has always been the subject of science. In this study, an ant/firefly hybrid heuristic algorithm has been developed to optimize the materials used in power transformer tanks and therefore to reduce tank costs. Based on this algorithm, an interface program has been created in Visual Studio Program. Using this power transformer tank design computer program, the materials used in the tanks have been optimized. As a result of the optimization, the materials used in the transformer tank, which is designed as a result, are saved between 5% and 15%. By this study, it has become possible to reduce the manufacturing costs of power transformers.

Keywords: *Power Transformers, Transformers Tanks, Hybrid Heuristic Algorithm, Optimization*

1. INTRODUCTION

Transformers are electrical machines that convert electrical energy into voltages and currents at the same frequency but in one or more circuits with the principle of electromagnetic induction. Since power plants are located close to the source used, they are often located far from consumption centers. For this reason, electrical energy must be able to be transmitted to remote areas from where it is produced. The voltage value of the alternating current produced in the alternators in the power plants is between 0.4 kV and 35 kV. These low voltages must be increased by 15 kV, 34.5 kV, 66 kV, 154 kV and 380 kV in order to transmit them to remote consumption centers. Increasing the voltage value of the alternating current to these values and lowering the operating voltage of 220 and 380 volts in consumption centers are made with expensive transformers. Reducing production costs in these expensive transformers has always been the subject of science. In this study, a computer program has been developed by using hybrid heuristic algorithms in the design of transformer tanks which constitute an important part of transformer. Using this computer program, design optimization of power transformer tanks has been made.

2. POWER TRANSFORMER TANKS

The tank forms the outer frame of the transformer. Oil cooling is used to prevent heating of the core, coil and switch. Hence, it needs to be in a closed environment. A power transformer tank is shown in Fig. 1.

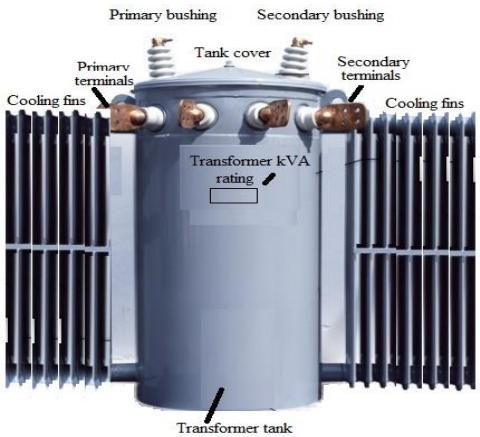

Fig. 1. Power transformer tank

This constitutes a closed environment tank. In order to prevent heating of iron sheets from conductive wires passing through the tank, the dimensions are determined by leaving distances between the active part and the sheet. Transformer tank can be of different shapes. It is a gated structure in which the electrical circuits pass through the tank and there is oil for cooling due to this electricity. Due to the presence of oil in the tank, it has a sealing feature. In addition, there are accessories such as bushing, expansion vessel, radiator on the tank. It also carries over supporting structures (Abi-Samra, 2009). In oil transformers, the iron body with the windings is placed in a container called a transformer tank. This container, made of sheet metal, is sealed in an oil-tight state. After the moisture is removed from the active part which is dried in the evacuated ovens, it is placed in the tank (Kothmann, 1995). Then, the tank is filled with the oil. Moisture must not get into the oil since the moisture reduces the insulation strength of the oil significantly. When the transformer container is slightly moistened, its puncture resistance value immediately drops to half. The dehumidified oil must be dried. The electrical puncture strength of the oil, ready for boiling according to standards and ready to be re-filled into the tank, shall not fall below 125 kV/cm (Moser, 1986).

The construction of the tank changes according to the size and shape of the transformer. Transformer tanks are manufactured as straight walled, curtain walled, corrugated walled, tubular and radiator from small to big powers (Moser, 1987). Transformer tanks with large forces, which are forced to be cooled, are also constructed as thick-walled, flat-walled. Oil tanks are made of 1 mm to 12 mm thick sheet metal according to the size and cooling type of the transformers. The cover and bottom parts of small and medium power transformers are generally made of 5 mm to 12 mm sheets. In transformers with large powers, the cover and bottom parts are made of 18 mm and 72 mm sheets. The thickness of the tank walls generally depends on the oil height. The flat sheet thickness is 3 mm at one meter height. Tank sheets are supported by various constructions in order not to use very thick sheets in higher walled flat tanks. Various reinforcement constructions are available to support tank sheets. The sheets forming the tank are generally welded together. The base plate is also welded to the side plates of the tank. The cover frame on the upper part of the tank is attached to the front and side wall sheets by making corner welding. The cover plate is either bolted to the cover frame or welded.

All transformer tanks are tested for leaks. Domes on the tank cover or sometimes on the side walls allow the bushings to be attached. Doms are generally circular. The diameters and heights of bushings vary according to the electrical stresses and forces. Dom and bushings are made to be mounted to the boiler. The flange is welded to the hole drilled in the lid to secure the dome to the tank. Radiators, oil-air and oil-water coolers are used for cooling the tanks. In radiator cooling, the radiator is generally mounted on the transformer. In cases where the number of radiators is too high to be placed on the transformer, it is made by placing on cooling benches separately from the transformer. The number of fans is determined according to the heat losses to be disposed of. It provides the circulation of oil in the radiators with pipes. These pipes are connected to the radiators from the top and bottom of the transformer. Here, the oil emerges from the top of the tank and passes through the radiators to cool down, and then the cooled oil re-enters the tank from the bottom. The pipes are placed in the region where the oil is the hottest and the transformer is cooled better. The oil expansion vessel is generally located on the top of the lid. Two pipes go from the expansion vessel to the boiler. One of them allows oil to flow from the tank to the other tank. The other pipe allows air to escape. There is an open hole in this expansion vessel to allow free expansion of the oil in case of sudden heating. This hole is bent downwards to prevent foreign objects from entering the oil.

In large transformers, buoys are placed in the container to prevent oxidation and moisture absorption of the oil in the expansion vessel by contact with air. Moisture absorbers are placed between the vent and the oil expansion vessel. In this way, the contact surface of the oil is reduced and moisture is removed .

3. ANT/FIREFLY HYBRID OPTIMIZATION ALGORITHM

The pheromones, which the ants actually use to find the shortest path, are a kind of chemical secretion that some animals use to influence other animals of their own species. As the ants move, they leave their pheromones that they have stored in the paths they have crossed (Dorigo, 2004). They prefer the path where pheromone is more likely to be the least. Its instinctive behavior explains how they find the shortest path to food, even if a pre-existing path is unavailable (Laptik, 2012). Considering that each ant leaves the same amount of pheromone at the same speed. It may take a little longer than the normal process if the ant recognizes the barrier and chooses the shortest path. Each ant takes a step-by-step decision-making policy starting from the source node and creates a solution to the problem. On each node, the local information is stored in the node itself or the arcs that exit from this node are read by the ant. The next step is to decide which node to use when going randomly (Laptik, 2017). Natural behavior of ants is given in Fig. 2.

Fig. 2. Natural behavior of ants

An ant hits the node from the node until it reaches the destination node, completes its forward movement and goes back to the motion mode. The optimization potentials through the behavior of ants colony and during the analysis has been realized that the ants are able to find the shortest path to reach the food from the nest that can be used in solving complex problems. Fireflies usually emit a flashing light at short intervals. The flashing rhythm of this light is part of the signaling system that enables fireflies to meet and distinguish fireflies from other light-scattering insects. The speed, frequency and the time before fireflies respond to each other have special meanings. The optimization method developed based on this logic that determines the survival patterns of fireflies is called the firefly algorithm. Population-based heuristic algorithms are selected to optimize multiple model functions. Natural behavior of fireflies is given in Fig. 3.

Fig. 3. Natural behavior of fireflies

Firefly herd optimization method has been developed by observing and imitating the social behaviors of fireflies. The main purpose of using this method is to capture all local maxima. In multi-model function optimization problems, the most important difference between firefly herd optimization and previous approaches is the dynamic decision area used by the individuals in the herd who efficiently place multiple peaks (Yang, 2009). Each individual in the herd uses the decision-making area to select his neighbors and determines his movement through the signal strength he receives from his neighbors (Yang, 2012). Meta heuristics studies have made possible improving of optimization techniques that have the aim of providing top quality solutions to complex systems. In the generated hybrid algorithm, mathematical modeling of ant and firefly colony behavior was performed. This method has been used to solve the continuous and discontinuous problems in the design of power transformer tank, mimicking the natural behavior of ants and fireflies. Hybrid optimization of generated ants and fireflies; It is a hybrid optimization technique which is used as a result of monitoring the paths used by ants and evaluating the light intensity of fireflies.

4. OPTIMAL DESIGN OF POWER TRANSFORMER TANKS USING HEURİSTİC ALGORITHMS

Power transformer tanks design algorithm improved is shown in Fig. 4. The basic steps of the algorithm are as follows:

Step 1. Enter the number of experiments, the maximum number of generations and the number of the population (N).

Step 2. Enter; tank internal length, tank internal width, surface pressure, cover sheet material type, base sheet material type, active part weight, oil level height, reinforcement sheet length, effective areas, forces, force branches, wall sheet thickness, maximum reinforcement height, boiler vacuum value, reinforcement shape, type of reinforcement material.

Step 3. Determine the tank model.

Step 4. Enter primary voltage, secondary voltage, number of primary winding, number of secondary winding.

Step 5. Generate N chromosomes for the initial population.

Step 6. Set total number of bars, number of rows, number of columns, depth of network embedding.

Step 7. Calculate suitability for each solution.

Step 8. If the maximum number of generations is reached, identify and store the chromosome that is the best fit in the experiment.

Step 9. Increase the number of experiments if maximum number of generations is reached, but maximum number of experiments is not reached.

Step 10. Start the experiment again.

Step 11. If the maximum number of generations is not reached, go to step 5.

Step 12. Go to Step 18 if both the maximum generation number and the maximum number of experiments are reached.

Step 13. Divide the N number of chromosomes into binary groups and cross.

Step 14. Apply mutation to N chromosomes.

Step 15. Select the best N number of chromosomes for the next generation from the chromosomes obtained by N number of chromosomes and N number of mutations.

Step 16. Increase the number of generation by 1 and go to Step 5.

Step 17. Calculate transformer tank parameters of the 3N number of chromosomes.

Step 18. Identify the best chromosome.

Step 19. Calculate the average of the best chromosome of each experiment.

Step 20. View results; cover sheet thickness, cover plate length, cover plate width, base sheet thickness, forcing the base plate, base sheet deflection, bearing forces, wall plate thickness, reinforcement thickness, reinforcement height, reinforcement top sheet thickness, reinforcement top sheet width, strength moments, reinforcement cross section, reinforcement weight.

Power transformer tank design program interface improved is shown in Fig. 5.

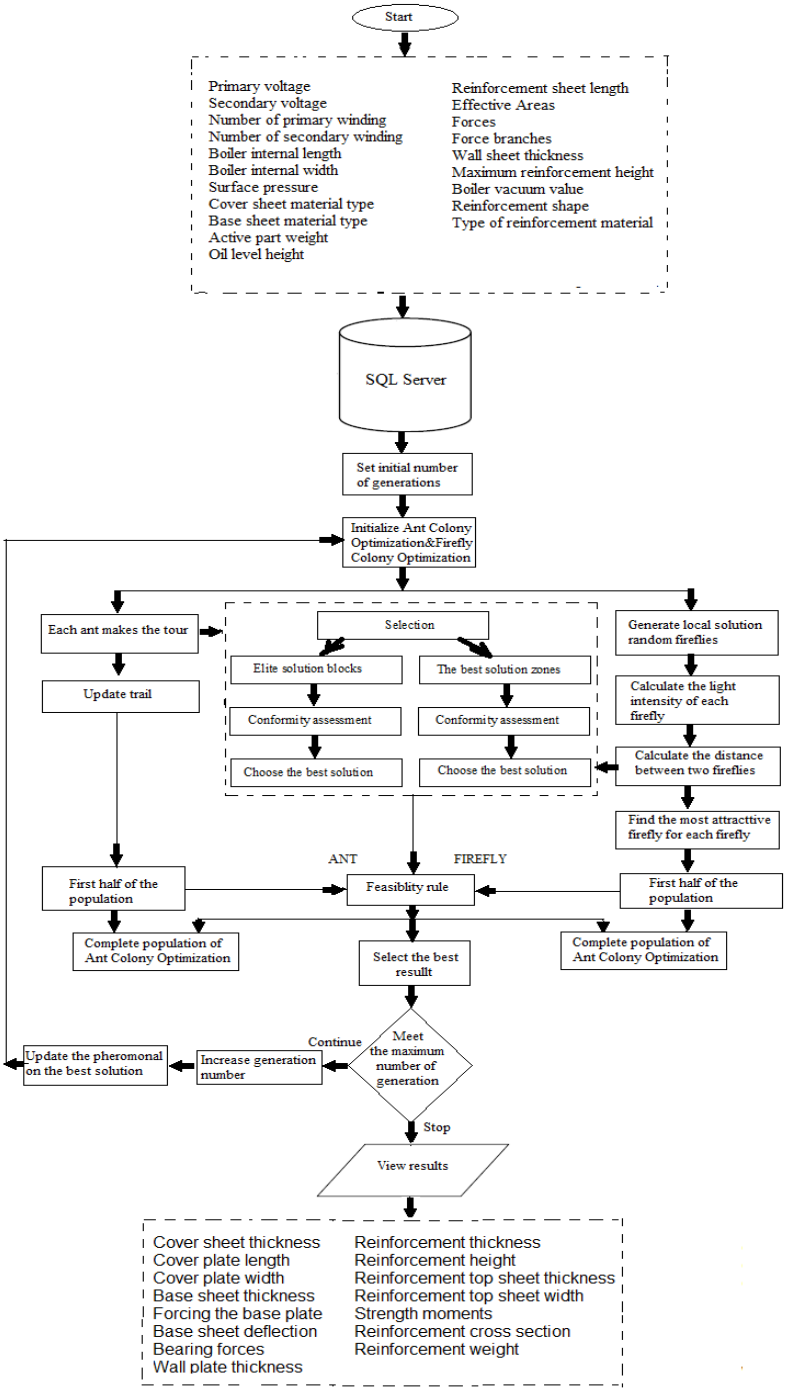

Fig. 4. Power transformer tank design algorithm improved

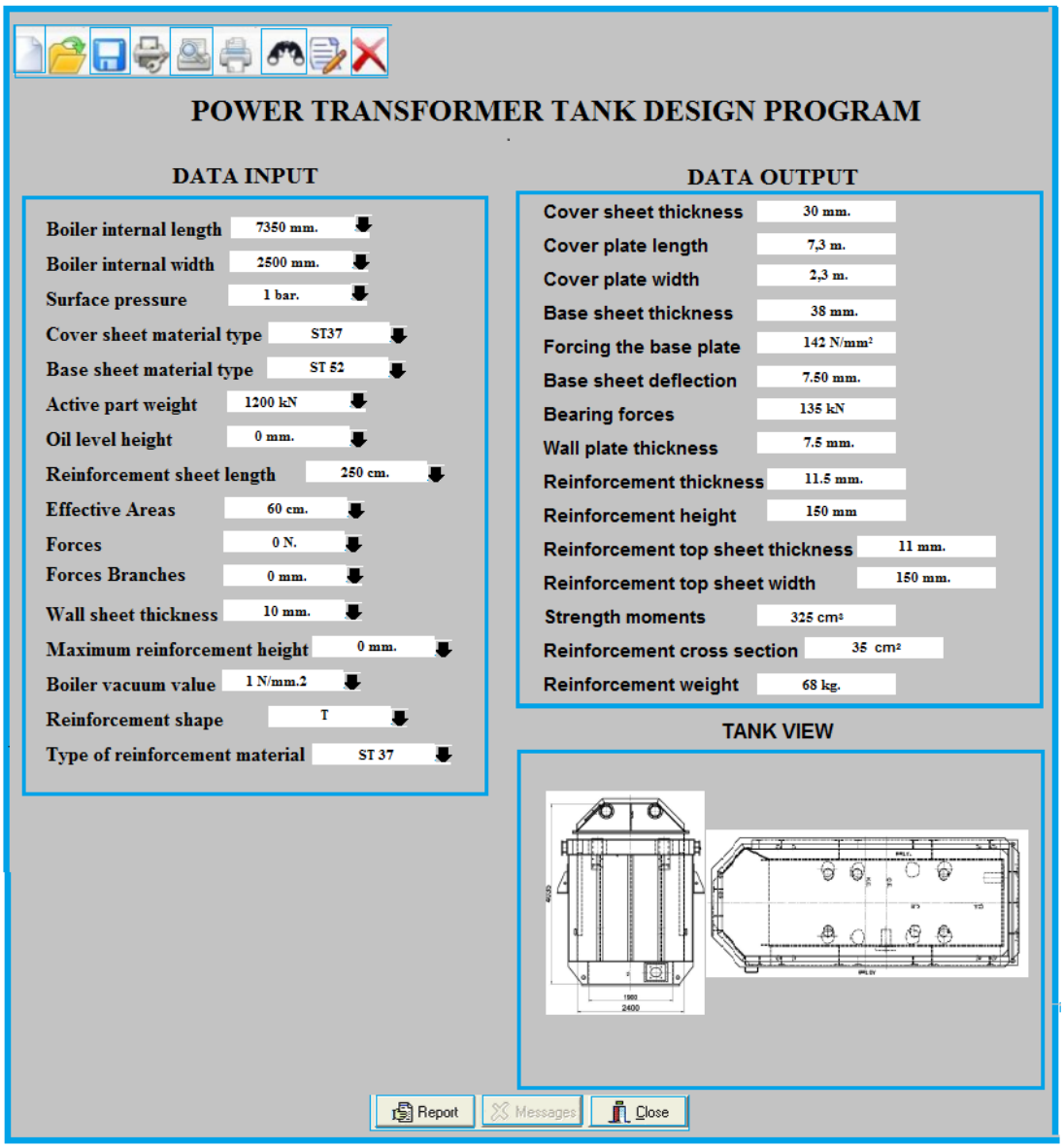

Fig. 5. Power transformer tanks design program interface improved

The variables of power transformer tank design optimization are given in Table 1.

Table 1. Optimization of variables for power transformer tank design

Transformer Tank's Detail	No-opt.	Opt.
Cover sheet thickness (mm.)	32	30
Cover plate length (m.)	7,5	7,3
Cover plate width (m.)	2,5	2,3
Base sheet thickness (mm.)	40	38
Forcing the base plate (N/mm^2)	144	142
Base sheet deflection (mm.)	7.70	7.50
Bearing forces (kN)	140	135
Wall plate thickness (mm.)	9	7.5
Reinforcement thickness (mm.)	13	11.5
Reinforcement height (mm.)	162	150
Reinforce top sheet thickness (mm.)	14	11
Reinforcement top sheet width (mm.)	162	150
Strength moments (cm^3)	340	325
Reinforcement cross section (cm^2)	38	35
Reinforcement weight (kg.)	72	68

In the conventional method design, the thickness of the transformer tank cover is 32 mm. In the generated optimization, it is understood that 2 mm of the cover thickness is unnecessary. In the design, the transformer tank cover plate length is 7.3 m. In the optimization, it is understood that 20 mm of the cover plate length is unnecessary. In the design, the transformer cover plate width tank cover plate length is 2.5 m. In the optimization, it is understood that 20 cm of the cover plate width is unnecessary. In the design, the thickness of the transformer tank base plate is 40 mm. In the optimization, it is understood that 2 mm of the base sheet thickness is unnecessary. In the design, the transformer tank wall plate thickness is 9 mm. In the optimization, it is understood that 1,5 mm of the wall plate thickness is unnecessary. In the design, the thickness of the transformer tank reinforcement is 13 mm. In the optimization, it is understood that 1,5 mm of the reinforcing thickness is unnecessary. In the design, the transformer tank reinforcement height is 162 mm. In

the optimization, it is understood that 12 mm of the reinforcement height is unnecessary. In the design, the thickness of the top layer of the transformer tank reinforcement is 14 mm. In the optimization, it is understood that 3 mm of the reinforcing top layer thickness is unnecessary. In the design, the top layer width of the transformer tank reinforcement is 162 mm. In the optimization, it is understood that 12 mm of the width of the reinforcing top sheet is unnecessary. In the design, the transformer tank reinforcement weight is 72 kg. In the optimization, it is understood that 4 kg of the tank reinforcement weight is unnecessary. By this study, it has been possible to optimize the material used in the production of transformer tanks.

5. CONCLUSION

There is no power transformer boiler design by using hybrid heuristic algorithms in the literature. In this study, it is aimed to present a conscious engineering approach to transformer boiler production which is designed and manufactured according to the experiences accumulated over the years. For this purpose, extensive material analyzes have been performed to identify the materials used in boiler manufacturing. The structure of the power transformer tank has been examined in detail. A firefly/firefly heuristic algorithm has been developed to optimize the materials used here. Power transformer tank design program interface has been created in Visual Studio by using this improved algorithm. In this optimization, wall sheet thickness, reinforcement thickness, base plate thickness, base plate strength, base plate deflection, bearing forces, wall plate thickness, reinforcement height, reinforcement top layer width, strength moments, reinforcement section and reinforcement weight have been changed. The best optimum design has been made considering the tensile and yield strength of the materials used in the analysis of power transformer tanks. As it is understood from the values obtained, the materials used in transformer tank are saved from 5% to 15%. By this study, it has become possible to provide a reduction in the cost of transformer tank production. Thus, manufacturing documentation of the power transformer tank whose optimization has been completed in the simulation environment can be prepared and realized.

REFERENCES

Abi-Samra, N., Artega, J., Daravny, B. and Foata, M., **"**Tank Rupture and Mitigation-A Summary of Current State of Practice and Knowledge", *IEEE Transactions on Power Delivery*, pp. 1959-1967, 2009.

Dorigo, M., Stutzle, T., "Ant Colony Optimization'', *The MIT Press*, pp 33-41, 2004.

Kothmann R.E., Thompson D.G., "Power transformer tank rupture risk assessment and mitigation" *EPRI Rep. TR-104994*, 1995.

Laptik, R., "Ant System with Distributed Values of Pheromone Evaporation", *Elektronika Ir Elektrotechnika*, Vol. 18, No.8, pp. 69-72, 2012.

Laptik R., Navakauskas D., "Application of Ant Colony Optimization for Image Segmentation'', *Elektronika Ir Elektrotechnika*, Vol. 80, No.8, pp. 13-18, 2017.

Moser H.P., Dahinden V., Transformerboard I, *Rapperswil*, 1986.

Moser H.P., Dahinden V., Transformerboard II, *Rapperswil*, 1987.

Yang, X.S., ''*Firefly Algorithms for Multimodal Optimization*'', Stochastic Algorithms: Foundations and Applications, SAGA 2009, Lecture Notes in Computer Science, 5792. Berlin: Springer Verlag, pp. 169–178, 2009.

Yang, X. S., ''Multiobjective Firefly Algorithm For Continuous Optimization'', *Engineering with Computers*, Online Fist, DOI: 10.1007/s00366-012-0254-1., 2012.

Turkish Journal of Engineering

Turkish Journal of Engineering (TUJE)
Vol. 4, Issue 1, pp. 23-29, January 2020
ISSN 2587-1366, Turkey
DOI: 10.31127/tuje.568965
Research Article

THE INVESTIGATION OF NANOMATERIALS IN TERM OF HUMAN HEALTH

Lezgin Kaya [1], Memduh Kara *[2] and Bahadır Sayıncı [3]

[1] Mersin Univerity, Faculty of Engineering, Mechanical Engineering, Mersin,Turkey
ORCID ID 0000 – 0002 – 4498 – 1387
lezginkaya24@gmail.com

[2] Mersin Univerity, Faculty of Engineering, Mechanical Engineering, Mersin,Turkey
ORCID ID 0000 – 0002 – 5201 – 5453
memduhkara@mersin.edu.tr

[3] Mersin Univerity, Faculty of Engineering, Mechanical Engineering, Mersin,Turkey
ORCID ID 0000 – 0001 – 7148 – 0855
bsayinci@mersin.edu.tr

* Corresponding Author
Received: 22/05/2019 Accepted: 06/09/2019

ABSTRACT
Nanotechnology is one of today's most popular research areas. The reason for this is that, thanks to this technology, production can be much better and much smaller. Investments in this technology increase each year and it is predicted that the increase will continue. The fact that more nanomaterials are in our lives has become a necessity for further research into this technology. Many studies have been done on nanomaterials for a long time, but most of them are those that highlight the positive aspects of nanomaterials on humans. Until a few years ago, studies on the negative effects of nanomaterials on living things, especially humans, are insufficient. In recent years, increasing use of nanomaterials necessitated the examination of the effect on human health. As a result of research, some nanomaterials have been determined to have negative effects on human health. These materials are especially risky for workers during production. People and institutions working with nanomaterials need to take some security measures. These measures should be determined according to the properties of nanomaterials. Taking the necessary precautions reduces the possibility of exposure. The negative effects of nanomaterials on human health are still being investigated. However, thanks to its superior features, its popularity is rapidly increasing and it is expected to continue to increase.

Keywords: *Nanotechnology, Nanomaterials, Occupational Health and Safety, Ergonomics*

1. INTRODUCTION

Nanotechnology; it is the technology where the substances are examined by going down to 1-100 nm dimensions and the information obtained as a result of these investigations are used for applications in various fields (Ramsden, 2011; Allhoff *et al.*, 2010). Nanotechnology has an impact on human life on a large scale. This change is clearly seen through many years of work. For example; mobile phones used today have been thought many years ago. However,due to technological deficiencies at that time, if they were to be produced, their size would have reached a building size (Ramden, 2011). The effect of technology on the dimensions of products can be clearly understood by this example. This is the most remarkable innovation of nanotechnology.

Nanotechnology addresses many different areas and continues to innovate in areas. Solar creams that do not emit ultraviolet light through nanotechnology, lighter and more robust tennis rackets, self-cleaning glass production (Ramden, 2011), along with some other technologies (ultrasonic, HC) to be successful in removing waste water (Beth *et al.*, 2018), increasing shelf life of foods by using nanomaterials in the food industry (Gokkur *et al.*, 2012). Such developments add quality to our lives but do not have the effect of changing our lives completely. Intensive studies are being carried out on developments that can be considered a revolution in nanotechnology.Wars can cause great changes on earth. Countries are investing in a lot of money to be successful in the wars which are extremely important for them.Nanotechnology can be very effective in the military because it provides more efficient and light products. In 2002, the United States established a research center called the Military Institute of Nanotechnology at the Massachusetts Institute of technology. (Allhoff *et al.*, 2010) the task of this research center is to make innovations that will increase the productivity of the soldiers at the time of the operation. A soldier weighs 45.it carries equipment and moving with this weight for a long time can cause soldiers to get tired early and decrease their productivity.Equipment produced using nanotechnology is much lighter. Only for this reason nanotechnology can be used for military purposes. But nanotechnology will not only bring lightweight on soldiers, it will have the potential to do innovations that will affect the course of the war. Superior products, for example, such as self-administered bullets, nano-sized robots that can disrupt electrical or chemical systems in a region, can play a major role in determining the end of the war (Allhoff *et al.*, 2010).

Nanotechnology is clearly known to bring benefits and innovations in many areas. However, the use of nanomaterials involves some risks and problems. In this study, the risks and precautions to be taken in the use of nanomaterials were investigated.

2. THE EFFECTS OF NANOMATERIALS ON HUMAN HEALTH

With the development of technology, new materials have been produced and used. Thanks to these materials, many new and superior products can be produced. However, changing materials can also cause some health problems. Besides many superior properties of nanomaterials, it can cause serious health problems especially if precautions are not taken (Buzea *et al.*, 2007; Esmaeillou *et al.*, 2012; Geraci *et al.*, 2015; Kuhlbusch *et al.*, 2018; Li *et al.*, 2018; Liu *et al.*, 2012; Mala *et al.*, 2018; Naqvi *et al.*, 2018; Pietroiusti *et al.*, 2018; Schulte *et al.*, 2008; Zalk *et al.*, 2009).

As a result of the research, there are more than 1600 Nano-active products today. By 2020, 6 million workers will be exposed to the ever-increasing nanomaterials (Li *et al.*, 2018). Fig. 1. shows the changes in nanotechnology investments over the years. As shown in Fig. 1., the investment in nanotechnology is expected to increase over the years and will continue to increase. For this reason, as time goes on, the risks of nanomaterials on human health will increase.

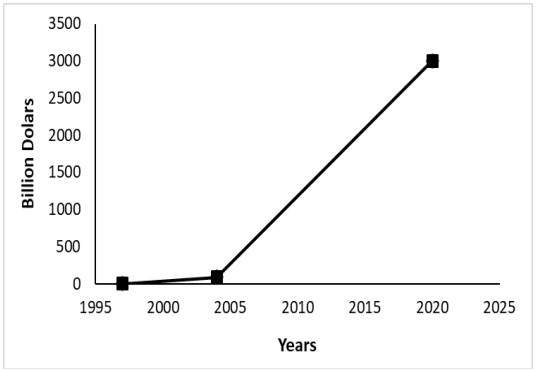

Fig. 1. Changes in Investments for Nanotechnology by Years (Esmaeillou *et al.*, 2012).

Studies to examine the effects of nanomaterials on human health are basically two types; in vitro (in laboratory) and in vivo (in living organisms). Studies conducted in vitro laboratory environment.The advantage is that getting quick results and low cost.It is also an ethically more appropriate method because there are no applications on living things. Some experiments that can be carried out include the polyphase test, the apoptosis test, the necrosis test, the oxidative stress test and DNA damage tests (Kumar *et al.*, 2017). In vivo is usually done on animals such as rats or mice. Nanoparticles in dead or alive organisms are determined by radio labels. The in vivo method also determines the level of toxicity of the nanoparticle by examining the organisms exposed to the nanoparticles. Histopathology of living organs, cells or tissues is used after exposure (Kumar *et al.*, 2017).

As a result of researches, nano-sized particles are observed to pose more risk to human health than macro-sized particles. Nano-sized particles damage the lungs through respiration. At the same time, these particles can easily penetrate the circulatory system and reach the nervous system and the brain (Ozdemir *et al.*, 2015; Unver, 2016). The effect of nanoparticles on human health has been shown to depend on particle size. For example, if the size of particles taken from the lungs is less than 100 Nm, they can reach the alveoli in our blood vessels (Köksal *et al.*, 2014). As mentioned, the particle size has a significant impact on human health. According to particle size, the accumulation areas in the human body (especially the respiratory system) are also different. Fig. 2. shows the accumulation zones of materials in the respiratory system according to particle size.

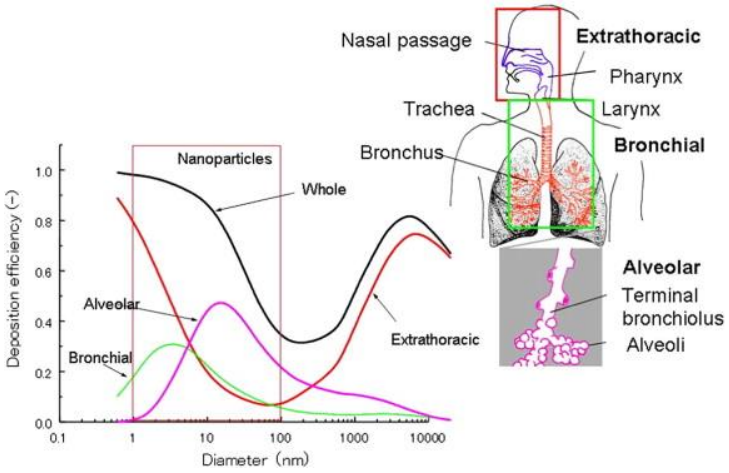

Fig. 2. Accumulation zones in respiratory system according to particle size (Geraci *et al.*, 2015)

Many animals and plants were used to investigate the damage of nanoparticles. For example, the effect of titanium dioxide nanoparticles on water flea ,the effect of silver nanoparticles on water lentils,the effect of zinc oxide nanoparticles on mussels, the effect of zinc oxide nanoparticles on offspring carp, as a result of many researches have shown that nanoparticles pose a risk for plants and animals. In light of these studies, the first study to determine the negative effects of nanoparticles on human health was carried out in 2009 (Özdemir, 2015).

In cases where nanoparticles are small enough, they can easily enter the cell and bind to DNA and cause some genetic damage. Especially silver, aluminum oxide, titanium dioxide, iron oxide, zinc oxide, such as nanoparticles can lead to DNA damage has been determined (Santos *et al.*, 2013; Collins *et al.*, 2017; Dogan *et al.*, 2018; Esmaeillou *et al.*, 2012, Akyol *et al.*, 2018; Sekeroglu, 2013).

2.1. Exposure Routes of Nanomaterials

Nanoparticles can enter the human body and cause some health problems when certain conditions are met. Nanoparticles can enter the human body through respiration, through skin and through digestion. Nanomaterials, which are extremely small and light, enter the human body by breathing the most. The nanoparticles that enter our body by inhalation can reach other organs by the circulatory system except the lung and brain. Nanoparticles entering the body through the digestive tract can reach the stomach and intestinal tract and from there with blood to other organs of the body. If the nanoparticles enter the body via the skin, they can be mixed into the lymph system (Unver, 2016). The ways in which nanoparticles enter the human body are shown in Fig. 3. As can be seen in Fig. 3., the nanoparticles can spread through the body after entering certain ways into the human body.

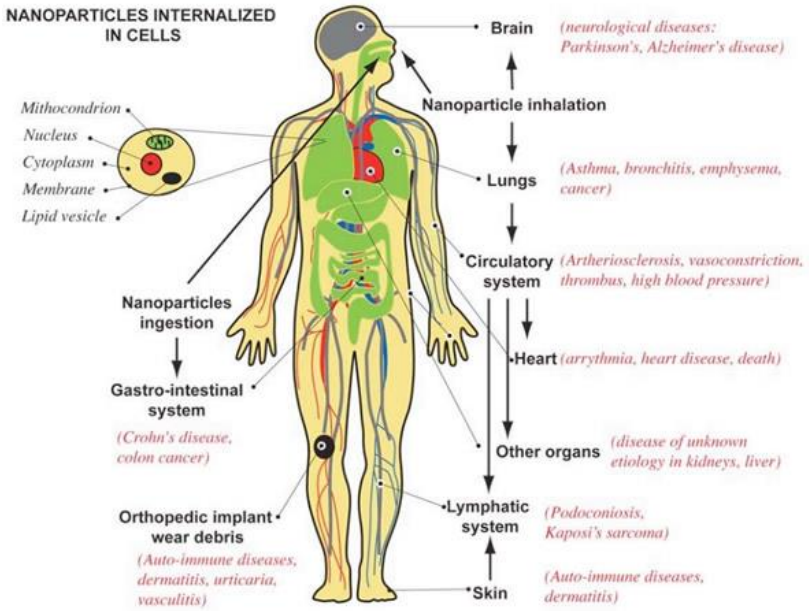

Fig. 3. Schematic representation of the ways nanoparticles enter the human body (Buzea *et al.*, 2007)

2.2. Determination of Exposure

The popularity of nanomaterials is increasing due to many extraordinary properties. As shown in Fig. 1., investments have increased from year to year and are expected to increase further. In addition to the many advantages of nanomaterials, it is known that they have characteristics that may pose a risk to humans and the environment. People interact intensively during the use and production of these materials. In particular, people who work in the production of nanomaterials are at greater risk of exposure. Nanomaterials are also important in the size, amount and in which way they enter the human body. Knowing the nanoparticle size and amount is important for the precautions to be taken and the procedures to be applied after exposure. For this reason, many devices have been produced to determine the exposure risks of people in working environments. These devices can determine the amount and size of nanoparticles in the environment (Naqvi *et al.*, 2018; Pietroiusti *et al.*, 2018). Fig. 4. shows the CPC device;

Fig. 4. CPC device (Babaarslan, 2014)

The CPC (Condensation Particle Counter) device serves to determine the number of particles. The operating principle of the device is based on the counting of droplets formed by the concentration of alcohol vapor and the optical detector. The device capacity is 1-1000 nm and is better than other similar devices if operated in single particle mode (Kuhlbusch *et al.*, 2018). Fig. 5. shows the mini-disk device. The main task of this device determines the amount of nanoparticles. It also measures the average diameter and surface areas of nanoparticles. These features differ from CPC. It is a simple and convenient device that is easy to use and does not work with an extra resource.

Fig. 5. CPC device (Babaarslan,2014)

The OPC (optical Particle counter) shown in Fig.6. is a different device used to determine the number of particles. OPC measuring range 200nm - 20μm (Kuhlbusch *et al.*, 2018).

Fig. 6 . OPC device (Babaarslan, 2014)

Fig. 7 shows SMPs (Scanning mobility Particle sizer). The task of the SMPs device is to determine the size distribution of particles.Although many devices are available in this function, it is the most widely used SMPs device (Babaarslan, 2014). SMPs device capacity is 1-1000mn. Although such devices have been developed for years, there are still some deficiencies and studies are continuing (Kuhlbusch *et al.*, 2018). The disadvantage of the SMPs device is that it is slow. It also performs different scans for each different dimension (Babaarslan, 2014).

Fig. 7. SMPs device(Babaarslan,2014)

Fig. 8. shows the SEM (Scanning Electron microscopy). SEM is based mainly on the study of the interaction of electrons from an electron source with the material to be studied. Some electrons come out of interaction with the material to be studied. These are secondary electrons and backscatter electrons. The secondary electron is the result of the collision of the incoming electron with the material to be studied. This electron occurs at a depth of about 10 nm.The secondary electrons that occur are collected and applied to obtain the surface image. Another type of electron is the scattering electron, which comes more deeply (at about 300nm depth) than the secondary electron.It also has higher energy than the secondary electrons. In addition to these, X rays occur as a result of another interaction between the electron and the material. X rays contain high energy and influence from the surface of the material to 1000 nm depth (Babaarslan, 2014). SEM devices achieve very precise results, and these results depend on the imaging capacity of the device. In general, their capacity is 0.1 nm-1 mm (Kuhlbusch *et al.*, 2018).

Fig. 8. SEM device (Reddy *et al.*, 2017)

3. RISK ASSESSMENT

Persons working with nanomaterials are at risk and should be decided how to take measures. Devices such as CPC, OPC, SMPS, SEM are used to determine the size and quantity of nanoparticles in the environment. Although these devices provide information about the size and quantity of nanoparticles, they do not provide information about the sources and chemical composition of nanoparticles (Pietroiusti *et al.*, 2018). Therefore, the presence of devices does not eliminate the risk in the environment while providing information about measures to be taken.

To assess the risk of the working environment, measurement can be carried out with the devices used to determine the exposure of workers in respiratory zones and in the environment. When the two measurements are compared, it can be interpreted that the workers are exposed to nanoparticles if the concentration of nanoparticles in the respiratory zone is greater (Pietroiusti *et al.*, 2018).

As result of the processes, information about the nanoparticles is obtained. Thus, the risk level and exposure are determined. However, in some cases, sufficient information cannot be obtained about the characteristics of nanoparticles in the environment. In these cases, other methods must be applied. Although there are multiple methods,the most reliable is the control banding method (Babaarslan, 2014). In this method, some properties are determined as the force parameter and some coefficients are assigned to these properties.In addition to these parameters, some probability factors have been determined and coefficients have been assigned to these parameters. The risk matrix is formed by collecting the coefficients of these two different parameters. The risk level is determined by means of charts from this risk matrix (the second parameter value corresponding to the first parameter is read) (Zalk *et al.*, 2009).

There are some important problems when making a risk assessment. For example, there are some situations that need to be taken into account in the control banding method. This is a matrix method used in this method. In matrix methods, some values are assigned in case an event or situation occurs. Therefore, the degree of violence is determined as a result of these acceptances. However, there are some uncertainties when determining the degree of intensity. In these cases, what to do should be considered and included in the evaluation. Calculations should be made based on the worst case that may occur in unknown uncertainties.So the Unknown should be considered the highest danger.

The risk assessment parameters in the control layers method are intensity and probability (Unver, 2016). Density factor score is mostly (70%) in nanomaterials and the rest is the main material. Intensity factors; particle shape of nanomaterials, surface chemistry of nanomaterials, solubility of nanomaterials, particle diameter of nanomaterials, the cancer-causing condition of the nanomaterials, effect of nanomaterials on reproduction system, effect of nanomaterials on dermal, the risk status of the main material (toxicity), the cancer-causing condition of the main material, the negative effect of the main material on the reproductive system, the muatajenlik of the main material, the dermal effect of the main material, the negative effect of the main material on asthma (causing asthma or worsening the situation) is determined. Another parameter the probability parameter, is the amount of nanomaterials used during the process (a suitable estimation should be obtained if coulnd't a precise result is obtained), the working environment is dusty, foggy or in a condition that makes breathing difficult, the number of people working in the environment that is thought to be exposed, working time factors.

3.1. Determination and implementation of measures

Considering the characteristics of nanomaterials, the precautions to be taken against the risks that may occur should differ according to other materials. During the production of nanomaterials, significant problems can occur in the aspect of employees. The procedures to be applied as a result of the risk assessments and measures to be taken are determined. Before making a risk assessment in a place where nanomaterials are produced, a pre-hazard analysis should be established to make the risk assessment more healthy (Unver, 2016). In the context of pre-hazard analysis,an analysis should be made on the subjects such as materials to be used during production,production methods,devices used ,workers having sufficient equipment related to the work, whether the company doing the job is sufficient in the work, ventilation system adequacy, material production being made by automatic or direct workers. It will be much easier to make a risk assessment in light of the information obtained as a result of this analysis. Fig. 9. shows the the hierarchy of control measures;

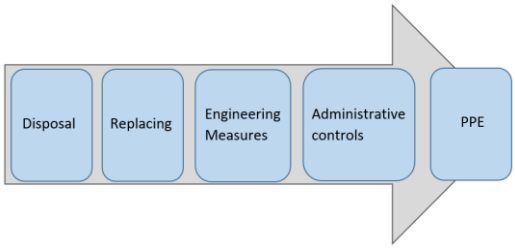

Fig. 9. Control Measures Hierarchy (Unver, 2016)

Control measures vary depending on the type of nanomaterials or process. For this reason, control measures can be examined under five headings. These titles are presented below.

Disposal: Disposal is the first and easiest method. It is to eliminate or reduce the amount of nanomaterials seen at risk. After the production starts, the demolition process can cause some problems. Therefore, it is the first step before the start of the process.

Replacing risky material with another material that is less risky or has no risk at all: The aim of this phase is to change the risky materials to a less risky or non-risky situation. For example, a volatile chemical is replaced with another non-volatile chemical. Thus, it is prevented from mixing the harmful chemical into the air and breathing of the employees.

Improvement of the process: The main purpose of this method with engineering measures is to protect employees from environmental hazards with engineering solutions. Expensive in the short run but cost-effective in the long run (Unver, 2016). For example, in a working environment where ventilation is inadequate, the protection of workers from the air known to be at risk with personal protective equipment (PPE) may seem less costly than the installation of an engineering solution ventilation system. But in the long run, process improvement creates a less costly situation. In addition, it can offer a more effective solution than PPE (Schulte *et al.*, 2008).

Administrative improvements: The aim of this method is to raise awareness about risky situations of employees and managers exposed to nanomaterials. In cases where engineering measures are inadequate, this method is applied. In this method, changes are made to allow workers to be exposed to less (change of working schedule, training and work rotation).

Personal protective equipment use: The use of personal protective equipment (PPE) is at the end of the step of measures that can be taken. In cases where all other methods are inadequate , equipment such as gloves, masks, protective clothing is used to prevent nanoparticles from entering the body (Schulte *et al.*, 2008). The very small nanoparticles can easily enter the human body through the skin. In order to prevent this,polyethylene gloves were found to be more resistant than cotton and polyester gloves (Unver, 2016).

Cotton aprons used in laboratories cannot provide effective protection against nanoparticles. Therefore, it is recommended that workers working with nanomaterials use aprons containing polyethylene instead of these aprons.

The presence of ventilation system is extremely important in the environment where nanomaterials are produced. HEPA filters should be used in ventilation systems. (Pui *et al.*, 2007). In the absence of ventilation system, selection of respiratory protector is important. Respiratory protector should be fully seated on the face first and there should not be any gaps.

4. CONCLUSION

It is known that nanomaterials have many superior properties and their use is increasing rapidly.But as a result of the studies, these materials which have superior properties can also have some effects on human health. Some nanomaterials have toxic properties. For this reason, it is inevitable that people working in production facilities are exposed to nanomaterials that show this toxic property. Very small nanoparticles can easily enter the human body and cause serious disturbances. Therefore, it is not enough to apply ordinary work safety rules during material production. Environmental conditions and persons with the necessary equipment are important in the Prevention of exposure. Nanomaterials will continue to improve the quality of life with superior features, if the necessary rules are clearly formulated and implemented.

REFERENCES

Akyol, M., Hayta, S. B. (2018). "Nanoteknolojinin dermatoloji alanında kullanımı" *Güncel Dermatoloji Dergisi*, Vol.3, No.2, pp. 44-55.

Allhoff, F., Lin, P., Moore, D. (2010). Nanoteknoloji nedir ve neden önemlidir?, *Tübitak popüler bilim kitapları*, Ankara, Turkey

Babaarslan, E. (2014). Mühendislik ürünü nanomalzemelerin güvenli üretiminin değerlendirilmesi, iş sağlığı ve uzmanlığı tezi, Çalışma ve sosyal güvenlik bakanlığı iş sağlığı ve güvenliği genel müdürlüğü, Ankara, Türkiye

Bethi, B., Sonawane, S., H., (2018). "*Nanomaterials and Its Application for Clean Environment"*. Nanomaterials for Green Energy, Bhanvase, B. A., Pawade, V. B., Dhoble, S. J., Sonawane, S. H., Ashokkumar, M.,Elsevier, Telangana State, India, pp. 385-409.

Buzea, C., Pacheco, I., I., Robbie, K. (2007) "Nanomaterials and nanoparticles: Sources and toxicity." *Biointer Phase*,Vol.2, No.4, pp.18-65.

Collins, A., Yamani, N., E., Dusinska, M. (2017). "Sensitive detection of DNA oxidation damage induced by nanomaterials" *Free Radical Biology and Medicine*, Vol. 107, pp. 69-76.

Dogan, B., T., Uslu, B., Ozkan, S., A., (2018). "*Detection of DNA damage induced by nanomaterials*" Nanoscale Fabrication, Optimization, Scale-Up and Biological Aspects of Pharmaceutical Nanotechnology, Grumezescu, A. M.,Elsevier, Ankara, Turkey, pp. 547-577.

Esmaeillou, M., Moharamnejad, M., Hsankhani, R., (2013). "Toxicity of ZnO nanoparticles in healthy adult mice." *Enviromental Toxicology and Pharmacology*, Vol.35, No.1, pp.67-71.

Geraci, C., Sayes, C., Schulte, P.,Heidel, D., Hodsan, L., Eastlake, A., Brenner, Sara. (2015) "Perspectives on the design of safer nanomaterials and manufacturing processes." *Journal of Nanoparticle Research*, Vol. 7, No. 9, pp. 13.

Gokkurt, T., Findık, F., Unal, H., Mimaroglu, A. (2012) "Extension in Shelf Life of Fresh Food Using Nanomaterials Food Packages" Polymer-Plastics Technology and Engineering, Vol.51, No.7., pp.701-706.
Köksal. F., Köseoğlu, R. (2014). *Nanobilim ve Nanoteknoloji*, Nobel Yayınları, Ankara, Turkey

Kuhlbusch, T., A., J., Wijnhoven S., W., P., Haase, A. (2018) "Nanomaterial exposures for worker, consumer and the general public." *NanoImpact*, Vol.10, pp. 11-25.

Kumar, V., Sharma, N., Maitra, S. S. (2017). "In vitro and in vivo toxicity assessment of nanoparticles." *International Nano Letters*, Vol. 7, No. 4, pp. 243-256.

Li, Z., Cong, H., Yan, Z., Liu, A.,Yu, B. (2018). "*The Potential Human Health and Environmental Issues of Nanomaterials.*" Handbook of Nanomaterials for Industrial Applications, Hussain, C. M., Elsevier, Qingdao, China, pp. 1049- 1054.

Liu, X., Tang, K., Harper, S., Harper, B., Steevens, J., A., Xu, R. (2018) "*Predictive Modeling of Nanomaterial Biological Effects*". Handbook of Nanomaterials for Industrial Aplication, Hussain, C., M., Elsevier, Nj, United States, pp. 1049-1054.

Mala, R., Celsia, R. (2018) "*Toxicity of nanomaterials to biomedical applications*". Fundamental Biomaterials: Ceramics, Thomas, S., Balakrishnan. P., Sreekala, M., S., Woodhead Publishing, Kalady, India, pp. 440-473.

Naqvi, S., Gopinath, P., Kumar, V., (2018) "*Nanomaterial Toxicity: A Challenge to End User*". Applications of Nanomaterials, Bhagyaraj ,M., S., Oluwafemi, S., O., Kalarikkal, N., Thomas, S.,Woodhead Publishing, Rooker, India, pp. 315-343.

Özdemir, L., Gök Metin, Z. (2015). "Nanoteknolojinin sağlık alanında kullanımı ve hemşirenin sorumlulukları." *Anadolu Hemşirelik ve Sağlık Bilimleri Dergisi*, Vol. 18, No. 3, pp. 235-244.

Pietroiusti, A., Juvala, H. S., Lucaroni, F., Savolainen, K. (2017). "Nanomaterial exposure, toxicity, and impact on human health" *Nanomedicine and Nanobiotechnology*, Vol. 10, No. 5, pp. 1-21.

Pui, D. Y. H., Kim, S. C. Harrington, M. S. (2006). "Experimental study of nanoparticles penetration through commercial filter media" *Journal of Nanoparticle Research*, Vol. 9, No. 1, pp. 117-125.

Ramsden, J. (2011). *Nanoteknolojinin Esasları*, ODTÜ Yayıncılık, Ankara,Turkiye.

Reddy, G. V., Akula, S., Malgikar, S., Babu, P. R., Reddy, G. J., Josephin, J. J. (2017). "Comparative scanning electron microscope analysis of diode laser and desensitizing toothpastes for evaluation of efficacy of dentinal tubular occlusion." *Journal of Indian Society of Periodontology*, Vol. 21, No. 2, pp. 102-106.

Santos, C. L., Albuquerque, A. J. R., Sampaio, F. C., Keyson, D. (2013). "*Nanomaterials with Antimicrobial Properties: Applications in Health Science*" Microbial pathogens and strategies for combating them: science, technology and education, Mendez-Vilas, A., Vol. 1. Formatex Research Center, Badajoz, Spain, pp. 143-154.

Schulte, P., Geraci, C., Zumwalde, R., Hoover, M., Kuempel, E., (2008). "Occupational Risk Management of Engineered Nanoparticle." *Journal of Occupational and Environmental Hygiene*, Vol. 5, No. 4, pp. 239-249

Şekeroğlu, Z. A., (2013). "Nanoteknolojiden nanogenotoksikolojiye: kobalt-krom nanopartiküllerinin genotoksik etkisi." *Türk Hijyen ve Deneysel Biyoloji Dergisi*, Vol. 70, No. 1, pp. 33-42.

Ünver, H. (2016). Nanomalzeme Üretiminde İş Sağlığı ve Güvenliği Risklerinin Değerlendirilmesi, İş Sağlığı ve Güvenliği Uzmanlık Tezi, Çalışma ve Sosyal Güvenlik Bakanlığı İş Sağlığı ve Güvenliği Genel Müdürlüğü, Ankara, Türkiye.

Zalk, D. M., Paik, S. Y., Swuste, P. (2009). "Evaluating the Control Banding Nanotool: a qualitative risk assessment method for controlling nanoparticle exposures." *Journal of Nanoparticle Research*, Vol. 11, No. 7, pp. 1685-1704.

Turkish Journal of Engineering

Turkish Journal of Engineering (TUJE)
Vol. 4, Issue 1, pp. 30-35, January 2020
ISSN 2587-1366, Turkey
DOI: 10.31127/tuje.600898
Research Article

FABRICATION OF TiO_2 BASED COMPOSITE MATERIALS BY HYDROTHERMAL METHOD

Canan Aksu Canbay *[1] and Furkan Özbey [2]

[1] Fırat University, Faculty of Science, Department of Physics, Elazığ, Turkey
ORCID ID 0000-0002-5151-4576
caksu@firat.edu.tr

[2] Fırat University, Faculty of Science, Department of Physics, Elazığ, Turkey
ORCID ID 0000-0003-4794-233X
furkanzby@hotmail.com

* Corresponding Author
Received: 02/08/2019 Accepted: 10/09/2019

ABSTRACT
Composite nanoparticles (nano powders) are nano-sized and can be synthesized with a wide range of organic, inorganic materials and production techniques. Titanium dioxide is one of the most commonly used materials in the production of composite materials. The reason why titanium dioxide is more preferred is that it has a minimum of any reactive step, it does not interfere with the human body and is an organic material that does not contain by-products. The photocatalytic properties of titanium dioxide can be improved by various methods. TiO_2 is the most widely used photocatalyst in air purification. In this study, titanium dioxide based composite material was fabricated by hydrothermal method. The electrical, optical and structural properties of the material were investigated with the contribution of three different compositions of cadmium oxide (CdO) for produced in the experiments. For this purpose, SEM, U-V (Vis), I-V and FTIR techniques were used for the characterization and obtained results evaluated.

Keywords: *Composite Material, TiO_2, CdO, Hydrothermal Method*

1. INTRODUCTION

Composite materials have been discovered and continue to be explored for a wide range of uses throughout human history. This process, which started with the addition of straw to mud, continues to develop in a wide range of areas from construction materials to photovoltaic nanoparticles. However, the use of the first composite word coincides with the early 1940s (Kinsinger *et al.* 2011). The purpose of producing composite materials is to gain new chemical and physical properties such as optical, electrical or mechanical, etc. to materials. There has been a rapid development in composite material technology in the near future. This rapid development has enabled them to be used increasingly in many sectors. The most preferred sector is the aviation industry (Akbulut *et al.* 2017).

Composite nanoparticles are nano-sized and can be synthesized with a wide range of organic, inorganic materials and production techniques. Titanium dioxide is one of the most used materials in the production of composite materials. The semiconductor property of titanium dioxide is used and its photocatalytic property is utilized. Inorganic metal based titanium dioxide (TiO_2) covers a wide range of catalysts, semiconductor films, etc. from the chemical industry to photovoltaic and semiconductor thin film applications. as used very often. In photovoltaic applications, it has been possible to synthesize titanium dioxide by using various additive and production methods to improve optical absorption capacity or electrical properties and researches continue along this direction.

Titanium dioxide is more preferred because it has a minimum of any reactive step, does not interfere with the human body and is an organic material (Kinsinger, Tantuccio, Sun, Yan and Kisailus 2011). TiO_2 is the most widely used photocatalyst in air purification (Zhang *et al.* 2006) and TiO_2 has been one of the most researched semiconductors since the discovery of water separation in the 1970s. TiO_2 has wide application areas such as; TiO_2 based catalyzes, cosmetics, dyes, antibacterial substances, lithium-ion cells, dye-sensitive solar cells, etc. are abundant. However, the white color and a broadband range of intact TiO_2 limit its application to the UV part of the sunlight spectrum in depth. Only a small proportion (~%5) of solar energy can be used well by copper TiO_2 and most of the solar energy is wasted. Therefore, it is necessary to reduce the recombination of electron-hole pairs to extend the absorption edge of the solar spectrum to the visible region and to increase the photocatalytic activity of TiO_2(Fang *et al.* 2017). Since titanium dioxide is a good catalyst, it can interact with different materials. The TiO_2 semiconductor can be combined with the cadmium oxide semiconductor, which has a narrow bandgap and can absorb visible light. The basic principle of this mechanism is based on the excitation of the electron in the valence band (VB) to the conductivity band (CB) by the absorption of light from the narrow band hollow semiconductor, and from there the passage of TiO_2 into the conductivity band. Thus, electrons move towards the surface of TiO_2 to form active oxidized species. There are such many studies in the literature.

There is a wide area of study with many different contributions such as; TiO_2:FeS_2,ZrO_2:TiO_2,SiO_2:TiO_2,TiO_2:CNSP etc (Rashid *et al.* 2018). Cadmium oxide is an important n-type semiconductor with a direct band gap of ~2.5 V and an indirect band gap of 1.18~1.20eV. Nonlinear materials have promising applications in catalysts. CdO nanoparticles are known to be highly reactive and have been used in processes such as energy storage systems, electrochromic thin films and heterogeneous catalyses. It forms an important component in the synthesis of nanoscience and nanotechnology. Nanomaterials produced by chemical methods have proved to be more effective by providing better control as well as providing different sizes, shapes, and functionalization than those produced by physical methods such as laser ablation, arc discharge and evaporation. Metal oxide nanoparticles can be produced by soft chemical methods such as co-precipitation, sol-gel and hydrothermal synthesis (Sayilkan *et al.* 2007).

In this study, cadmium oxide (CdO) nanoparticles are added to titanium dioxide (TiO_2), which is a good semiconductor, to improve optical absorber and electrical conductivity properties. For this purpose, using SEM, UV-Vis, I-V and FTIR measurements of unadulterated TiO_2 sample produced by hydrothermal method and also CdO: TiO_2 (10:90) and CdO: TiO_2 (20:80) composite samples with two different ratios of CdO added into TiO_2 were produced and characterized.

2. MATERIALS AND METHODS

Synthesis steps of TiO_2; first, titanium isopropoxide (Ti (OC3H7) 4) ethyl alcohol (ethanol (CH3CH2OH)) were put in a beaker, while hydrochloric acid (HCl) and ethanol were added to each other in a separate beaker. The mixtures were stirred for one hour on a magnetic stirrer and the two mixtures formed were added, too. The resulting new sample was again stirred in the magnetic stirrer for half an hour. The solution was determined as TiO_2 and in the following process, two different doped samples were obtained by adding 10% and 20% cadmium oxide (CdO) calculated as molar ratios to the solution prepared by the same experimental procedures. Thus, the samples; TiO_2, CdO: TiO_2 (10:90), CdO: TiO_2 (20:80) were produced. These mixtures were subjected to the hydrothermal process, drying and annealing, respectively, in accordance with the literature. As a result of these steps, three powder samples in powder forms were obtained.

SEM, UV-VIS, I-V and FTIR analyses of the three physical and chemical properties of the powder samples were performed to determine the physical and chemical properties.

3. RESULTS

3.1. Scanning Electron Microscope (Sem) Results

Fig. 1 shows SEM images of pure TiO_2 and TiO_2 doped with CdO as; CdO: TiO_2 (10:90) and CdO: TiO_2 (20:80), respectively. The SEM images of the samples showed that the pure sample consisted of smooth spherical structures. In CdO: TiO_2 composites, these spherical structures were not observed. In composite samples, these spherical structures were disintegrated and

disrupted by CdO effect, and instead of these spheres random particle structures of large and small dimensions were formed. Based on these findings, it was found that the structural properties of the samples varied depending on the sample composition ratio.

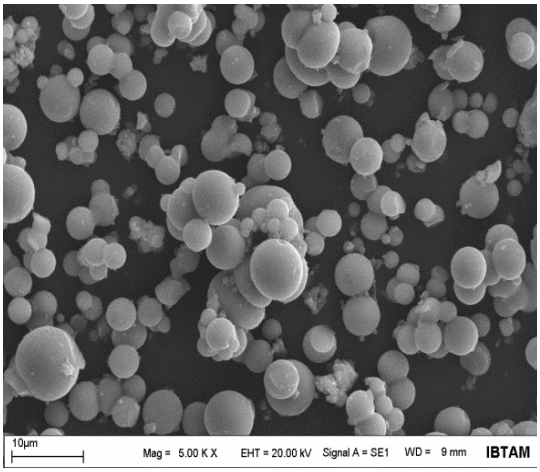

a

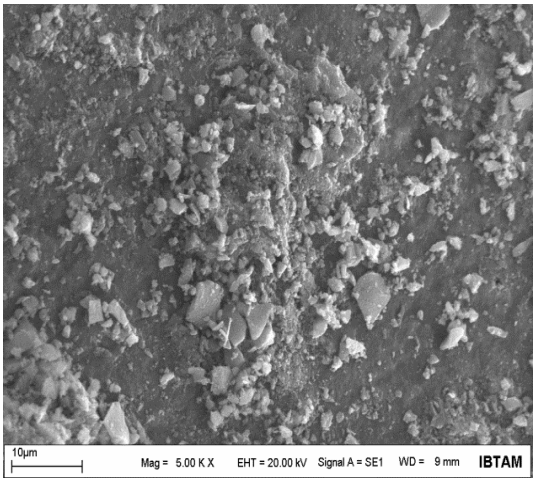

b

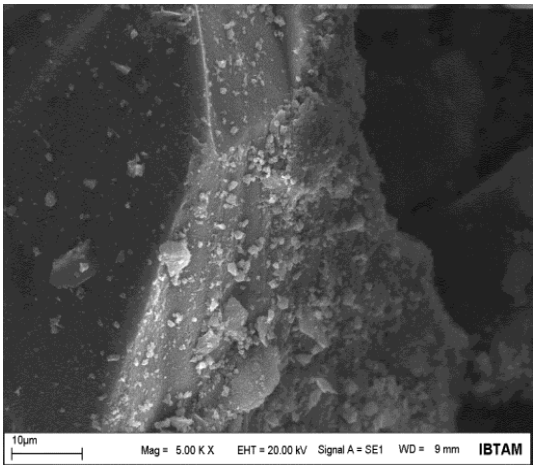

c

Fig 1. SEM images of the specimens; a)TiO_2, b) CdO:TiO_2(10:90), c) CdO:TiO_2(20:80).

3.2. Optical Analysis Results

Optical band intervals of pure TiO_2, CdO: TiO_2 (10:90) and CdO: TiO_2 (20:80) samples were investigated. The samples were pelletized and optical measurements were taken. The transmittance method was not used because the samples were not transmissible and instead of this diffuse reflectance method was used. According to this method, reflectance measurements of the samples were taken and optical band intervals were calculated. The Kubelka-Munk function developed for this is expressed as follows (Morales *et al.* 2007);

$$\boldsymbol{F(R)} = \frac{\boldsymbol{(1-R)^2}}{\boldsymbol{2R}} \qquad (1)$$

Here, F (R) is the Kubelka-Munk function and corresponds to absorbance and R is reflectance. The most important feature of the Kubelka-Munk function is that the samples with weak absorbance coefficients convert the measured reflectance values into absorbance values.

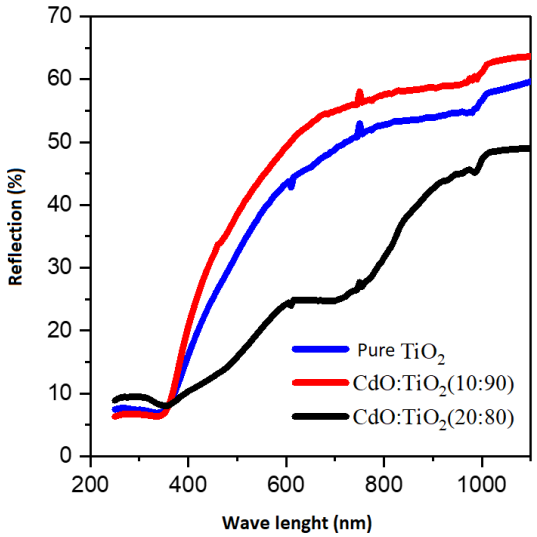

Fig 2. Reflection spectra of samples

Reflection spectra of pure TiO_2, CdO: TiO_2 (10:90) and CdO: TiO_2 (20:80) samples are given in Fig. 2. Variations of the reflection spectra with wavelength can be seen in the figure. Looking at all three samples, around 400 nm is seen as the reflection limit. Reflection increases with increasing wavelength. When the reflection properties of the three samples are examined, it is seen that they exhibit similar behaviors. As shown in the figure, it has been observed that as the doping ratio increases, the percentage of reflection of the sample first increases and then decreases(He *et al.* 2002; Sun *et al.* 2009; Wojcieszak *et al.* 2015).

The relationship between absorbance and optical band is expressed in the following equation.

$$\alpha h\nu = A\,(h\nu - E_g)^n \qquad (2)$$

The α value in this equation corresponds to the value of F (R) / d (d = sample thickness). A is a constant, Eg is a forbidden energy (optical band) range, n is a constant and determines the type of optical transition. The

forbidden energy ranges (αhν) of the samples were obtained from the $(\alpha h\nu)^2$–hν graph.

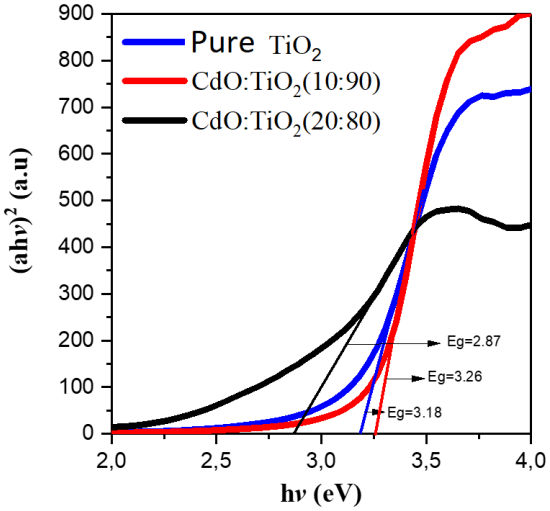

Fig 3.Specimens $(\alpha h\nu)^2$–hν spectrum

$(\alpha h\nu)^2$–hν spectra were plotted to calculate the forbidden energy range of the obtained samples and are given in Fig. 3 (Lebukhova *et al.* 2017). Eg values were obtained from linear parts of the$(\alpha h\nu)^2$–hν spectra. Eg values were calculated as 3.18 eV for pure TiO_2 sample, 3.26 eV for CdO: TiO_2 (10:90) sample and finally 2.87 eV for CdO: TiO_2 (20:80) sample(A.Aadim *et al.* 2016; Laatar *et al.* 2017; Kamil *et al.* 2018). The optical band spacing of the composite materials produced varies depending on the composite ratio of the material.

3.3. Electrical Conductivity Results

In order to determine the electrical characteristics of the prepared samples, their electrical conductivity was measured by 2-probe method and I-V graphs were obtained and the results were given in Fig. 4.

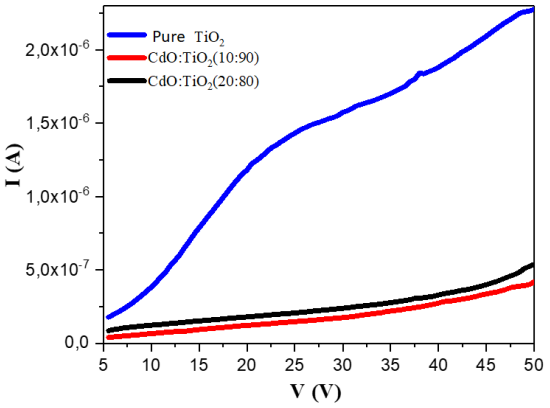

Fig. 4. Specimens I-V curves

The following equation was used to calculate the electrical conductivity of the samples.

$$\sigma = \frac{I}{V} \cdot \frac{d}{A} \qquad (3)$$

Where **σ** is the electrical conductivity, I current, V potential difference, d is the thickness of the sample and A is the cross-sectional area of the sample ($A = \pi r^2$ r radius of contact point).

The calculated electrical conductivity of the samples are; $6{,}08\times10^{-7}\ \Omega^{-1}cm^{-1}$ for pure TiO_2 sample, $1{,}29\times10^{-7}\ \Omega^{-1}cm^{-1}$ for CdO: TiO_2 (10:90) sample and CdO: TiO_2 (20:80) for sample and $1{,}58\times10^{-7}\ \Omega^{-1}cm^{-1}$.

Accordingly, it was observed that the electrical conductivity of the samples varied depending on the ratio of TiO_2 and CdO in the material. The results obtained are similar to the results of the previous study. (Nagashima *et al.* 2012).

3.4. FTIR Results of Samples

Variations of FTIR spectra with the number of waves for chemical structure analysis of the samples are given in Fig. 5. Characteristic vibration bands were observed in the FTIR spectrum of TiO_2 at $1200cm^{-1}$ and $1700\ cm^{-1}$. The presence of these bands confirms the chemical structure of titanium dioxide. The change in peak intensities indicated the presence of cadmium oxide but also showed good addition.

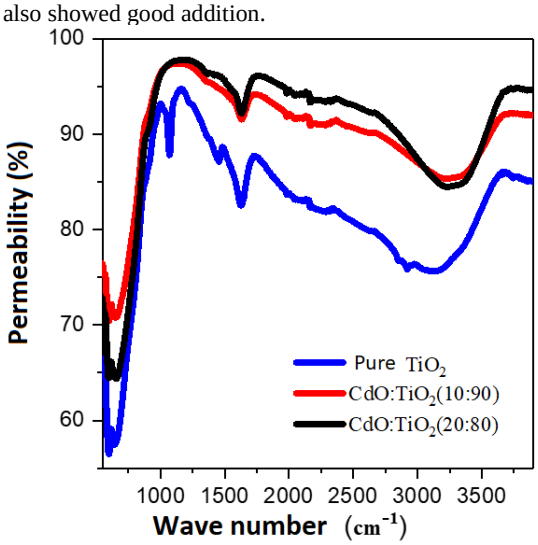

Fig 5.Specimen FTIR spectrums

When the curves given in Fig. 5 are examined, it is observed that the permeability is maximum between 900–1300 cm^{-1}. This increase can be said to be typical bands of TiO_2 and similar results can be found in the literature. (A.Aadim *et al.* 2016). In the figure, the wide vibration bands observed in the range of 500-700cm^{-1} were caused by vibrations in the Ti-O-Ti bonds in the TiO_2 mesh. 598 cm^{-1} Ti-O vibration band and 1638cm^{-1} Ti-O-Ti stretch band corresponded to(Nithya *et al.* 2013; Mashkour *et al.* 2017).

4. DISCUSSION

In this study, cadmium oxide (CdO) doped titanium dioxide (TiO_2) composites and pure titanium dioxide (TiO_2) were produced as semiconductor materials. The samples produced; additive titanium dioxide (TiO_2) and CdO: TiO_2 (10:90) and CdO: TiO_2 (20:80) are composite materials. Structural, electrical, optical and chemical,

properties of the three samples were analyzed by SEM, I-V, UV-VIS and FTIR measurements.

When the SEM images of composite materials were evaluated; The structure of pure TiO_2 sample was observed as spherical particles and these spherical structures were determined to be uniform. In composite samples, spherical structures disappeared and instead of the particles of different sizes formed in varying sizes and shapes depending on CdO contribution ratio. The dielectric property was increased by adding CdO into TiO_2. The electrical conductivity of the samples was calculated from the current-voltage (I-V) plots drawn by electrical measurements. Accordingly, the electrical conductivities were found as $6{,}08x10^{-7}\Omega^{-1}cm^{-1}$ for pure TiO_2 sample, $1{,}29x10^{-7}\ \Omega^{-1}cm^{-1}$ for CdO: TiO_2 (10:90) sample and $1{,}58x10^{-7}\Omega^{-1}cm^{-1}$ for CdO: TiO_2 (20:80) sample. The forbidden energy ranges of the samples were calculated from the absorbance spectrum. It was found to be 3.18 eV for pure TiO_2 sample, 3.26 eV for CdO: TiO_2 (10:90) and finally 2.87 eV for CdO: TiO_2 (20:80). FTIR analyses were performed to examine the structural properties of the samples and the average characteristic band of the samples was around 1300 cm^{-1}.

ACKNOWLEDGMENTS

This work is financially supported by FÜBAP, Project No: FF.16.13

REFERENCES

A.Aadim, K., K. I. Khaleel and Ayman A.Noori (2016). "The effect of the concentration ratio of Cadmium oxide on the optical properties for Titanium dioxide films." *IOSR Journal of Applied Physics*, Vol. 8, No. 5, pp. 46-49.

A.Aadim, K., K. I. Khaleel and AymanA.Noori (2016). "The effect of the concentration ratio of Cadmium oxide on theoptical properties for Titanium dioxide films." *IOSR Journal of Applied Physics*, Vol. 8, No. 5, pp. 46-49.

Akbulut, H. and Y. Kara (2017). "Karbon elyaf takvİyelİ karbon nanotüp katkili epoksİ kompozİt helİsel yaylarin mekanİk davranişlari." *Gazi Üniversitesi Mühendislik-Mimarlık Fakültesi Dergisi*, Vol. 32, No. 2.

Aksoylu, B. (2007). Kompozit Malzemelerde Elyaf Burkulmasının Sayısal Olarak İncelenmesi, Yüksek Lisans Tezi, İstanbul Teknik Üniversitesi Fen Bilimleri Enstitüsü, 127s.

Fang, W., M. Xing and J. Zhang (2017). "Modifications on reduced titanium dioxide photocatalysts: A review." *Journal of Photochemistry and Photobiology C: Photochemistry Reviews*, Vol. 32, No., pp. 21-39.

He, J., I. Ichinose, T. Kunitake and A. Nakao (2002). "In situ synthesis of noble metal nanoparticles in ultrathin TiO_2− gel films by a combination of ion-exchange and reduction processes." *Langmuir*, Vol. 18, No. 25, pp. 10005-10010.

Kamil, A. M., H. T. Mohammed, A. A. Balakit, F. H. Hussein, D. W. Bahnemann and G. A. El-Hiti (2018). "Synthesis, Characterization and Photocatalytic Activity of Carbon Nanotube/Titanium Dioxide Nanocomposites." *Arabian Journal for Science and Engineering*, Vol. 43, No. 1, pp. 199-210.

Kinsinger, N., A. Tantuccio, M. Sun, Y. Yan and D. Kisailus (2011). "Photocatalytic titanium dioxide composite." *Journal of nanoscience and nanotechnology*, Vol. 11, No. 8, pp. 7015-7021.

Laatar, F., H. Moussa, H. Alem, L. Balan, E. Girot, G. Medjahdi, H. Ezzaouia and R. Schneider (2017). "CdSe nanorod/TiO2 nanoparticle heterojunctions with enhanced solar-and visible-light photocatalytic activity." *Beilstein journal of nanotechnology*, Vol. 8, No., pp. 2741.

Lebukhova, N., N. Karpovich, S. Pyachin, E. Kirichenko, K. Makarevich and M. Pugachevskii (2017). "Synthesis and optic properties of titanium dioxide nanostructures doped with alkali metals." *Theoretical Foundations of Chemical Engineering*, Vol. 51, No. 5, pp. 820-824.

Mashkour, M., M. Rahimnejad, S. Pourali, H. Ezoji, A. ElMekawy and D. Pant (2017). "Catalytic performance of nano-hybrid graphene and titanium dioxide modified cathodes fabricated with facile and green technique in microbial fuel cell." *Progress in Natural Science: Materials International*, Vol. 27, No. 6, pp. 647-651.

Morales, A. E., E. S. Mora and U. Pal (2007). "Use of diffuse reflectance spectroscopy for optical characterization of un-supported nanostructures." *Revista mexicana de física*, Vol. 53, No. 5, pp. 18-22.

Nagashima, K., T. Yanagida, M. Kanai, K. Oka, A. Klamchuen, S. Rahong, G. Meng, M. Horprathum, B. Xu and F. Zhuge (2012). "Switching properties of titanium dioxide nanowire memristor." *Japanese Journal of Applied Physics*, Vol. 51, No. 11S, pp. 11PE09.

Nithya, A., K. Rokesh and K. Jothivenkatachalam (2013). "Biosynthesis, characterization and application of titanium dioxide nanoparticles." *Nano vision*, Vol. 3, No. 3, pp. 169-174.

Rashid, J., S. Saleem, S. U. Awan, A. Iqbal, R. Kumar, M. Barakat, M. Arshad, M. Zaheer, M. Rafique and M. Awad (2018). "Stabilized fabrication of anatase-TiO 2/FeS 2 (pyrite) semiconductor composite nanocrystals for enhanced solar light-mediated photocatalytic degradation of methylene blue." *RSC Advances*, Vol. 8, No. 22, pp. 11935-11945.

Sayilkan, F., M. ASİLTüRK, Ş. Şener, S. Erdemoğlu, M. Erdemoğlu and H. Sayilkan (2007). "Hydrothermal Synthesis, Characterization and Photocatalytic Activity of Nanosized TiO_2 Based Catalysts for Rhodamine B Degradation." *Turkish Journal of Chemistry*, Vol. 31, No. 2, pp. 211-221.

Sun, L., J. Li, C. Wang, S. Li, Y. Lai, H. Chen and C. Lin (2009). "Ultrasound aided photochemical synthesis of Ag loaded TiO2 nanotube arrays to enhance photocatalytic

activity." *Journal of Hazardous Materials*, Vol. 171, No. 1-3, pp. 1045-1050.

Wojcieszak, D., M. Mazur, J. Indyka, A. Jurkowska, M. Kalisz, P. Domanowski, D. Kaczmarek and J. Domaradzki (2015). "Mechanical and structural properties of titanium dioxide deposited by innovative magnetron sputtering process." *Materials Science-Poland*, Vol. 33, No. 3, pp. 660-668.

Zhang, K., W. Xu, X. Li, S. Zheng and G. Xu (2006). "Effect of dopant concentration on photocatalytic activity of TiO2 film doped by Mn non-uniformly." *Open Chemistry*, Vol. 4, No. 2, pp. 234-245.

Turkish Journal of Engineering

Turkish Journal of Engineering (TUJE)
Vol. 4, Issue 1, pp. 36-46, January 2020
ISSN 2587-1366, Turkey
DOI: 10.31127/tuje.571598
Research Article

INVESTIGATION OF THE MOMENT–CURVATURE RELATIONSHIP FOR REINFORCED CONCRETE SQUARE COLUMNS

Saeid Foroughi *[1] and Süleyman Bahadır Yüksel [2]

[1] Konya Technical University, Faculty of Engineering and Natural Sciences, Department of Civil Engineering, Konya / Turkey
ORCID ID 0000-0002-7556-2118
saeid.foroughi@yahoo.com

[2] Konya Technical University, Faculty of Engineering and Natural Sciences, Department of Civil Engineering, Konya / Turkey
ORCID ID 0000-0002-4175-1156
sbyuksel@ktun.edu.tr

* Corresponding Author
Received: 29/05/2019 Accepted: 11/09/2019

ABSTRACT
In this study; the effect of the material model, axial load, longitudinal reinforcement ratio, transverse reinforcement ratio and transverse reinforcement spacing on the behavior of reinforced concrete cross-sections were investigated. Squared cross-section column models have been designed. The effect of axial load, transverse reinforcement diameter and transverse reinforcement spacing on the behavior of reinforced concrete column models have been analytically investigated. The behavior of the columns was evaluated from the moment-curvature relation by taking the nonlinear behavior of the materials into account. The moment-curvature relationships for different axial load level, transverse reinforcement diameter and transverse reinforcement spacing of the reinforced concrete column cross-sections were obtained considering Mander confined model. Moment-curvature relationships were obtained by SAP2000 Software which takes the nonlinear behavior of materials into consideration. The examined effects of the parameters on the column behavior were evaluated in terms of ductility and the strength of the cross-section. In the designed cross-sections, the effect of transverse reinforcement diameter and transverse reinforcement variation on the confined concrete strength and the moment-curvature relationship was calculated and compared for constant longitudinal reinforcement ratio. The examined behavioral effects of the parameters were evaluated by comparing the curvature ductility and the cross-section strength. It has been found that transverse reinforcement diameters and transverse reinforcement spacing are effective parameters on the ductility capacities of the column sections. Axial load is a very important parameter affecting the ductility of the section. It has been observed that the cross-sectional ductility of the column sections increases with the decrease in axial load.

Keywords: *Transverse Reinforcement, Nonlinear, Confined Concrete Strength, Axial Load, Moment-Curvature, Curvature Ductility.*

1. INTRODUCTION

Understanding the nonlinear response and damage characteristics of reinforced concrete buildings subjected to significant earthquakes is essential for assessment of seismic performance of existing buildings, as well as safe and economic design of new buildings (Ucar *et al.*, 2015). In the reinforced concrete structures, that is known reinforced concrete columns are one of the most crucial elements under earthquake loads. Column mechanisms are very critical to prevent total collapse in earthquakes. The objective performance levels of reinforced concrete structures could not be ensured due to the failure of some critical reinforced concrete columns. Because of this, determining the behavior of the structures should be known well to design earthquake-resisting structures. In the reinforced concrete structures, the structural behavior can be changed according to the behavior of the reinforced concrete members. Moment-curvature relationship is one of the best solutions to evaluate and represent the behavior of reinforced concrete cross sections (Dok *et al.*, 2017).

The moment-curvature relationships of critical cross-sections of reinforced concrete members are essential for non-linear analysis of reinforced concrete structures. Realistic moment-curvature relationships can only be obtained if realistic material constitutive models are utilized for confined and unconfined concrete, and reinforcing steel during the cross-sectional moment-curvature analysis (Bedirhanoglu and Ilki, 2004). The behavior of reinforced concrete elements are determined by the cross-sectional behavior of elements. Cross-sectional behavior depends on the material used, the geometry of the cross-section and the loading on that particular cross-section. The behavior of a reinforced concrete cross-section under bending moment or bending moment plus axial force can be monitored from moment-curvature relationship (Ersoy and Özcebe, 2012). Moment-curvature relationship and stress-strain curves of steel and concrete are calculated by selecting Mander model (Mander et. al., 1988) and using the equilibrium equations and conformity equations to be written. Generally, the ductility is defined as the capacity of a material, section, structural element, or structure to undergo an excessive plastic deformation without a great loss in its load-carrying capacity (Arslan and Cihanli, 2010).

Ductility of reinforced structures is a desirable property where resistance to brittle failure during flexure is required to ensure structural integrity. Ductile behavior in a structure can be achieved through the use of plastic hinges positioned at appropriate locations throughout the structural frame. These are designed to provide sufficient ductility to resist structural collapse after the yield strength of the material has been achieved. The available ductility of plastic hinges in reinforced concrete is determined based on the shape of the moment-curvature relations (Olivia and Mandal, 2005). Ductility may be defined as the ability to undergo deformations without a substantial reduction in the flexural capacity of the member (Park and Ruitong, 1988). According to Xie et al, (1994), this deformability is influenced by some factors such as the tensile reinforcement ratio, the amount of longitudinal compressive reinforcement, the amount of lateral tie and the strength of concrete. The ductility of reinforced concrete section could be expressed in the form of the curvature ductility ($\mu_\emptyset$):

$$\mu_\emptyset = \emptyset_u / \emptyset_y \quad (1)$$

where $\emptyset_u$; is the curvature at ultimate when the concrete compression strain reaches a specified limiting value, $\emptyset_y$; is the curvature when the tension reinforcement first reaches the yield strength. Theoretical moment-curvature analysis for reinforced concrete structural elements indicating the available flexural strength and ductility can be constructed providing that the stress-strain relations for both concrete and steel are known. Moment-curvature relationship can be obtained from curvature and the bending moment of the section for a given load increased to failure (Olivia and Mandal, 2005).

In order to be able to understand the behavior of reinforced concrete members, cross sectional behavior should be known. Cross sectional behavior can be best evaluated by moment-curvature relationship. On a reinforced concrete cross section moment-curvature relationship can be determined by some complicated iteration methods. Making these iterations manually is very difficult and not practical. Some spread sheet programs can be used for this purpose (Çağlar *et al.*, 2013). Usually it is desirable to design a reinforced concrete member with sufficient curvature ductility capacity to avoid brittle failure in flexure and to insure a ductile behavior, especially under seismic conditions. Firstly, information about stress-strain relationships, confined concrete and unconfined concrete models, moment-curvature relationship is given for a better understanding of non-linear behavior (Foroughi and Yüksel, 2018).

In this study, squared reinforced concrete column cross section models with equal cross-sectional area were designed and the effect of the longitudinal reinforcement ratio, axial force level and transverse reinforcement ratio on the behavior of these models were investigated. The behavior of the column models was investigated through the relation of moment-curvature. In last decades various stress-strain relationships for unconfined and confined concrete were proposed by different researchers. A concrete model proposed by Mander *et al.* (1988) which is widely used, universally accepted and mandated in Turkish Seismic Code (TSC, 2018) has been used to determine the moment-curvature relationships of reinforced concrete members based on the SAP2000 Software (CSI, Ver. 20.1.0). Moment-curvature relations were obtained and presented in graphical form using SAP2000 Software which takes nonlinear behavior of materials into consideration. The examined behavioral effects of the parameters were evaluated by the curvature ductility and the cross-section strength. The stress-strain curves and moment-curvature curves were drawn in various models and were interpreted by comparing the curves.

2. MATERIAL AND METHOD

In order to investigate the effect of longitudinal reinforcement ratio and transverse reinforcement ratio, column models with dimensions of 400mm×400mm were designed. A total of 14 models were designed for different transverse reinforcement diameters, transverse

reinforcement spacing and different axial loads of each model. The parameters investigated in the stress-strain relationships, confined concrete models, moment-curvature relations and ductility of the reinforced concrete column models are the transverse reinforcement diameter, transverse reinforcement spacing and axial load levels. The designed reinforced concrete cross section models are considered to be composed of three components; cover concrete, confined concrete and reinforcement steel. Material models are defined considering the Mander unconfined concrete model, for cover concrete, and the Mander confined concrete model for core concrete. For all column models, C30 was chosen as concrete grade and S420 was selected as reinforcement for the reinforcement behavior model, the stress-strain curves given in TSC (2018) were used (Table 1).

Table 1. Material parameters in property values (TS-500, 2000)

Standard Strength	Parameters	Value
Concrete: C30	Strain at maximum Stress of Unconfined Concrete (ε_{co})	0.002
	Ultimate Compression Strain of Concrete (ε_{cu})	0.0035
	Characteristic Standard Value of Concrete Compressive Strength (f_{ck})	30MPa
Reinforcement: S420	Yield Strain of Reinforcement (ε_{sy})	0.0021
	Spalling strain in reinforcing steel (ε_{sp})	0.008
	Strain in reinforcing steel at maximum strength (ε_{su})	0.08
	Characteristic Yield strength of Reinforcement (f_{yk})	420MPa
	Ultimate strength of Reinforcement (f_{su})	550MPa

The details of the cross-sections with different transverse reinforcement diameters and transverse reinforcement spacing for different cross-sections are given in Table 2. As shown in Table 2, for the parametric study; transverse reinforcement spacing were taken as 50mm, 75mm, 100mm, 125mm, 150mm, 175mm and 200mm. Diameters of the transverse reinforcement diameters were taken as 8mm and 10mm.

Table 2. Details for the designed square column model cross-sections

No	Longitudinal Reinforcement	Transverse reinforcement	N/N_{max}
C1	8Φ22	Φ8/50mm	0
C2		Φ8/75mm	0.10
C3		Φ8/100mm	0.20
C4		Φ8/125mm	0.30
C5		Φ8/150mm	0.40
C6		Φ8/175mm	
C7		Φ8/200mm	
C8	8Φ22	Φ10/50mm	0
C9		Φ10/75mm	0.10
C10		Φ10/100mm	0.20
C11		Φ10/125mm	0.30
C12		Φ10/150mm	0.40
C13		Φ10/175mm	
C14		Φ10/200mm	

The combined effect of N_{dmax} vertical loads and seismic loads, gross section area of column shall satisfy the condition $A_c \geq N_{dmax}/0.40f_{ck}$, (TSC, 2018). To investigate the effect of axial force on the cross-section behavior, the models were investigated under five different axial forces; $N_1 = 0$, N_2=480kN, N_3=960kN, N_4 =1440kN and N_5 =1920kN. Moment-curvature relationships for the designed column cross-sections are presented from the analytical results of different axial load, transverse reinforcement diameter and transverse reinforcement spacing. By using the Mander model, with the consideration of the lateral confining stress, the σ-ε relationships of the reinforced concrete columns are obtained by using the SAP2000 Software. The reinforcement diameters and reinforcement ratio used in the cross-sections were determined by considering the limitations given TS500 (2000) and TSC (2018). In all the models the longitudinal column reinforcement was 8Φ22. The monotonic envelope curve introduced by Mander *et al.* (1988) was adopted in this study for its computational efficiency. The following equation is used to calculate the unconfined concrete strength (f'_{cc}). The effectively confined area of concrete at hoop level is found by subtracting the area of the parabolas containing the ineffectively confined concrete. Thus the total plan area of ineffectually confined core concrete at the level of the hoops when there are n longitudinal bars is;

$$A_i = \frac{\sum_i^n (w_i')^2}{6} \tag{1}$$

Incorporating the influence of the ineffective areas in the elevation, the area of effectively confined concrete core at midway between the levels of transverse hoop reinforcement is:

$$A_e = \left(b_c\, d_c - \sum_i^n \frac{(w_i')^2}{6}\right)\left(1 - \frac{S'}{2b_c}\right)\left(1 - \frac{S'}{2d_c}\right) \tag{2}$$

Where b_c; concrete core dimension to center line of perimeter hoop in x-direction, d_c ; concrete core dimension to center line of perimeter hoop in y direction, s'; clear vertical spacing between hoops. Therefore, the confinement effectiveness coefficient (k_e) , which represents the ratio of the smallest effectively confined concrete area (A_e) to the net confined concrete core area (A_{cc}), could be given by the following Equations.

$$k_e = \frac{A_e}{A_{cc}} \quad , \quad A_{cc} = b_c\, d_c(1 - \rho_{cc}) \tag{3}$$

ρ_{cc} is ratio of area of longitudinal reinforcement to area of concrete core.

It is possible for rectangular reinforced concrete members to have different quantities of transverse confining steel in the x and y directions. These may be expressed as,

$$\rho_s = \rho_x + \rho_y = \frac{A_{sx}}{s\, d_c} + \frac{A_{sy}}{s\, b_c} \tag{4}$$

The lateral confining stress on the concrete (total transverse bar force divided by vertical area of confined concrete) are given in the x and y direction as,

$$f_{lx} = \rho_x\, f_{yh} \quad , \quad f_{ly} = \rho_y\, f_{yh} \tag{5}$$

Effective lateral confining stresses in the x and y directions are,

$$f'_{lx} = k_e\, f_{lx} \quad , \quad f'_{ly} = k_e\, f_{ly} \quad , \quad f'_l = f_l\, k_e \tag{6}$$

To determine the confined concrete compressive strength f'_{cc}, a constitutive model involving a specified maximum strength surface for multiaxial compressive stresses is used in this model. f'_l is the effective lateral confining stress.

$$f'_{cc} = f'_{co}\left(-1.254 + 2.254\sqrt{\frac{1+7.94f'_l}{f'_{co}}} - 2\frac{f'_l}{f'_{co}}\right) \tag{7}$$

The longitudinal concrete stress (f_c) is given by the following relation as the function of the longitudinal concrete strain (ε_c). In the following equations, f_c and ε_c represent the concrete strength and the corresponding strain value, respectively.

$$f_c = \frac{f'_{cc}\, x\, r}{r - 1 + x^r} \quad , \quad x = \frac{\varepsilon_c}{\varepsilon_{cc}} \tag{8}$$

Where ε_c: longitudinal compressive concrete strain. The calculation of f'_{cc} is not sufficient to obtain stress-strain curve of confined concrete. Therefore, the corresponding strain at maximum concrete stress (ε_{cc}) has to be calculated too. In addition, the maximum unit strain value 'ε_{cu}' in the concrete must be calculated at the first hoop fracture occurring in transverse reinforcement.

$$\varepsilon_{cc} = \varepsilon_{co}\left[1 + 5\left(\frac{f'_{cc}}{f'_{co}} - 1\right)\right] \tag{9}$$

Where f'_{co} and ε_{co}; the unconfined concrete strength and corresponding strain, respectively (generally ε_{co} = 0.002 can be assumed), and

$$r = \frac{E_c}{E_c - E_{sec}} \tag{10}$$

$$E_c = 5000\sqrt{f'_{co}}\, MPa\,, \quad E_{sec} = \frac{f'_{cc}}{\varepsilon_{cc}} \tag{11}$$

E_c: modulus of elasticity of concrete
E_{sec}: secant modulus of confined concrete at peak stress

Maximum concrete compressive strain (fracture strain ε_{cu}) is defined as the fracturing of the confining reinforcement. Maximum concrete compressive strain for confined concrete is given (Paulay and Priestley, 1992);

$$\varepsilon_{cu} = 0.004 + \frac{1.4\, \rho_s\, f_{yw}\, \varepsilon_{su}}{f'_{cc}} \tag{12}$$

ρ_s: ratio of volume to transverse confining steel to volume of confined concrete core
ε_{su}: Strain in reinforcing steel at maximum strength
f_{yw}: yield strength of transverse reinforcement

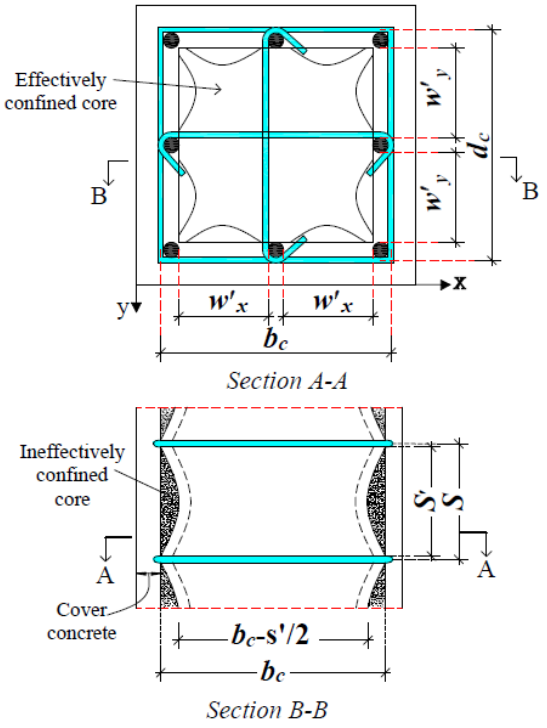

Fig. 1. Effectively confined core for square hoop reinforcement (Mander *et al.*, 1988)

3. NUMERICAL STUDY

The computed results for the models are summarized in the following Tables. When the calculated values of the designed models were examined, the following results were obtained. The values given in the tables are prepared according to the different confining reinforcement diameters and spacing for the column models. Effective lateral confining stress in *x* and *y* direction and compressive strength of confined concrete and ε_{cc} and ε_{cu} values are given in Table 3. The obtained σ-ε relationship of the longitudinal concrete stress (f_c) as the function of the longitudinal concrete strain (ε_c) is summarized in Fig. 2. The σ-ε curve shown in Fig. 1 for different transverse reinforcement spacing has been prepared according to 8mm (Fig. 2a) and 10 mm (Fig. 2b) transverse reinforcement diameter.

Table 3. The calculated f_{lx}, f_{ly}, f'_{lx}, f'_{ly}, f'_{l}, f'_{cc} , ε_{cc} and ε_{cu} values to Mander models

No	Hoops spacing(mm)	f_{lx}, f_{ly} (MPa)	f'_{lx}, f'_{ly}, f'_{l} (MPa)	f'_{cc} (MPa)	ε_{cc}	ε_{cu}
C1	Φ8/50	3.838	2.767	40.91	0.0080	0.0302
C2	Φ8/75	2.558	1.698	35.69	0.0059	0.0240
C3	Φ8/100	1.919	1.168	32.81	0.0048	0.0203
C4	Φ8/125	1.535	0.845	30.98	0.0041	0.0178
C5	Φ8/150	1.279	0.648	29.73	0.0036	0.0160
C6	Φ8/175	1.096	0.503	28.83	0.0033	0.0146
C7	Φ8/200	0.959	0.396	28.15	0.0030	0.0135
C8	Φ10/50	5.961	4.341	47.48	0.0106	0.0391
C9	Φ10/75	3.974	2.666	40.45	0.0078	0.0315
C10	Φ10/100	2.980	1.836	36.41	0.0062	0.0269
C11	Φ10/125	2.384	1.344	33.79	0.0052	0.0237
C12	Φ10/150	1.987	1.020	31.96	0.0045	0.0214
C13	Φ10/175	1.703	0.793	30.62	0.0040	0.0195
C14	Φ10/200	1.490	0.626	29.60	0.0036	0.0180

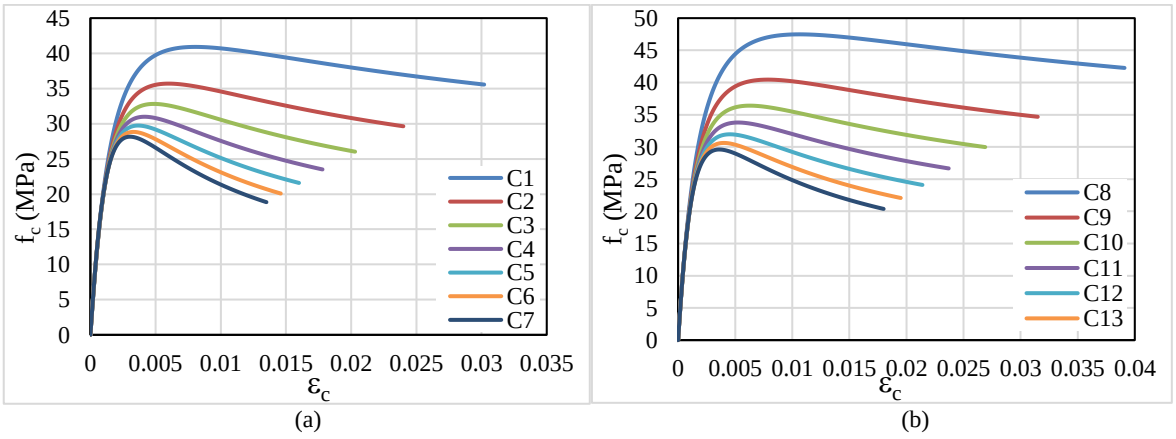

(a) (b)

Fig. 2. Stress-strain relationships for different transverse reinforcement spacing according to Mander model

The moment-curvature relationships obtained from the analytical results are presented in graphical form. Fig. 3 shows the moment-curvature comparisons for different transverse reinforcement spacing and different axial loads in the designed cross sections. In Fig. 3, moment-curvature relationships are given for different transverse reinforcement spacings according to the transverse reinforcement diameters of 8mm and 10mm respectively. In the column models designed from the analytical results, while the axial load is fixed in Fig. 4, the moment-curvature relationships are compared with respect to the diameter and spacing of different transverse reinforcements.

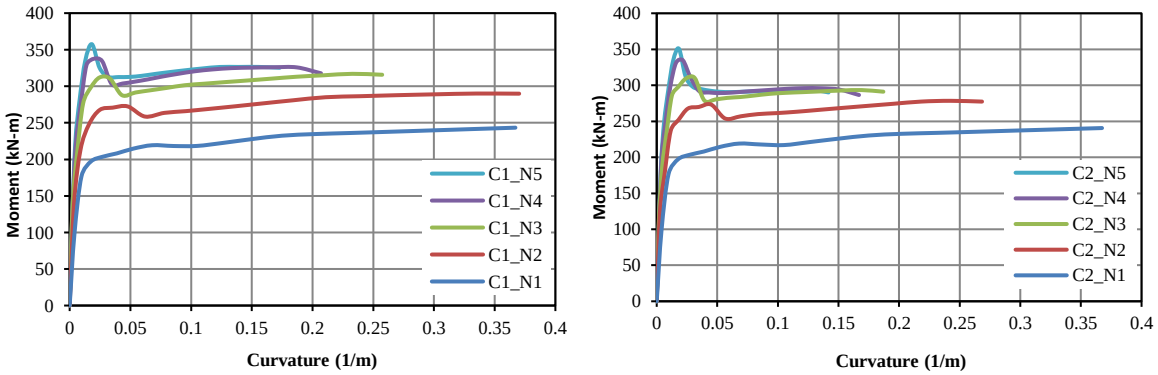

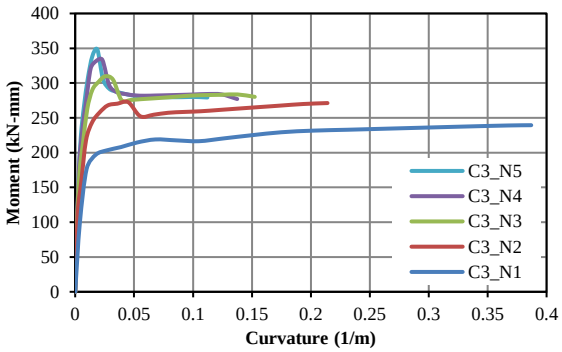
Moment (kN-mm)
Curvature (1/m)
C3_N5
C3_N4
C3_N3
C3_N2
C3_N1

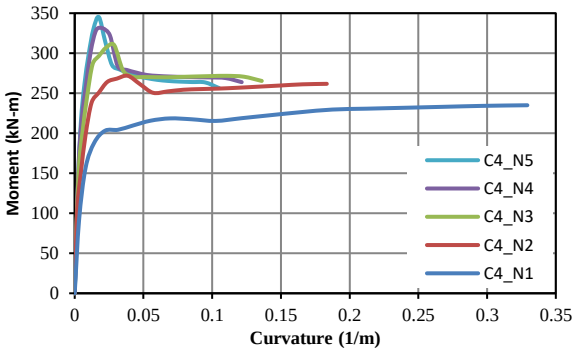
Moment (kN-m)
Curvature (1/m)
C4_N5
C4_N4
C4_N3
C4_N2
C4_N1

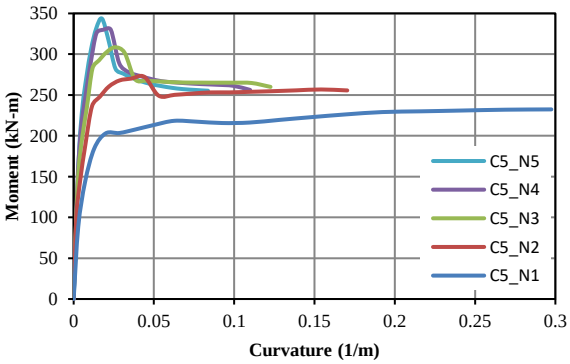
Moment (kN-m)
Curvature (1/m)
C5_N5
C5_N4
C5_N3
C5_N2
C5_N1

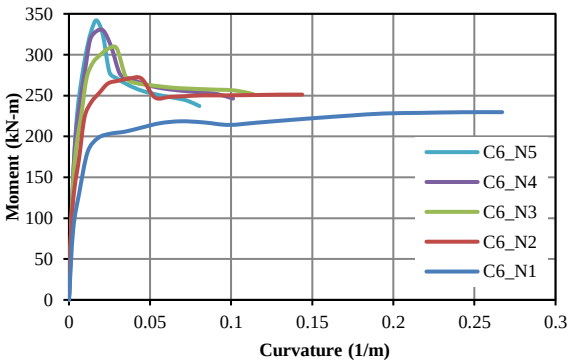
Moment (kN-m)
Curvature (1/m)
C6_N5
C6_N4
C6_N3
C6_N2
C6_N1

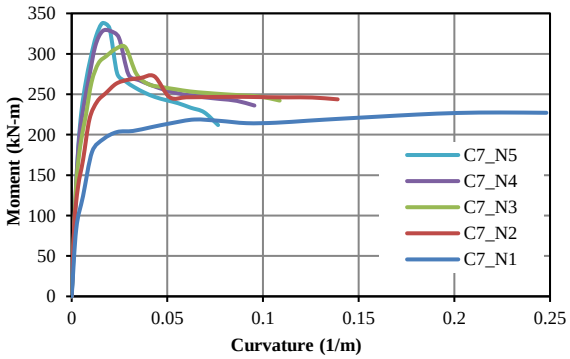
Moment (kN-m)
Curvature (1/m)
C7_N5
C7_N4
C7_N3
C7_N2
C7_N1

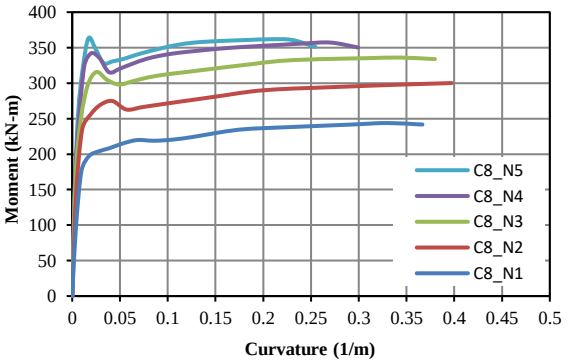
Moment (kN-m)
Curvature (1/m)
C8_N5
C8_N4
C8_N3
C8_N2
C8_N1

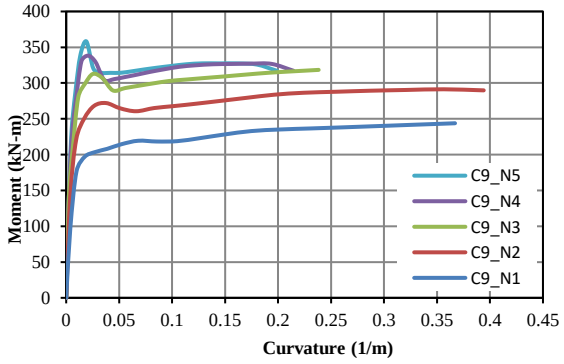
Moment (kN-m)
Curvature (1/m)
C9_N5
C9_N4
C9_N3
C9_N2
C9_N1

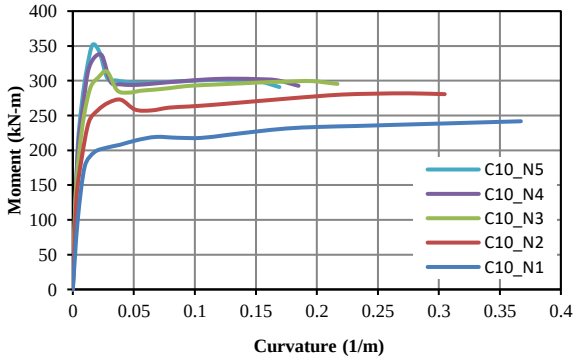
Moment (kN-m)
Curvature (1/m)
C10_N5
C10_N4
C10_N3
C10_N2
C10_N1

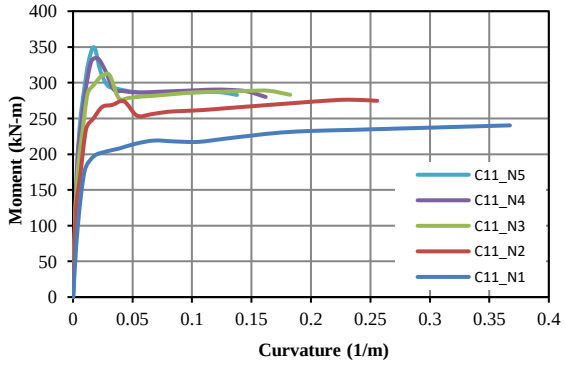
Moment (kN-m)
Curvature (1/m)
C11_N5
C11_N4
C11_N3
C11_N2
C11_N1

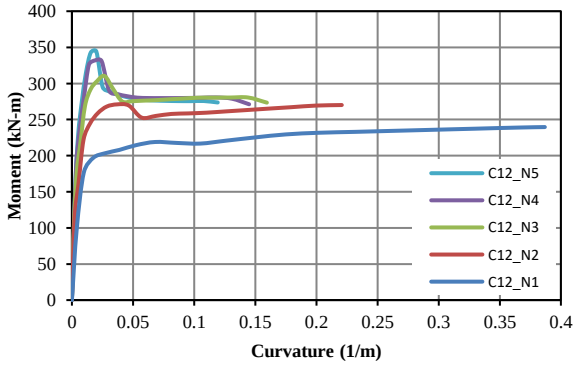
Moment (kN-m)
Curvature (1/m)
C12_N5
C12_N4
C12_N3
C12_N2
C12_N1

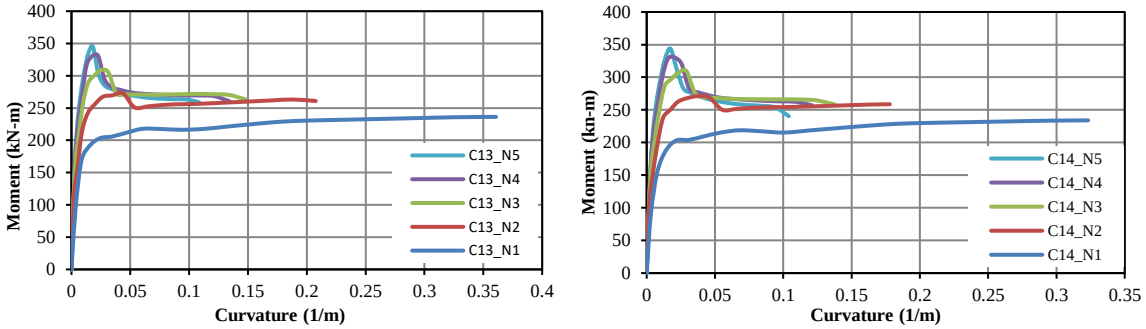

Fig. 3. Moment-curvature relationships of the columns for different load axial

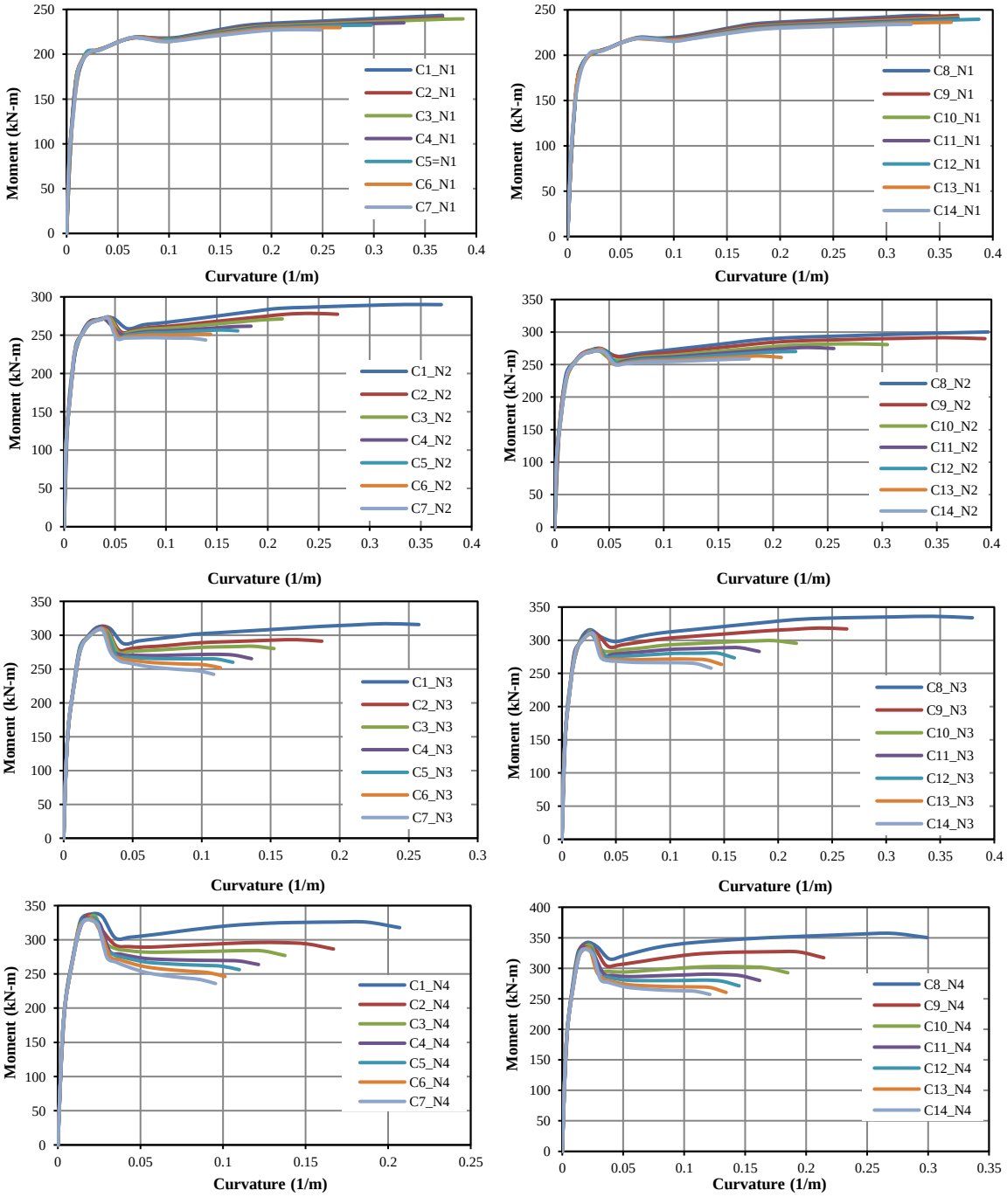

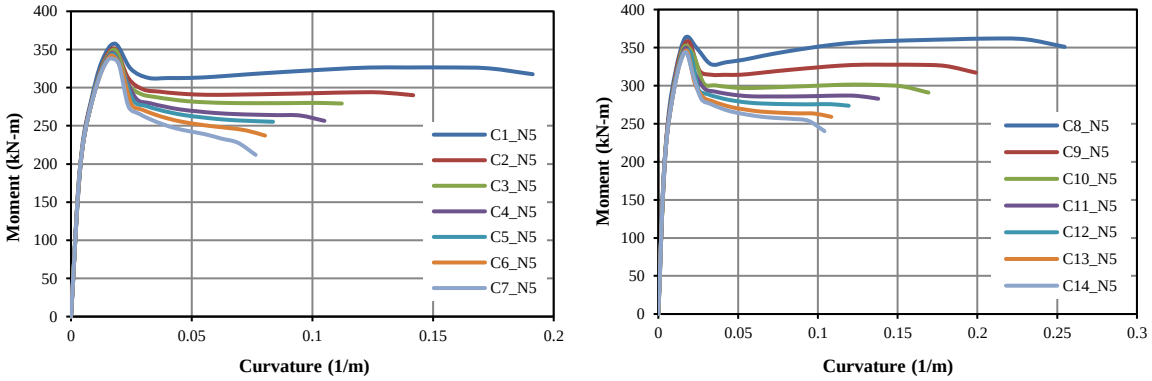

Fig. 4. Moment-curvature relationships of the columns for different hoops spacing

Moment-curvature relationships for the designed column cross-sections are presented for different axial load level, transverse reinforcement diameter and transverse reinforcement spacing. Yield moment ($\boldsymbol{M_y}$), ultimate moment ($\boldsymbol{M_u}$), yield curvatures ($\boldsymbol{\emptyset_y}$), ultimate curvatures ($\boldsymbol{\emptyset_u}$) and curvature ductility ($\boldsymbol{\mu_\emptyset}$) values are calculated from the moment-curvature relationships (Table 4 and Table 5).

Table 4. Calculation results of bending moment-curvature (transverse reinforcement Φ8)

Kesit No	Axial Load Level N/N_{max}	M_y $(kN.m)$	$\emptyset_y$ $(1/m)$	M_u $(kN.m)$	$\emptyset_u$ $(1/m)$	$\mu_\emptyset$
C1	0	165.03	0.0088	243.32	0.4060	46.1
	0.1	218.78	0.0101	290.0	0.3258	32.3
	0.2	278.27	0.0116	317.0	0.2574	22.2
	0.3	322.15	0.0132	337.54	0.2070	15.7
	0.4	345.35	0.0153	357.52	0.1913	12.5
C2	0	164.56	0.0088	240.58	0.4063	46.2
	0.1	220.07	0.0101	278.43	0.2688	26.6
	0.2	275.65	0.0116	291.10	0.1870	16.1
	0.3	312.53	0.0132	334.72	0.1669	12.6
	0.4	342.07	0.0157	350.88	0.1418	9.0
C3	0	164.41	0.0088	239.42	0.4064	46.2
	0.1	222.45	0.0101	272.42	0.2141	21.2
	0.2	271.35	0.0116	309.77	0.1524	13.1
	0.3	321.69	0.0134	333.42	0.1375	10.3
	0.4	341.57	0.0159	348.16	0.1122	7.1
C4	0	161.15	0.0087	234.96	0.3293	37.9
	0.1	218.33	0.0101	271.76	0.1834	18.2
	0.2	272.56	0.0116	310.29	0.1361	11.7
	0.3	313.68	0.0133	263.84	0.1215	9.1
	0.4	339.80	0.0161	345.20	0.1050	6.5
C5	0	155.18	0.0087	232.37	0.2975	34.2
	0.1	221.70	0.0101	272.26	0.1704	16.9
	0.2	282.77	0.0117	308.54	0.1226	10.5
	0.3	318.12	0.0134	329.95	0.1099	8.2
	0.4	338.59	0.0161	343.63	0.0837	5.2
C6	0	154.09	0.0087	229.66	0.2671	30.7
	0.1	226.30	0.0101	270.75	0.1438	14.2
	0.2	275.13	0.0116	308.07	0.1135	9.8
	0.3	319.52	0.0134	329.25	0.1012	7.6
	0.4	337.90	0.0159	341.98	0.0804	5.1
C7	0	156.52	0.0087	227.42	0.2481	28.5
	0.1	223.78	0.0101	272.11	0.1390	13.8
	0.2	273.01	0.0116	308.02	0.1087	9.4
	0.3	315.11	0.0134	328.22	0.0955	7.1
	0.4	336.94	0.0158	338.0	0.0765	4.8

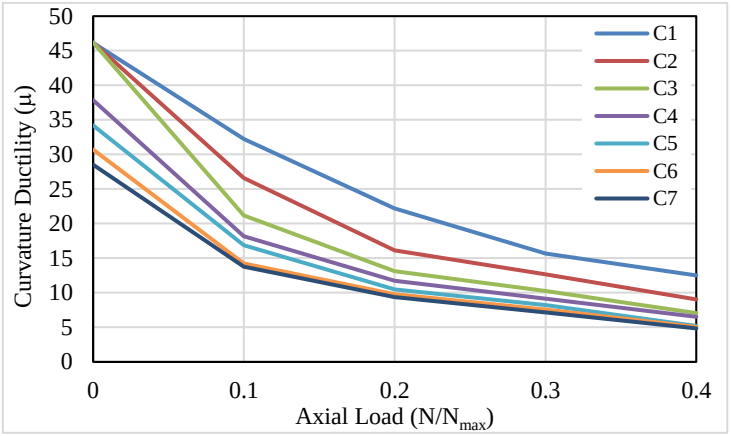

Fig. 5. Influence of axial loads on the ductility (transverse reinforcement Φ8).

Table 5. Calculation results of bending moment-curvature (transverse reinforcement Φ10)

Kesit No	Axial Load Level N/N_{max}	M_y $(kN.m)$	$\emptyset_y$ $(1/m)$	M_u $(kN.m)$	$\emptyset_u$ $(1/m)$	$\mu_\emptyset$
C8	0	165.53	0.0089	243.81	0.4120	46.3
	0.1	232.02	0.0102	300.10	0.3671	36.0
	0.2	265.02	0.0114	336.07	0.3297	28.9
	0.3	326.50	0.0131	357.16	0.2994	22.9
	0.4	349.53	0.0151	351.02	0.2547	16.9
C9	0	165.06	0.0088	243.85	0.4058	46.1
	0.1	223.98	0.0101	291.33	0.3423	33.9
	0.2	280.96	0.0116	318.39	0.2635	22.7
	0.3	318.20	0.0132	338.32	0.2145	16.3
	0.4	345.66	0.0153	358.20	0.1990	13.0
C10	0	164.66	0.0088	241.70	0.4061	46.1
	0.1	213.57	0.010	281.82	0.3048	30.5
	0.2	268.11	0.0115	313.14	0.2169	18.9
	0.3	316.68	0.0133	336.15	0.185	13.9
	0.4	349.44	0.0159	351.59	0.1693	10.6
C11	0	164.50	0.0088	240.29	0.4062	46.2
	0.1	224.67	0.0101	276.25	0.2557	25.3
	0.2	278.35	0.0117	310.92	0.1825	15.6
	0.3	312.89	0.0132	333.79	0.1619	12.3
	0.4	341.62	0.0158	349.44	0.1378	8.7
C12	0	164.38	0.0088	239.58	0.4063	46.2
	0.1	224.88	0.0101	271.02	0.2208	21.9
	0.2	273.50	0.0116	310.35	0.1595	13.8
	0.3	320.98	0.0134	331.76	0.1450	10.8
	0.4	342.99	0.0161	344.22	0.1193	7.4
C13	0	170.62	0.0088	236.27	0.3608	41.0
	0.1	220.34	0.0101	272.89	0.2076	20.6
	0.2	270.50	0.0116	308.37	0.1477	12.7
	0.3	318.40	0.0134	331.42	0.1344	10.0
	0.4	338.95	0.0161	345.02	0.1084	6.7
C14	0	159.74	0.0087	234.02	0.3232	37.1
	0.1	219.22	0.0101	271.09	0.1780	17.6
	0.2	271.78	0.0116	309.52	0.1380	11.9
	0.3	313.48	0.0133	330.44	0.1210	9.1
	0.4	338.36	0.0160	343.85	0.1041	6.5

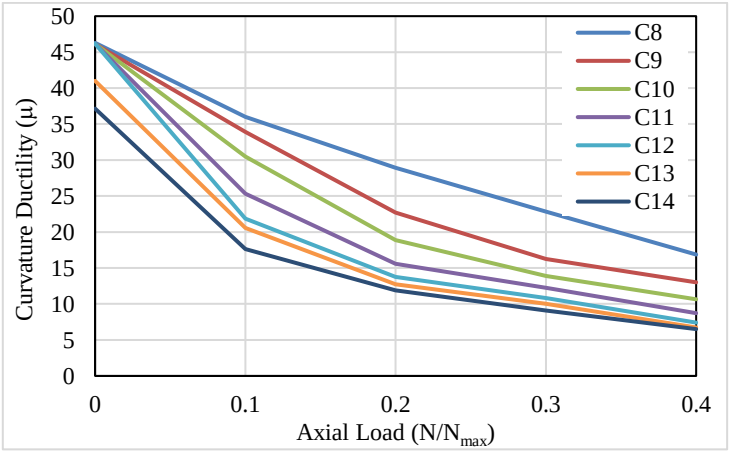

Fig. 6. Influence of axial loads on the ductility (transverse reinforcement Φ10).

In this part of the study, the moment-curvature diagrams are obtained from the SAP2000 Software by changing the transverse reinforcement diameter, transverse reinforcement spacing and axial load level. When the analysis results are examined, it is observed that the variation of the axial load and transverse reinforcement have important effect on the moment-curvature behavior of the reinforced concrete cross-sections. As a result, axial load is a very important parameter affecting the ductility of the section. As it shall be seen from moment-curvature relations, ductility decreases with the increase of axial load ($N/N_{max} \geq 0$) ratio where the transverse reinforcement is constant. However, when the axial load is small in the same cross-sections (transverse reinforcement is constant), the ductility in the cross-section is high. As it can be seen from the moment-curvature graphs, it is observed that the cross-section ductility decreases when the transverse reinforcement spacing is increased under a constant axial load. It is observed that the cross-section ductility and the curvature increase significantly with the reduction of the transverse reinforcement spacing. It is observed that the ratio of transverse reinforcement is effective on cross-section behavior of reinforced concrete cross section. The increase in transverse reinforcement diameter increases the ductility of the cross section and the maximum moment bearing capacity.

4. CONCLUSION

The following results were obtained from the stress-strain and moment-curvature analyses of the square columns:

The stress-strain relationship graphs of confined compressive strength and corresponding axial strain, of the core regions of the reinforced concrete columns are investigated based on the numerical study. The following results were obtained from the comparison of the columns with different characteristics of the examined factor in the study. The models were examined according to the conditions given in the TSC, (2018). Concrete stress-strain graphs were obtained by using Mander confined concrete models. Although the longitudinal reinforcement diameters and reinforcement yield strengths used in the models are constant, the effect of the use of different transverse reinforcement diameters and transverse reinforcement spacing on the lateral effective strength was investigated.

- It has been found that for all models, transverse reinforcement diameters and transverse reinforcement spacing are effective on the lateral load bearing capacity.
- The transverse reinforcement spacing densification has a greater effect on the ductility and the bearing capacity (moment capacity) of a cross section.
- The increase of the transverse reinforcement ratio increases the ductility and the maximum bearing capacity of a cross section.
- The moment-curvature relationship is determined according to the cross-sectional analysis of reinforced concrete columns by using SAP2000. The moment-curvature relationships are compared according to transverse reinforcement diameters, transverse reinforcing spacing and the axial load levels of reinforced concrete columns.
- The result is that the axial load is a very important parameter affecting the ductility of the cross-section. The relationship between axial load and ductile behavior is generally inversely proportional (Figs. 3 and 4).
- The increase in the axial load level causes the curvature values to decrease (brittle behavior), although it usually increases the moment capacity of the cross section.
- It has been observed that the cross-sectional ductility increases with the decrease in axial load.
- In cases where the axial load is small, reinforced concrete sections have a ductile behavior.
- As the diameter of the transverse reinforcement increases, the moment capacity of the cross section increases as expected.
- Significant reductions in ductility capacities under increasing axial force have been observed.
- The effect of axial load on cross-sectional behavior appears to be more explicit in cross sections where the transverse reinforcement spacing is minimum.
- If the analysis results are compared, yielding and ultimate moment capacities of the sections increase when decrease of the transverse reinforcement spacing.
- Moreover, the more ductile behavior for reinforced concrete cross sections is observed due to

increment of curvature ductility on reinforced concrete square columns with the increase of transverse reinforcing ratio.

- Additionally, according to the analysis results, the increment of transverse reinforcement ratio affects the yielding and ultimate moment capacities of the members for each type of concrete material.
- In order to see the actual behavior of the column sections, the transverse reinforcement ratio, transverse reinforcement spacing, and axial load ratio should be taken into consideration in the analyses.

REFERENCES

Arslan, G. and Cihanli, E. (2010). "Curvature Ductility Prediction of Reinforced High-Strength Concrete Beam Sections." *Journal of Civil Engineering and Management*, Vol. 16, No. 4, pp. 462–470.

Bedirhanoglu, I. And Ilki, A. (2004). "Theoretical Moment-Curvature Relationships for Reinforced Concrete Members and Comparison with Experimental Data." *Sixth International Congress on Advances in Civil Engineering*, 6-8 October 2004 Bogazici University, Istanbul, Turkey, pp. 231-240.

Caglar, N., Ozturk, H., Demir, A., Akkaya, A. and Pala, M. (2013). "Betonarme Kesitlerdeki Moment-Eğrilik İlişkisinin Yapay Sinir Ağları ile Belirlenmesi." *Akademik Platform Mühendislik ve Fen Bilimleri Dergisi*, pp. 1018-1029.

Ersoy, U. ve Özcebe, G. (2012). *Betonarme 1*, Evrim Yayınevi ve Bilgisayar San. TİC. LTD. ŞTİ. İstanbul, Türkiye.

Dok, G., Ozturk, H. and Demir, A. (2017). "Determining Moment-Curvature Relationship of Reinforced Concrete Columns." *The Eurasia Proceedings of Science, Technology, Engineering and Mathematics*, (EPSTEM), Vol. 1, pp. 52-58.

Foroughi, S. and Yuksel, S.B. (2018). "Moment Curvature Relationship of Square Columns." *International Congress on Engineering and Architecture*, (ENAR), Alanya, Turkey, pp. 681-688.

Olivia, M. and Mandal, P. (2005). "Curvature Ductility Factor of Rectangular Sections Reinforced Concrete Beams." *Journal of Civil Engineering*, Vol. 16, No. 1, pp. 1-13.

Mander, J. B., Priestley, M. J. N. and Park, R. (1988). "Theoretical stress-strain model for confined concrete." *Journal of Structural Engineering*, Vol. 114, No. 8, pp. 1804-1826.

Paulay, T., and Priestley, M.J.N. (1992). *Seismic Design of Reinforced Concrete and Masonry Buildings*, John Wiley & Sons, Inc, New York, USA.

Park, R. and Ruitong, D. (1988). "Ductility of doubly reinforced concrete beam section." *ACI Structural Journal*, Vol. 85, No. 2, pp. 217-225.

SAP2000, Structural Software for Analysis and Design, Computers and Structures, Inc, USA.

TSC (2018). *Specification for Buildings to be Built in Seismic Zones*, Ministry of Public Works and Settlement Government of the Republic of Turkey.

TS500 (2000). *Requirements for Design and Construction of Reinforced Concrete Structures*, Turkish Standards Institute, Ankara, Turkey.

Ucar, T., Merter, O. and Duzgun, M., (2015). "Determination of lateral strength and ductility characteristics of existing mid-rise RC buildings in Turkey." *Computers and Concrete*, Vol. 16, No. 3, pp. 467-485.

Xie, Y., Ahmad, S., Yu, T., Hino, S. and Chung, W. (1994). "Shear ductility of reinforced concrete beams of normal and high strength concrete." *ACI Structural Journal*, Vol. 91, No. 2, pp. 140-149.

Turkish Journal of Engineering

Turkish Journal of Engineering (TUJE)
Vol. 4, Issue 1, pp. 47-56, January 2020
ISSN 2587-1366, Turkey
DOI: 10.31127/tuje.599359
Research Article

THE IDENTIFICATION OF SEASONAL COASTLINE CHANGES FROM LANDSAT 8 SATELLITE DATA USING ARTIFICIAL NEURAL NETWORKS AND K-NEAREST NEIGHBOR

Mustafa Hayri Kesikoglu [1], Sevim Yasemin Cicekli *[2] and Tolga Kaynak [3]

[1] Erciyes University, Engineering Faculty, Department of Geomatics, Kayseri, Turkey
ORCID ID 0000-0001-5199-0815
mkesikoglu@gmail.com

[2] Cukurova University, Ceyhan Engineering Faculty, Department of Geomatics, Adana, Turkey
ORCID ID 0000-0002-8140-1265
yoturanc@cu.edu.tr

[3] Erciyes University, Engineering Faculty, Department of Geomatics, Kayseri, Turkey
ORCID ID 0000-0002-0718-9091
tolgakaynak@erciyes.edu.tr

* Corresponding Author
Received: 31/07/2019 Accepted: 01/10/2019

ABSTRACT
Coastline boundaries are constantly changing due to natural or human-induced events that take place in the world. Therefore it is necessary to correctly observe coastline boundaries. Remote sensing is one of the most frequently used methods to monitor the changes in coastal areas. In this study, it is aimed to solve the problem of choosing the right method for coastal change observation. This paper introduces a spatial pixel-based and object-based image classification approach to recognize changing areas in coastline. The coastline boundary changes occurred in a part of Yamula Dam Lake in Kayseri province were examined using three multispectral Landsat 8 satellite images of March, August and November 2016. Firstly, image-to-image registration processing was performed to register the three satellite images. Then, each satellite image was classified into two information classes either 'Lake' and 'Other Field' by using pixel-based Artificial Neural Networks (ANNs) and object-based K-Nearest Neighbor (KNN) method. Classification accuracies for ANNs method were obtained 99.97%, 99.90% and 99.80% respectively in March, August and November. As for the accuracies of the classification for the KNN method, in March, August and November were obtained 99.99%, 99.93% and 99.92% respectively. The change images were formed for March-August and August-November pairs by using the obtained classification images. The post classification comparison method was used to determine the changes in coastline boundaries. At the end of the study, seasonal changes from water to land and from land to water were detected. According to the result of the changes there is a 5,67 km^2 increase from March to August and a 3,14 km^2 decrease from August to November in Yamula Dam Lake.

Keywords: *Artificial Neural Networks; k-nearest Neighbor; Change Detection; Landsat 8*

1. INTRODUCTION

Remote sensing is a frequently preferred surveying method because it is useful and reliable in many disciplines. The remote sensing technique is one of the most successful methods in land cover and land use determination, planning, monitoring and mapping with different time intervals. It is also used for determination of emerging deformations and management of natural resources such as the determination of water beds, investigation of water pollution, determination of mineral and oil resources (Lillesand *et al.*, 2014).

Coastlines are permanent intersections where established seas and lakes or rivers (excluding situations such as floods) meet sections of land. Coastlines are one of the features identified by the International Geographic Data Committee (Karaburun and Demirci, 2010). Coastlines also have boundaries, which change according to meteorological phenomena, natural environment and human-induced effects. Efforts to identify changes in coastal boundaries at different times have a major impact on the management, conservation and sustainability of coastal resources. In recent years, there has been an increase in the utilization of remote sensing to monitor the changes in coastline management, coastline or coastal use (Ozpolat and Demir, 2014). Kuleli *et al.* (2011) determined coastline change in Yumurtalık and Gediz Ramsar wetland between 1989 and 2009 by using Digital Shoreline Analysis System, which is a statistic-based method. They used Landsat satellite images while doing this work. Prabaharan *et al.* (2010) investigated changes in the Vedaranniyam coastline, India. They utilized Landsat-1998, IRS 1C LISS III-2003 and IRS-Cartosat1-2008 satellite images to detect the changes. Guney and Polat (2015) used images of Landsat MSS of 1975, Landsat TM of 1987 and Landsat ETM of 2000 to determine coastline changes. They observed coastline changes by utilizing post classification comparison technique. Erener and Yakar (2012) used Landsat TM obtained in 1987, Landsat ETM+ obtained in 2000 and Landsat ETM+ obtained in 2006 and determined the water level changes from 1987 to 2006. Wang *et al.* (2013) used satellite images for determining the effect of coastal change on erosion by utilizing five different times and taken from three type satellites which are Landsat 5 TM, Landsat 7 ETM+ and HJ-1A. Shetty *et al.* (2015) used Landsat 5 TM images obtained from IRS 1C / 1 D in 1991, from IRS P6 in 2001, 2005 and 2009, from Landsat 8 OLI in 2013 satellite images and observed that sand was carried by erosion during the 46-year period (Shetty *et al.*, 2015).

The algorithms used in remote sensing studies to detect change can be separated in two types of method. The first is the unsupervised change detection approach. This method is based on the principle of the determination in land use and land cover changes obtained from satellite images taken on different dates and converting to single or multi-band image. The second method is the supervised change detection approach. This approach needs training and test classes as supervised classification for the determination in land use and land cover changes (Kesikoğlu *et al.*, 2013). For this reason, this approach is more challenging but, despite this, it allows us to achieve a more effective result in determining the direction of change.

The accuracy of the change detection process depends on the image classification process. Therefore, the selection of which classification method is used in change detection studies is important. There are many image classification methods used in literature such as membership function and, decision tree (DT) (Im and Jensen, 2005), random forest (RF) (Rodriguez-Galiano *et al.*, 2012), support vector machine (SVM) (Duro *et al.*, 2012, Kesikoglu *et al.*, 2019), maximum-likelihood (ML) (De Giglio *et al.*, 2019). In this study, we used two approaches: artificial neural networks (ANNs) and k-nearest neighbor (KNN). ANNs have a system that simulates the human brain. ANNs has been successfully used to classify satellite images in recent years (Pradhan and Lee, 2010; Chebud *et al.*, 2012; Hassan-Esfahani *et al.*, 2015). KNN is a nonparametric discriminatory analysis. The use of KNN method in image classification goes to 1990s (Denoeux, 1995) and it uses various image classification studies (Franco-Lopez *et al.*, 2001; McRoberts *et al.*, 2002; Yu *et al.*2006).Shiba *et al.* (2003) compared Case Slicing Technique as a new classification approach with K-Nearest Neighbor, C4.5 Learning Algorithm and Naive Bayes methods. Case Slicing Technique improved accuracy of the classification. Isa *et al.* (2005) used ANNs to classify the type of cervical cancer in its early stage and compared different ANNs. Zhang *et al.* (2017) used Spot-5 images to compare pixel-based and object-based classification method in the Heine River basin. They observed that object-based classification gave better results. Al Fugara *et al.* (2009) used Landsat 7 satellite images to compare pixel-based and object-based classification in the Klong valley of Malaysia. As a result of the work, object-based classification gave better results than pixel-based classification.

In this study, we aim to identify the changes at the Yamula dam coastline by using Landsat-8 satellite images obtained in March, June and November of 2016. In this context, we selected two-classification method and compared classification accuracies to obtain better results. ANNs and KNN methods were used for classification of satellite images and post classification comparison method was used to determine the coastline change. The study also briefly describes the planning of the work and the steps before the change is determined. It is aimed to contribute to the selection of the correct method in coastal line studies.

2. STUDY AREA

The Yamula Dam Lake is one of the most important dams due to producing electric energy and irrigation in Central Anatolia Region, Turkey (Kesikoğlu *et al.*, 2017). The dam is located 25 kilometers northwest of Kayseri and lies on the Kızılırmak River. The only water source that feeds the Yamula Dam is the Kızılırmak River. The river originates from Kızıldağ mountain in Sivas and flows into the Black Sea. The dam started holding water on December 27, 2003 (Yamula Barajı, n.d.). Landsat-8 satellite images of the year 2016 used in this study were chosen to include the Yamula Dam Lake and the change of coastline of the lake. The satellite image of the dam lake is demonstrated in Fig 1.

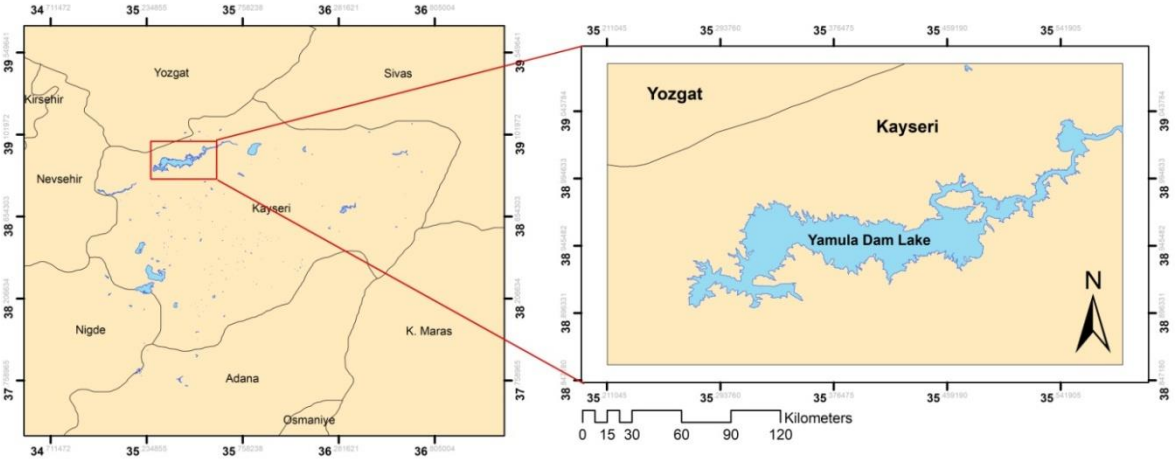

Fig. 1. Location map of study area

3. MATERIALS AND METHODS

In this study, Landsat 8 satellite images owning to the spring, summer and autumn seasons were used. These images were from March 5, 2016; August 26, 2016 and November 4, 2016. None of the winter season satellite images were evaluated due to the cloudy weather in December, January and February for the year 2016. Landsat 8 OLI / TIRS bands and their properties are given in detail in Table 1.

Table 1. Landsat-8 OLI / TIRS satellite image bands and features ("What are the band designations", 2017)

Sensor	Spectral Bands	Wavelength(μm)	Resolution(m)
	Band-1 Ultra Blue (Coastal Aerosol)	0.43-0.45	30
	Band-2 Blue	0.45-0.51	30
	Band-3 Green	0.53-0.59	30
	Band-4 Red	0.64-0.67	30
OLI	Band-5 Near Infrared (NIR)	0.85-0.88	30
	Band-6 Shortwave Infrared (SWIR-1)	1.57-1.65	30
	Band-7 Shortwave Infrared(SWIR-2)	2.11-2.29	30
	Band-8 Panchromatic	0.50-0.68	15
	Band-9 Cirrus	1.36-1.38	30
TIRS	Band-10 Thermal Infrared 1	10.60-11.19	100*30
	Band-11 Thermal Infrared 2	11.50-12.51	100*30

3.1. Artificial Neural Networks (ANNs)

ANNs is based on model of the biological brain. It is inspired from learning capability, structure and processing method of biological brain. ANNs consist of simple linear or nonlinear computing elements called "neurons", which are interconnected in complex ways and are usually arranged in layers (Sarle, 1994). There are numerous links between these elements. Information is distributed via links. Results are acquired through a learning process.

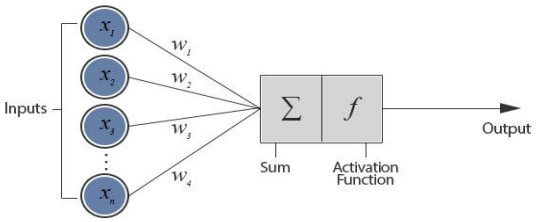

Fig. 2. Neurons structure of the ANNs (Haykin, 1994)

The structure of the neuron is demonstrated in Fig. 2, where $x_1,x_2,x_3....\ x_n$, are inputs and $w_1,w_2,w_3....\ w_n$, are the weights of these inputs. The weights determine the influence of inputs on the cell. The addition function calculates net data entering the cell. This can be mathematically identified as given in Eq. (1) (Haykin, 1994).

$$NetInput = \sum x_i w_i \quad (1)$$

The activation function can be identified as given in Eq. (2).

$$y = F(x) \quad (2)$$

All artificial nerve cells come together to form ANNs composed of three layers as shown in Fig. 3: input layer, hidden layer and output layer.

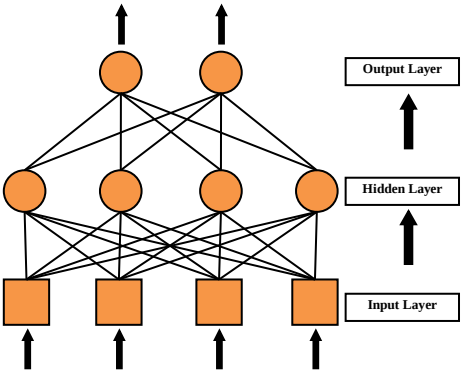

Fig. 3. Layers of the ANNs

The input layer receives the data from the outside and transmits it to the hidden layer. The hidden layer multiplies incoming data with weights and weighted data are collected. The results of the transfer function transmits output layer. Then, the output layer sends the result to the outside (Haykin, 1994).

3.2.K-Nearest Neighbor (KNN) Algorithm

K-Nearest Neighbor is one of the simplest and easiest methods to implement for image classification. Unlike other algorithms as ANNs, KNN does not need to train a dataset. Since the output value is only related to the partial number of neighboring samples, errors arising from the number of unstable training examples can be avoided in this algorithm. Due to these advantages, the algorithm has recently been used in many areas such as text classification, data processing and earthquake prediction (Sang *et al.*, 2011).

The KNN algorithm process is defined as follows. A stable database (D) based on the measured results is established. K is set to the nearest neighbor number. Since K strongly influences the output values, there is no special way to set it. The value is usually determined experimentally. M (m_1, m_2 ... m_n) which is the feature vector are computed and generated for each point. The distances between each point of M' and D collection are (M): dist (M', M). The commonly used Euclidean Distance is shown in the Eq. 3 (Sang *et al.*, 2011).

$$d(M', M) = \sqrt{\sum_i^n (m_i - m_j)^2} \quad (3)$$

According to the calculated distance, the nearest K point, D, is selected and a new data is collected according to the above equation (D_k). The output value of M is used the following equation according to D_k is calculated.

$$M' = \frac{\sum_{i=1}^{K} M_j}{K} \quad (4)$$

3.2.Post Classification Comparison

The most commonly used change detection techniques are image differencing, image rationing, principal component analysis, change vector analysis and post-classification comparisons (Kesikoğlu, 2013).Image differencing, image rationing, change vector analysis and principal component analysis are used for unsupervised change detection, whereas post-classification comparisons are used for supervised change detection process.

In this study post-classification comparison is used in change detection analysis. In this approach, satellite images belonging to two different times are classified and recorded independently. Then, the classified images are compared with each other. Thus, the direction and amount of change are determined (Tabarroni, 2010).

4. APPLICATION AND RESULTS

The direct use of raw images obtained from satellites in change detection studies is an obstacle for producing meaningful results because these images contain non-systematic errors. These errors arise from the height and position of satellite (Sertel *et al.*, 2007).The geometric correction process with image registration must be performed in order to correct these errors (geometric distortions) in the images. The process followed in the study is demonstrated in Fig. 4.

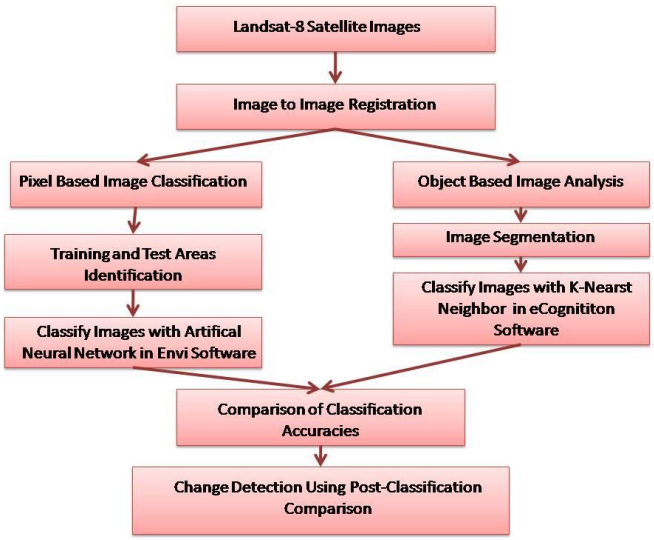

Fig. 4. Coastline change detection diagram

First of all, "Image to Image Registration" process was performed for satellite images. Satellite image for March were selected as reference and the other images were registered in that image. In the "Image Registration" process, image mapping was done by using ground control points (GCPs) that were known in the image. 30 well-distributed GCPs were used during implementation

and it was noted that the root mean square error (RMSE) value was less than 0.5. Furthermore, the images were cut based on the specified study area after registration. Blue bands of the each registered images are demonstrated in Fig. 5.

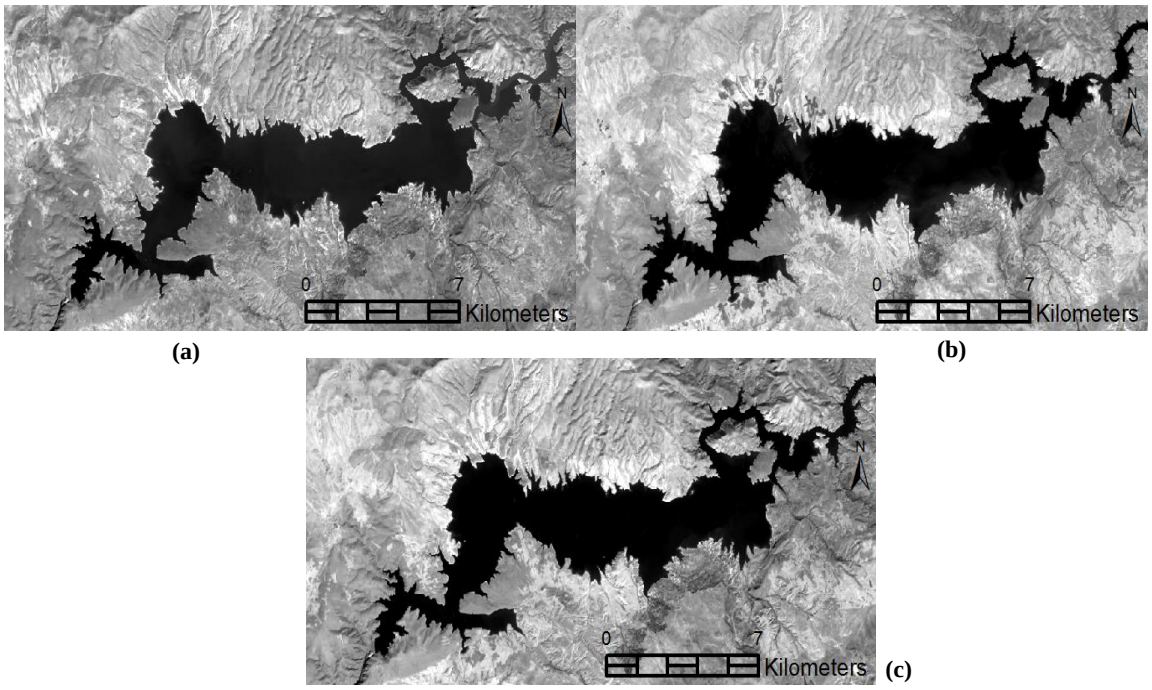

Fig. 5. Registered images for (a) March, (b) August, (c) November

Our study area was divided into two classes; 'Lake' and 'Other_field'. It was chosen 2454 pixels for training and 2501 pixels for testing to use in satellite images of different dates in the study. Due to the fact that the selected train and test areas represented the right classes in each images, a single train and test data was used. The selected training areas were used to classify the images with both ANNs and KNN classification algorithms. The test data were used to evaluate the accuracy of the classification process.

4.1. Pixel-based classification of the Landsat 8 data

Pixel-based image classification, using an ANNs classifier, was performed using ENVI, which is image analysis software. While classification was being done, parameters such as number of iterations, learning rate, training RMS output value and momentum related to ANNs were used. Since pixels are considered separately in pixel based classification, it is important to evaluate all pixels. Therefore, multispectral bands (bands 2-7) were used for doing classification. The training was stopped when the specified RMS output value was reached. The learning rate is a variable used for changing weight values of the ANNs. Momentum used to reduce error and to provide a correction for changing weights is a number value from 0 to 1 (Kesikoğlu, 2013). In this study, the number of iterations was 1000, the RMS output value was 0.1, the learning rate was 0.2 and the momentum was 0.9. After that, the multispectral images were divided into two classes as 'Lake' and 'Other_field'. Classified images are shown in Fig. 6.

4.2. Object-based classification of the Landsat 8 data

The KNN approach is similar to the supervised classification because samples are chosen as supervised classification. However, the selected samples are not as independent as selected in the supervised classification. The first step of object-based classification is segmentation. There are various segmentation types such as chessboard, quadtree, multi-resolution and spectral difference. Before using this method, training and test data in the ANNs was integrated into the eCognition software. Then, multi-resolution segmentation method was applied to the remaining areas. The scale parameter was 50, the shape parameter was 0.1 and the compactness parameter was 0.5 for the multi-resolution segmentation.

Prior to the classification, instead of pixels, objects (segments) formed by combining pixels are used in object-based classification. When classifying these objects, an input parameter is required, unlike pixel-based classification. This parameter was Normalized Difference Water Index (NDWI) (McFeeters, 1996). The reasons for choosing this parameter are that, NDWI is an internationally accepted index to extract water areas and it distinguishes water from other field easily. For this reason it has been sufficient to use two bands (band 3 and 5) required for NDWI method in object based classification. NDWI formula is given in Eq. 5.

$$NDWI = \frac{GREEN-NIR}{GREEN+NIR} \quad (5)$$

Classification was then carried out using the KNN according to the training data selected in the ANNs method. The multispectral images are divided into two classes as 'Lake' and 'Other field' by using KNN. Classified images are demonstrated in Fig. 7.

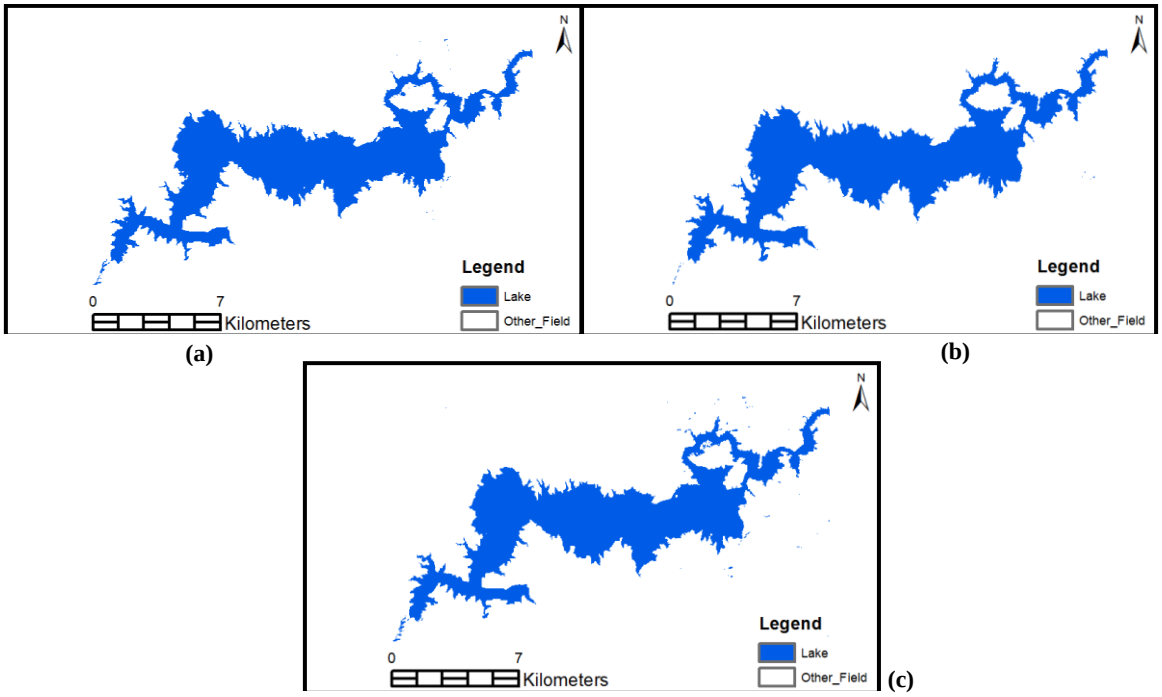

Fig. 6.Classification images classified by ANNs (a) March, (b) August, (c) November

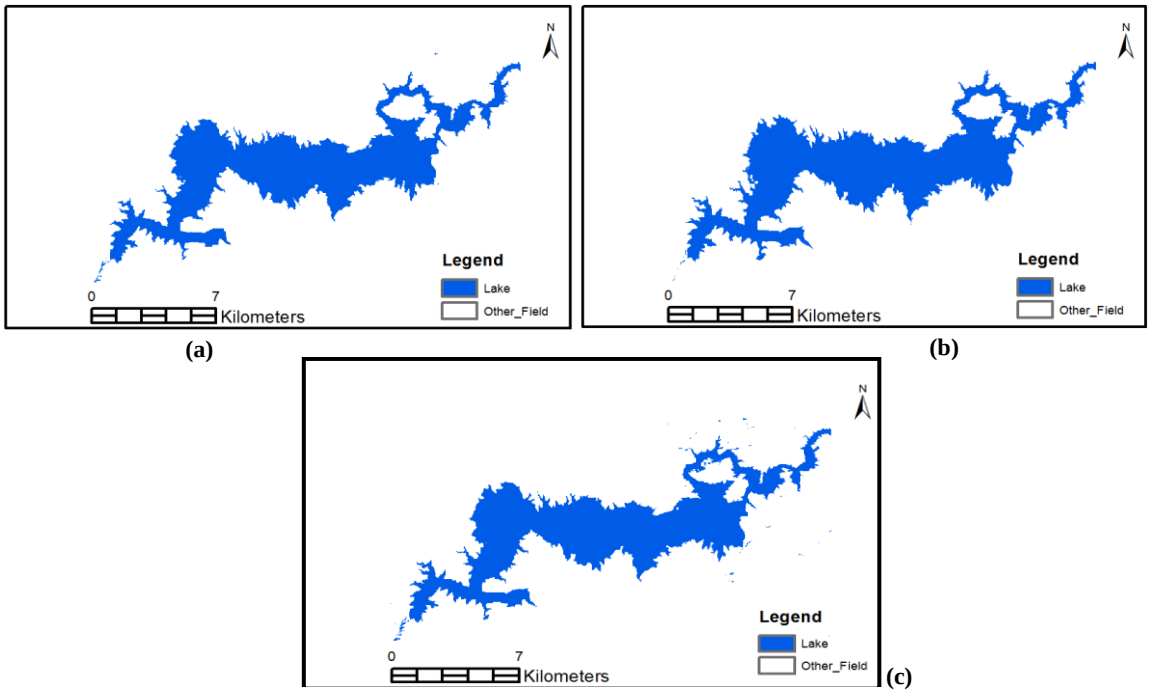

Fig. 7.Classification images of Yamula Dam Lake classified by KNN for (a) March, (b) August, (c) November

The image classification accuracies are presented in Table 2. Results obtained with KNN classification was observed at 99.99% overall accuracy for March image, 99.93% overall accuracy for August image and 99.92% overall accuracy for November image. Results obtained with ANNs classification was observed at 99.97% overall accuracy for March image, 99.90% overall accuracy for August image and 99.80% overall accuracy for November image.

Table 2. Results of accuracy analysis for classification

	ANNs		KNN	
Month	Overall Accuracy (%)	Kappa Coefficient	Overall Accuracy (%)	Kappa Coefficient
March	99.97	0.9991	99.99	0.9998
August	99.90	0.9969	99.93	0.9983
November	99.80	0.9938	99.92	0.9955

Although the results are close to each other, the KNN method seems to give better results. For this reason, the thematic maps obtained from KNN method are used to determine the change map. Change detection maps are shown in Fig. 8.

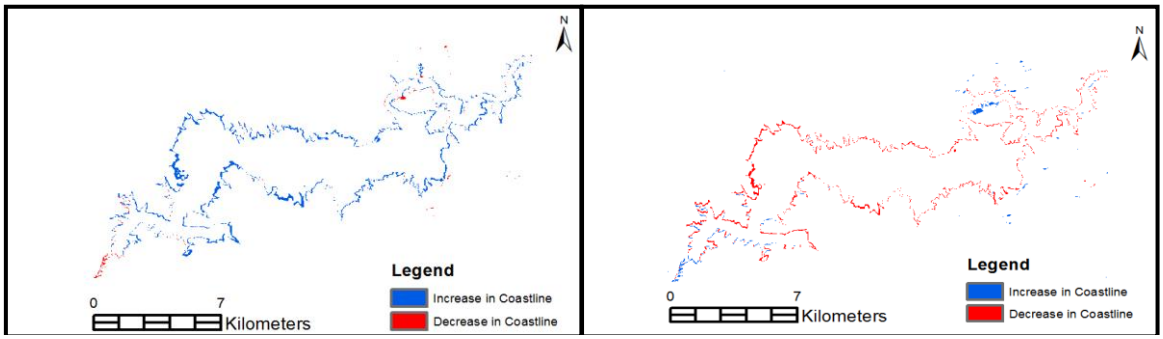

Fig. 8.(a) Map of changes by KNN method from March to August (b) Map of changes from August to November

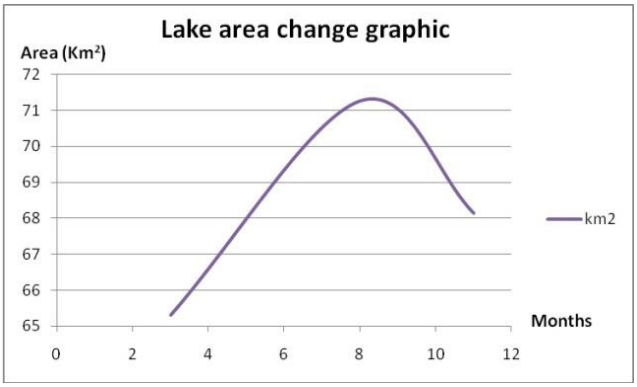

Fig. 9.The graphic of lake area from March to August and November in Yamula Dam Lake

According to the obtained findings (Fig. 9), lake area has a 5,67 km^2 increase from 65,82 km^2 to 71,49 km^2 between March and August; a 3,14 km^2 decrease from 71,49 km^2 to 68,35 km^2 between August and November.

In Kayseri the total precipitation was 430 mm in 2016. Whereas August is the driest month, April is the rainiest month. The precipitation in August was 6 mm while it was 54 mm in April. The precipitation increased after August illustrated in Fig. 10 (a).

In Sivas, total precipitation was 500 mm in 2016. Whereas August is the driest month, May is the rainiest month. The precipitation in August was 6 mm while, it was 60 mm in May. The precipitation increased after August illustrated in Fig. 10 (b).

The annual spatial precipitation in Sivas causes changes in the amount of water coming to the Yamula dam as it affects the occupancy rate of the Kızılırmak River. Therefore, due to the effect of the precipitation regime in Sivas on the study area, the precipitation regime in Sivas was also taken into consideration. The melting snow sometimes causes the flow of Kızılırmak Rivers to rise. This situation leads to an increase in the amount of water coming to the Yamula Dam Lake. Thus, the increase in the amount of incoming water is seen in Fig. 8, which leads to the expansion of the Yamula Dam Lake boundaries. The highest rainfall in Sivas province in 2016 took place in April and May according to the Sivas annual areal rainfall graphic. It also affected the increase in water boundaries of the Yamula Dam. After August, a decrease in the dam lake boundaries was observed.

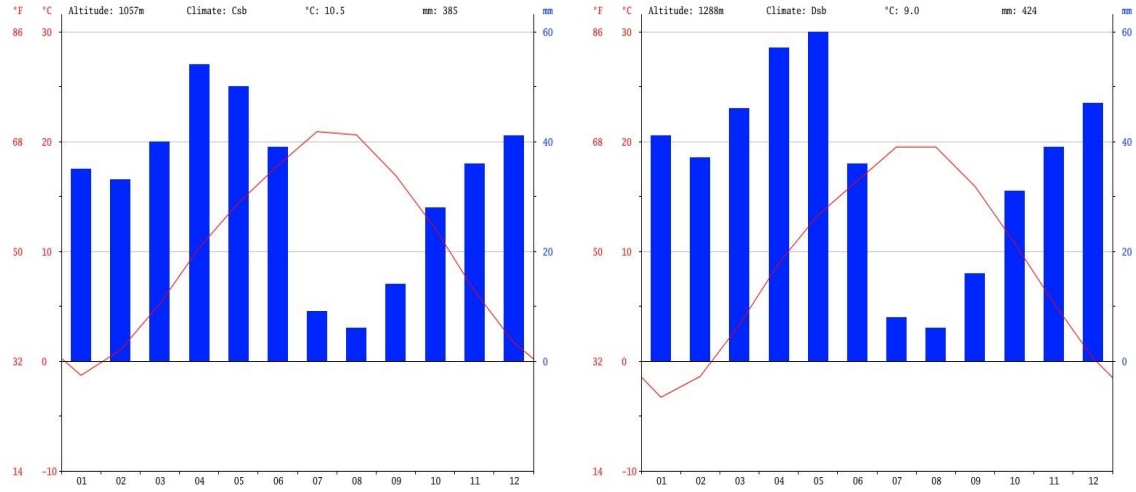

(a) **(b)**

Fig. 10. (a) Kayseri annual areal rainfall ("Iklim Kayseri", 2017) (b) Sivas annual areal rainfall ("Iklim Sivas", 2017)

5. CONCLUSION

Water is vital for the survival of livings. Rivers, lakes and dams form natural and artificial water resources. It is seen that both natural and human-induced effects are increasing or decreasing day by day in water resources. Therefore, determining the changes occurring in water sources is of great importance. Yamula is one of the most important dams in Turkey in terms of irrigation and electricity generation. In this study, both pixel-based and object-based classification methods were used to determine the water areas in the dam and the results were evaluated. While in the pixel-based classification method training data is selected pixel-by-pixel, in the object-based classification training data object by object is selected. For this reason the segmentation phase that forms the objects is very important. At the segmentation stage, pixels having similar reflection characteristics are grouped so that instead of working with a large number of pixels, segments consisting of pixels having these common characteristics are formed, at which point the heterogeneity between the segments is minimized. Therefore, object-based classification gives higher accuracy.

In this study, since the test area was a small area and only two classes were created, high accuracy was obtained by both methods. Different results were obtained as a result of using both algorithms. However, increase in the lake area until August and decrease after this month was detected in result of both algorithms. As the KNN method gave better results, the classification images obtained from this method was used to determine seasonal variations. The seasonal change information was obtained by using post classification comparison method on the classified Landsat 8 satellite images. It is seen that post classification comparison method used in this study produced meaningful change results in satellite images of different months.

The results of the study show that there is both an increase and decrease in Yamula Dam Lake. A lot of studies about the Yamula dam have been reviewed. As a result of the news, it was determined that the changes in the dam were not human-origin but climate-related. The change in the dam area was results from snow melting, rainfall and evaporation. It was detected that the increase until August was both snow melting and rainfall. The decrease in the lake area after August was results from the decrease in rainfall. Moreover, the evaporation which was caused by the increase of the air temperature negatively affected the lake area. In the context of this study, it has been was observed increase in the amount of the water in the Yamula Dam Lake until August and decrease in the amount of water in the Yamula Dam Lake after August In addition, KNN method gave better results than ANNs method to identify Yamula Dam Lake.

REFERENCES

A. M. Al Fugara, A., M., B. Pradhan, B., and T. A. Mohamed, T., A., (2009). "Improvement of land-use classification using object-oriented and fuzzy logic approach." *Applied Geomatics*, 1(4), 111.

Baek, S., and Sung, K. M. (2000). "Fast K-nearest-neighbour search algorithm for nonparametric classification." *Electronics Letters*,36(21), 1821-1822.

Chebud, Y., Naja, G. M., Rivero, R. G., and Melesse, A. M. (2012). "Water quality monitoring using remote sensing and an artificial neural network." *Water, Air, and Soil Pollution*, 223(8), 4875-4887.

De Giglio, M., Greggio, N., Goffo, F., Merloni, N., Dubbini, M., and Barbarella, M. (2019). "Comparison of Pixel-and Object-Based Classification Methods of Unmanned Aerial Vehicle Data Applied to Coastal Dune Vegetation Communities: Casal Borsetti Case Study." *Remote Sensing*, 11(12), 1416.

Denoeux, T. (1995). "A k-nearest neighbor classification rule based on Dempster-Shafer theory. "*IEEE Transactions on Systems, Man, and Cybernetics*,25(5), 804-813.

Duro, D. C., Franklin, S. E., and Dubé, M. G. (2012). "A comparison of pixel-based and object-based image

analysis with selected machine learning algorithms for the classification of agricultural landscapes using SPOT-5 HRG imagery". *Remote sensing of environment*, 118, 259-272.

Erener, A., and Yakar, M. (2012). "Monitoring Coastline Change Using Remote Sensing and GIS Technologies. "*Lecture Notes in Information Technology*, 30, 310-314.

Franco-Lopez, H., Ek, A. R., and Bauer, M. E. (2001). "Estimation and mapping of forest stand density, volume, and cover type using the k-nearest neighbors method. "*Remote Sensing of Environment*, 77(3), 251-274.

Güney, Y., and Polat, S. (2015). "Coastline Change Detection Using Remote Sensing Data: The Case of Aliaga and Candarli. "*Journal of Aeronautics and Space Technologies/ Havacılık ve Uzay Teknolojileri Dergisi*, 8(1).

Hassan-Esfahani, L., Torres-Rua, A., Jensen, A., and McKee, M. (2015). "Assessment of surface soil moisture using high-resolution multi-spectral imagery and artificial neural networks. "*Remote Sensing*,7(3), 2627-2646.

Haykin, S. (1994). *Neural networks: A comprehensive foundation*, Macmillan College Publishing Company, New York, USA.

Iklim Kayseri, https://tr.climate-data.org/asya/tuerkiye/kayseri/kayseri-250/ [Accessed 25 June 2017]

Iklim Sivas, https://tr.climate-data.org/asya/tuerkiye/sivas/sivas-255/ [Accessed 25 June 2017]

Im, J., & Jensen, J. R. (2005). A change detection model based on neighborhood correlation image analysis and decision tree classification. *Remote Sensing of Environment*, *99*(3), 326-340.

Isa N. A. M., Mashor M. Y, Othman N. H., Zamli K.Z., (2005). "Application of artificial neural networks in the classification of cervical cells based on the Bethesda system." *Journal of JICT*, 4, 77-97.

Karaburun, A., and Demirci, A. (2010). "Coastline changes in Istanbul between 1987 and 2007."*Scientific Research and Essays*, 5(19), 3009-3017.

Kesikoglu, M. H., Atasever, U. H., Dadaser-Celik, F., & Ozkan, C. (2019). Performance of ANN, SVM and MLH techniques for land use/cover change detection at Sultan Marshes Wetland, Turkey. *Water Science and Technology*.

Kesikoğlu, M. H., Atasever, Ü. H., and Özkan, C. (2013). "Uzaktan Algılamada Kontrolsüz Değişim Belirleme."*Tmmob Harita Ve Kadastro Mühendisleri Odası, 14. Türkiye Harita Bilimsel Ve Teknik Kurultayı*, Ankara.

Kesikoğlu, M. H. (2013). Research Of Coastal Change In Sultan Marshes National Park And Ramsar Site With Satellite Image Analysis, MSc. Thesis, University of Erciyes, Kayseri, Turkey.

Kesikoğlu M.H., Çiçekli S.Y., Kaynak T., Özkan C. (2017). "The determination of coastline changes using artificial neural networks in Yamula Dam Lake, Turkey. "*The 8th International Conference on Information Technology*, Amman, Ürdün, 1-4.

Kuleli, T., Guneroglu, A., Karsli, F., and Dihkan, M. (2011). "Automatic detection of shoreline change on coastal Ramsar wetlands of Turkey. "*Ocean Engineering*,38(10), 1141-1149.

Lillesand, T., Kiefer, R. W., and Chipman, J. (2014). *Remote sensing and image interpretation*. John Wiley and Sons.

McFeeters, S. K. (1996). "The use of the Normalized Difference Water Index (NDWI) in the delineation of open water features. "*International Journal of Remote Sensing*,17(7), 1425-1432.

McRoberts, R. E., Nelson, M. D., and Wendt, D. G. (2002). "Stratified estimation of forest area using satellite imagery, inventory data, and the k-Nearest Neighbors technique. "*Remote Sensing of Environment*, 82(2), 457-468.

Ozpolat, E. and Demir, T. (2014). "Coğrafi Bilgi Sistemleri Ve Uzaktan Algılama Yöntemleriyle Kıyı Çizgisi Değişimi Belirleme : Seyhan Deltası."*Xvi., Akademik Bilişim*, Mersin Üniversitesi ,Mersin.

Prabaharan, S., Raju, K. S., Lakshumanan, C., and Ramalingam, M. (2010). "Remote sensing and GIS applications on change detection study in coastal zone using multi temporal satellite data." *International Journal of Geomatics and Geosciences*, 1(2), 159.

Pradhan, B., and Lee, S. (2010). "Landslide susceptibility assessment and factor effect analysis: backpropagation artificial neural networks and their comparison with frequency ratio and bivariate logistic regression modelling" *Environmental Modelling and Software*, 25(6), 747-759.

Rodriguez-Galiano, V. F., Ghimire, B., Rogan, J., Chica-Olmo, M., & Rigol-Sanchez, J. P. (2012). An assessment of the effectiveness of a random forest classifier for land-cover classification. *ISPRS Journal of Photogrammetry and Remote Sensing*, 67, 93-104.

Sang, L., Xu, Y., Cao, R., Chen, Y., Guo, Y., and Xu, R. (2011). "Modelling of GaN HEMT by using an improved k-nearest neighbors algorithm. "*Journal of Electromagnetic Waves and Applications*, 25(7), 949-959.

Sarle, W. S. (1994). "Neural networks and statistical models. "*Proceedings Of The Nineteenth Annual Sas Users Group International Conference*.

Shetty, A., Jayappa, K. S., and Mitra, D. (2015). "Shoreline change analysis of Mangalore coast and

morphometric analysis of Netravathi-Gurupur and Mulky-Pavanje spits."*Aquatic Procedia*, 4, 182-189.

Tabarroni, A. (2010). Remote sensing and image interpretation change detection analysis: case study of borgo panigale and reno districts, MSc. Thesis, University of Florence, Florence, Italy.

Wang, X. Z., Zhang, H. G., Fu, B., and Shi, A. Q. (2013). "Analysis on the coastline change and erosion-accretion evolution of the Pearl River Estuary, China, based on remote-sensing images and nautical charts." *Journal of Applied Remote Sensing*, 7(1), 073519-073519.

What are the band designations for the Landsat satellites?,http://landsat.usgs.gov/band_designations_landsat_satellites.php[Accessed 22 June 2017].

Yamula Barajı (n.d.), http://www.kayseri.gov.tr/yamula-baraji [Accessed 8 March 2017]

Yu, Q., Gong, P., Clinton, N., Biging, G., Kelly, M., and Schirokauer, D. (2006). "Object-based detailed vegetation classification with airborne high spatial resolution remote sensing imagery." *Photogrammetric Engineering and Remote Sensing*, 72(7), 799-811.

Zhang, H., Li, Q Liu, J., Du, X., Dong, T., McNairn, H., Champagne, C., Liu, M., and Shang, J.(2017). "Object-based crop classification using multi-temporal SPOT-5 imagery and textural features with a random forest classifier."*Geocarto International*, 1-19.

CONTENTS

ISSN 2587-1366

TURKISH JOURNAL OF ENGINEERING

VOLUME 4 ISSUE 1 JANUARY 2020